Grad. School
Form No. 9
Revised

PURDUE UNIVERSITY

Graduate School

This is to certify that the thesis prepared

By Derli Prudente Santana

Entitled Soil Formation in a Toposequence of Oxisols from Patos de Minas Region, Minas Gerais State, Brazil.

Complies with the University regulations and that it meets the accepted standards of the Graduate School with respect to originality and quality

For the degree of:

Doctor of Philosophy

Signed by the final examining committee:

____________________, chairman

____

____

____

Approved by the head of school or department:

3/1 1984 ____________________

To the librarian:

This thesis is not to be regarded as confidential

____
Professor in charge of the thesis

SOIL FORMATION IN A TOPOSEQUENCE OF OXISOLS FROM PATOS DE MINAS REGION, MINAS GERAIS STATE, BRAZIL

A Thesis

Submitted to the Faculty

of

Purdue University

by

Derli Prudente Santana

In Partial Fulfillment of the

Requirements for the Degree

of

Doctor of Philosophy

May 1984

To my wife, Maria Célia, for her constant sacrifice,
companionship and love.

ACKNOWLEDGMENTS

I am deeply indebted to Dr. D. P. Franzmeier, my major professor, for the kind of advice and leadership that makes him a respected major professor as well as a friend. He continually gave me encouragement, advice and enough intellectual freedom to pursue my own ideas throughout my thesis work. I appreciate his faithful belief in my abilities.

A special thanks goes to Dr. D. G. Schulze for his strong support in the iron oxide mineralogy study and for taking time for the many stimulating and challenging discussions. I also appreciate the counsel of Drs. M. F. Baumgardner, W. N. Melhorn and J. L. White who served on my advisory committee.

The author wishes to express his deep appreciation to his friend Joaquim R. Almeida for representing the author and efficiently taking care of the author's affairs in Brazil. Also in Brazil, the assistance of Dr. Mauro Resende in helping to plan the research, to collect the samples and to provide support in so many ways is sincerely recognized.

Appreciation is expressed to Empresa de Pesquisa Agropecuária de Minas Gerais (EPAMIG) and to Empresa Brasileira de Pesquisa Agropecuária (EMBRAPA) for the leave of absence granted and for providing financial support which made this research possible.

The warm friendship and cooperation extended to the author by the staff members and fellow graduate students in the Agronomy Department is gratefully acknowledged and will be long remembered.

Last but by no means least, the author wants to acknowledge his wife Maria Célia for her love, understanding and support especially at times when completion of the thesis seemed remote indeed. To his children Arthur, Cecília and Lucas, the author also expresses appreciation for their expressions of love and understanding for the many nights and weekends that Daddy had to leave to do his "special work". Finally the author acknowledges his parents and sisters who struggled to give him a better education.

TABLE OF CONTENTS

LIST OF TABLES

LIST OF FIGURES

Figure | Page

Figure | Page

ABSTRACT

Santana, Derli Prudente. Ph.D., Purdue University, May 1984. Soil formation in a toposequence of Oxisols from Patos de Minas Region, Minas Gerais State, Brazil. Major Professor: Dr. D. P. Franzmeier.

Tuffite-derived soils, widespread in the Patos de Minas Region, are among the most productive soils of Minas Gerais State, Brazil, and have potential for greater agricultural development. To understand how properties of these Ustox soils relate to landscape features, a toposequence with 40 m relief in 500 m, was sampled on the flatter stretches of a valley slope. From summit to footslope positions the following trends in properties of the B horizon (about 1 m depth) were observed: 1. moist soil color graded progressively from dusky red to strong brown with mottles; 2. mica content increased; 3. hydroxy interlayered vermiculite, present in very small amounts, showed no clear trends; 4. kaolinite content decreased in an irregular fashion; 5. gibbsite and anatase decreased; 6. hematite decreased; 7. goethite decreased slightly; 8. maghemite was absent in the footslope positions and present in small amounts in backslope and summit positions; and 9. magnetic susceptibility decreased steadily. Downslope movement of Si or preferential removal of Si from upper slope positions controls the weathering and formation of clay minerals in the landscape. In the

lower slope positions, which are wetter than upper positions, goethite formation apparently is favored relative to hematite and maghemite. Goethite was found to have a smaller crystallite size and more Al-substitution than hematite.

Differential X-ray Diffraction Analysis (DXRD) combined with multipleregression analysis provided a quantitative estimate of the different iron oxide minerals present in the sample. A hand magnet attached to a small spring balance provided a quick and reliable quantitative estimate of soil magnetic susceptibility in the field. A simple redness index was calculated for mottled horizons. Also, a new redness index that emphasizes the role of hue in soil color relationships was used.

INTRODUCTION

Over the years, it has been learned that the most effective soil classification criteria are those in which the differentiating characteristics (the properties chosen as the basis of defining classes) are based, to some extent, on properties which covary with the general nature of the parent rock. In general, the younger the soil the greater the influence of parent material on soil properties. However, after long periods of weathering, even small differences in parent material composition cause significant variation in soil properties. Without fertilizer these small variations can result in very significant differences in yield. This is very pertinent in Brazil where higher base-status soils derived from mafic (basic) rocks are surrounded by extremely base-depleted soils derived from other rocks. Oxisols derived from mafic rocks are separated, in the Brazilian Soil Classification System, from Oxisols formed from other rocks even if they have the same color, same amount of clay and same organic matter content. This separation appears to be well-justified in terms of the productivity of the soils, because Oxisols derived from mafic rock have potential for greater agricultural development than those derived from other rocks.

Landscape position is a critical factor influencing many co-varying soil properties even in highly weathered soils, such as Oxisols that tend to have a high degree of homogeneity. Water movement and distribution on slopes, even where the gradient is slight and not readily apparent, is responsible for pedogenic differences that are a function of slope position. Thus, sites at the upper slope positions tend to be impoverished, to the advantage of sites on lower slopes, and particularly those of depressions, that are enriched in materials from all higher positions. This downslope process forms a three-dimensional continuum on the landscape in such a way that soils are similar laterally along a given contour line but vary continuously downslope. A gradual change in color is one of the more obvious variations and is typical of many Brazilian Oxisol landscapes.

Color is a very important soil characteristic, and because of its striking appearance is probably the most obvious feature of the soil. For most pedologists and soil surveyors, relatively slight differences in the color or color pattern of only one horizon in the profile may, at times, be significant in classifying soils into different groups. The importance of color in soil classification is evident in the widespread use of color terms in soil names, for example, Podzol (ash color), Chernozem (black earth), and Red Yellow Podzolic. In U.S.A. Soil Taxonomy, although color names are not frequently expressed in class names, the characteristic itself is important in many class definitions.

In Brazil, soil color names are used for almost all classes, especially for Latosols (Oxisols) where color criteria have been quite important.

In recent years there has been a gradual emergence of interest in magnetic susceptibility of soils, because it reflects the nature of the parent material and shows the results of soil forming processes. In Brazilian soil survey work, magnetic susceptibility, as observed in the field with a hand magnet, is used to help identify classes of soil developed from mafic rocks.

The objectives of this work are: (1) To determine the influence of hillslope positions on the mineralogy, chemistry, color and magnetic properties of soils developed from tuffite (a mafic rock) and to determine the interrelationships among these soil properties.

(2) To develop practical ways to measure and express magnetic properties and soil color.

(3) To use these measurements to predict fundamental soil properties, especially as they relate to use and management of the soils.

LITERATURE REVIEW

All the soils sampled in this work are Oxisols, the predominant soils of Brazil, so the main emphasis in this section is on Oxisols.

General Background

Oxisols are mineral soils with an oxic horizon within 2 m of the surface, or plinthite that forms a continuous phase within 0.30 m of the mineral surface of the soil, and with no spodic or argillic horizon overlying the oxic horizon (Soil Survey Staff, 1975). Differences in properties with depth in Oxisols are so gradual that in much of the profile they are nearly featureless soils without clearly marked horizons. The lack of marked changes, especially in terms of texture, color, and structure, is perhaps the most obvious distinctive feature of an oxic horizon.

The most important processes in the transformation of primary minerals leading to the formation of an oxic horizon are removal of basic cations and desilication. The net result of silica loss appears to be the relative accumulation of iron, or ferritization (Buol et al., 1980). It is assumed that these pedogenetic processes are, or were, generated under climatic conditions humid enough to favor the removal of

soluble weathering products and produce the residual concentration of sesquioxides and kaolinitic clays (Van Wambeke et al., 1983). However, Oxisol distribution tends to be independent of present rainfall patterns, suggesting that many Oxisols, mostly found in transported sediments, attained their weathered mineralogical characteristics by processes not related to present climate (Buol et al., 1980). This could indicate that the time factor may be more important than the present climate in explaining the genesis of some Oxisols.

Most well-drained Oxisols cover stable landforms or continental shields, or are formed in sediments derived from them (Buol et al., 1980). In general, there are no Oxisols in areas which belong to orogenic belts, except where they are associated with extremely weatherable rock formations such as basic and ultrabasic rocks (Bennema et al., 1962). Thus, the extreme degree of chemical decomposition may be as much the result of age as well as weatherability.

Almost all Oxisols occur between the tropical parallels, predominantly in the southern hemisphere. They generally occur where there is small seasonal variation in soil temperature, no seasonal soil freezing, and a maximum of rain when the sun is directly overhead (Van Wambeke et al., 1983). The temperature regimes of most Oxisols fall within the range from isomesic to isohyperthermic, and Oxisols have been reported with all moisture regimes except xeric. Oxisols support a rather wide range of vegetational-ecologic zones, but by far the greatest areas are in tropical rain forests, scrub and thorn forests, semideciduous forests, and savanna vegetational zones (Buol et al., 1980).

Oxisols Landscape

Soil genesis can be viewed as consisting of two steps: 1) the accumulation of parent material; and 2) the differentiation of horizons in the profile (Simonson, 1959). Differentiation of horizons depends on the variations in weathering rate and rate of removal of weathering products. If weathering rates are more rapid than removal processes, a thick soil cover develops. Conversely, if removal processes are more rapid than weathering, only a thin soil cover will exist because material is removed as fast as it becomes loose. Thus, on gentle slopes removal will be minimal and deep soils and regolith will develop, whereas at more erosionally active sites, soils will remain thin and youthful (Gerrard, 1981). However, soils on a landscape are all interrelated and the processes that occur in the soils of the higher portions of the landscape have an influence on soils that occur in lower parts of the landscape. Materials, suspensions and solutions move through and over soil landscapes rather than through only a single soil at a given point (Hall, 1983). Therefore, relief, affecting directly the stability of the surface determines, to a large extent, the degree of soil formation in the landscape.

One of the main features of the older landscapes of Brazil is the presence of widespread erosion surfaces at different levels (King, 1967). Some of the various erosion surfaces present in the landscape originated in the Quaternary, some in the Tertiary, and some even as far back as Mesozoic time. Surfaces formed during Tertiary time covered

broad areas and many are still well preserved, particularly the one which is believed to date from the mid-Tertiary (some thirty million years ago) and which forms a vast plateau in Central Brazil (The Brazilian Central Plateau), at a mean altitude of 750 m above sea level (Bennema et al., 1962). Locally known as "Chapadas" or "Chapadões", these surfaces have slopes of 0 to 3 percent and they represent a "master surface" from which most of the existing landscape of Brazil has subsequently been carved (King, 1967). These smooth, ancient land surfaces, and their slightly modified derivatives with accentuated relief, are covered with considerable quantities of detrital material. Detritus may be more than 30 m thick and consists of rock in an advanced stage of weathering, of boulders and fragments of rotten rock, and a superficial layer of allochthonous or pseudo-autochthonous material "drift" (Bennema et al. 1962). The "drift" mantle normally consists of a mixture of materials, representing contributions from many different rock-types, and commonly occurs as very strongly weathered mineral residues. Significant differences exist, however and they influence the kind of soils formed in drift materials (Bennema et al., 1962). The soils most commonly developed from drift materials are various kinds of Oxisols. For example, in the almost flat surface on which is located the Brazilian capital, Brazilia, complete associations of Acrustox, Haplustox and Ochraquox are present (Fewer, 1956; Bennema et al., 1962; Cline and Buol, 1973; Sanchez, 1976). This landscape consists of three erosion surfaces. The Acrustox tend to be associated with the highest

surfaces which have slopes of 0 to 3 percent. This surface terminates abruptly at an escarpment of 100 to 150 m elevation below which is a second gently-sloping erosion surface. The escarpments have little soil development on the weathered rock, and there are some plinthite outcrops. The second erosion surface is often several kilometers long with 2 to 8 percent slopes. Haplustox are the dominant soils. Ochraquox are present on both surfaces; they are apparently more prevalent along drainageways on and in depressions. The third erosion surface consists of 8 to 20 percent valley slopes parallelling narrow flood plains. Soils on this surface have higher base status and probably are Ustalfs. The first two surfaces are covered by scrub savanna vegetation (cerrado) indicative of low soil fertility. The third surface supports semideciduous forests reflecting a high base status.

In southeastern and eastern Brazil under udic, perudic and sometimes ustic moisture regimes, Oxisols may form on hilly or even mountainous relief (Bennema and Camargo, 1979). Where Oxisols are present there is a deep mantle of weathered material covering most of the hills which led scientists to infer that all the surfaces are very old in this region of Brazil (King, 1956, Valverde, 1958). Rezende (1972), studying a toposequence of soils in the Zona da Mata de Minas Gerais, concluded that most of the soils are actually either Oxisols or intergrade into them. The grading of Oxisols to Ultisols and Alfisols is common in areas of medium and high altitudes with deeply weathered regolith and strongly

undulating topography. Leptsch et al. (1977) studied an Oxisol-Ultisol-Inceptisol toposequence in Sao Paulo State, Brazil, and found that argillic horizons apparently formed in material that would qualify as an oxic horizon before it was exposed. Their data suggest that Oxisols are not always older than Ultisols or Alfisols since a geomorphic surface that has both Ultisols and Alfisols was inferred as older than another surface dominated by Oxisols. Moniz and Buol (1982), studying another toposequence in Sao Paulo State, also found a situation where, on hillslopes below the Oxisols but in material of oxic composition, profile differentiation processes have resulted in the formation of soils with subsoils displaying the morphological features of argillic horizons. This type of landscape association is also observed in several other Brazilian states (Camargo, 1980, cited by Moniz and Buol, 1982). According to a double-water flow model developed by Moniz and Buol (1982), the argillic horizon in this situation is formed from oxic materials through the action of both lateral and base-water flow integrated in the landscape.

With some exceptions, most Oxisols on residual material are from mafic (basic) parent material (Bennema et al., 1962; Buol, 1979; Van Wambeke et al., 1983). Thus, on these extremely weatherable rocks, weathering occurs in a shorter time than otherwise would be required. No consistent pattern with respect to geomorphic position appears to apply to these soils. Rauen (1980) studied a very common toposequence of soils from basaltic rocks in the tropical part of the state of

Parana, Brazil. The toposequence described has 90 m relief in approximately 1800 m. On smooth and gently sloping summits with rolling shoulders, the dominant soils are Oxisols; on rolling (8-20% slopes) backslopes or footslopes they are Alfisols; and on rolling and hilly topography near streams or erosional surfaces where bedrock is near the surface, they are Entisols and Mollisols. Hematite content decreases from the summit to the bottom of the valley and so does the gibbsite/kaolinite ratio, indicating that leaching and weathering decrease in the same fashion. Curi and Franzmeier (1984), studying a toposequence of Oxisols with 2 m relief in approximately 180 m developed from basalt in the Central Plateau of Brazil (Goias State), found that moist soil color changed from dark reddish brown (2.5YR3/4) in upper slope positions to dark yellowish brown (10YR4/4) in lower slope positions, and the following trends were observed: hematite content decreased and goethite content increased, the amount of Al substitution in the goethite structure increased, gibbsite content decreased and kaolinite content increased, and magnetic susceptibility and maghemite content of fine clay decreased.

In summary, where soil material has been transported, Oxisols can occupy geomorphic positions on surfaces of almost any age. In residual soils where weathering in situ produces an extreme degree of chemical decomposition, parent rocks of mafic (basic) composition appear the most prevalent, and no distinct geomorphic position appears especially favorable. Oxisols usually occupy more stable geomorphic surfaces, and less

weathered soils are on younger surfaces, but in southeastern and eastern Brazilian landscapes Oxisols may form on hilly or even mountainous relief. In Oxisol toposequences variation in soil color is one of the more obvious changes and generally is associated with relative elevation and thus with changes in hydrological characteristics.

Mineralogy

The removal of silica and bases and relative accumulation of oxides (hereafter including oxides, hydroxides and oxyhydroxides) of iron and aluminum are the major processes affecting the mineral components of Oxisols. These processes yield a product consisting of low activity clays, iron and aluminum oxides, a few unaltered fragments of weatherable minerals, and the various resistant minerals originally present in the rock. Kaolinite, gibbsite, goethite and hematite in different proportions are the main clay size minerals in Brazilian Oxisols (Leal and Veloso, 1973; Moniz, 1967; Moura Filho, 1972; Santana, 1973; Gomes, 1976; Fasolo, 1978; Rauen, 1980; Kämpf, 1981; Curi, 1983; and others). Maghemite has been reported in some Oxisols developed from basaltic (Rauen, 1980; Curi, 1983) and itabiritic rocks (Curi, 1983). Anatase and/or rutile may be present in low amounts in the clay fraction of Oxisols derived from mafic rocks (Moura Filho, 1972; Resende, 1976; Carmo, 1977; Santana and Moura Filho, 1978). Mica (mainly muscovite) is common in Oxisols derived from pellitic parent material (Almeida, 1979;

Resende and Franzmeier, 1982). Aluminum-interlayered vermiculite may form part of the clay-mineral association (Lepsch et al., 1977; Rodrigues, 1978; Fasolo, 1978; Santana and Moura Filho, 1978; Rauen, 1980). Truly amorphous iron compounds seem to be absent or are present in very small amounts in most Oxisols (Rauen, 1980).

Most clay-size kaolinites found in the oxic horizon are poorly crystallized and generally belong to the more disordered types and have a higher structural iron content compared with kaolinites found in deep geological deposits (Herbillon et al., 1979). Recent observations indicate that most iron oxides in Oxisols are highly aluminum substituted (Norrish and Taylor, 1961; Juo et al., 1974). In hematite the upper limit seems to be about 16 mole % Al substitution (Curi, 1983). The goethite structure appears to accommodate more Al than the hematite structure: 28% (Rezende, 1980); 30% (Resende 1976); 31% (Curi, 1983); 38% (Bigham, 1977). A reduction in unit cell size is expected since the Al^{3+} ion has a smaller radius (0.057 nm) than the Fe^{3+} ion (0.067 nm) and this could modify some properties of these minerals. Due to their low crystallinity, small particle size and high degree of substitution, these clay minerals may develop a relatively high specific surface with associated pH dependent positive and negative charges (Van Wambeke et al., 1983).

The silt fraction does not constitute much of the soil, except in some Oxisols derived from mafic rocks (Dusky Red Latosols) in spite of problems with dispersion of clay. Kaolinite, gibbsite, mica, quartz,

interstratified minerals, and hematite have been reported in this fraction (Camargo and Beinroth, 1978; Fasolo, 1978; Almeida, 1979; Rauen, 1980).

Quartz is the dominant mineral in the sand fraction of most Brazilian Oxisols. Magnetite and ilmenite are common in soils from mafic rocks (Resende, 1976). Micas, chalcedony, tourmaline, apatite, sillimanite, garnet, zirconite, hornblende, titanite, epidote, pyrite, pyroxene, etc. have been recorded in soil survey reports. Kaolinite (mostly pseudomorphs after feldspar or mica) and gibbsite also occur in the sand fraction (Pinto, 1971; Gomes, 1976; Fasolo, 1978; Rezende, 1980).

Color

Secondary iron oxides are usually the dominant pigments in well-drained soils that contain little organic matter. Goethite (yellowish brown), hematite (red), and perhaps maghemite (dark brown) are the main iron oxides in Brazilian Oxisols. Soils containing only, or almost exclusively, goethite are yellowish brown (10YR-2.5Y Munsell hue) but if hematite is present the soil is usually reddish (7.5YR and redder) (Eswaran and Sys, 1970; Davey et al., 1975; Bigham et al., 1978; Childs et al., 1979; Kämpf and Schwertmann, 1983) because the red color of hematite is very effective in masking the yellow color of goethite. The

greater pigmenting power of hematite over goethite can produce soils which actually have dominant amounts of goethite rather than hematite appear red (Resende, 1976; Taylor, 1982).

Maghemite is dark brown (Taylor and Schwertmann, 1974), but varies from yellow to dark red as a function of particle size (Van Houten, 1968). Black colors on ped faces and along cracks in soils commonly result from thin coatings of manganese oxides (Taylor, 1982). Finely-divided manganese oxide is said to be responsible for low chroma (dusky red) color of some Brazilian soils developed from basaltic rock (Bennema, 1966).

One way by which soil colors have been described is by Munsell notation, which allows soil scientists to give reproducible color codes immediately recognized by others. Various degrees of success have been obtained in attempts to correlate Munsell notations with different soil components. Krishna Murti and Satyanarayana (1971) found that titanium and ferrous iron influence soil hue, and clay and organic matter influence soil value. Eswaran and Sys (1970) analyzed a large number of soil clays and found a general correlation between free iron and color hue of the parent soils; that is, redder soils tended to have higher secondary iron contents in their clay fractions.

In view of the pigmenting power of hematite it is not surprising that numerical color indices based on the Munsell notation, such as Munsell hue (H), Munsell hue x value (H x V), or Munsell hue x chroma/value (H x C/V) correlate more with hematite content of soils (Childs

et al., 1979; Torrent et al., 1980; Curi, 1983; Kämpf and Schwertmann, 1983) than with either the hematite/goethite ratio (Bigham, 1978) or the total iron oxide content (Soileau and McCracken, 1967; Hurst, 1977).

Magnetic Susceptibility

The electronic structure of one atom determines its magnetic behavior. An electron rotates around the nucleus (orbital rotation) and around itself (spin rotation); these rotations are related to the orbital and spin magnetic moment (a moving charged particle produces a magnetic field). The observed magnetic moment arises from a combination of the orbital and spin moments, and it will depend on the presence or absence of unpaired electron(s) in the system (Mulay, 1963). Two electrons that are paired in an orbital have opposite spins and thus their spin magnetic moments cancel each other. In this situation, the magnetic moment is caused by orbital motion of electrons only (Mulay, 1963). On the other hand, shells of electrons that contain an odd number of electrons will have a net spin magnetic moment that they impart to the atom (Brailsford, 1966). Iron is an atom with unpaired electrons; however, the spins of these electrons (six) are arranged in a special way: the partially full 3d shell of Fe contains five electrons with spins pointing one way and only one electron with spin pointing in the other way. The result is a large net spin moment which primarily determines the magnetic properties of Fe, as the orbital moments make

little or no contribution to the observed magnetic moment (Beiser, 1969). All elements resembling iron in electronic configuration and strongly attracted to a magnet are called ferromagnetic. A similar behavior is displayed by magnetite and maghemite, the two most important magnetic minerals in soils, but in this case two out of three spin magnetic moments due to iron atoms in the crystal line up in one direction, and the other moment is oppositely aligned. Such behavior is called ferrimagnetism (Mullins, 1977). Ilmenite, hematite and goethite display a further type of behavior called antiferromagnetism: adjacent atomic magnetic moments spontaneously align themselves in opposite directions, giving an overall magnetic moment of zero (Mullins, 1977). Ferrimagnetic substances have very much stronger magnetic properties than ferromagnetic substances. It must be emphasized that these properties are dependent not only on the elements present, but also on the crystal structure which determines spacing of the constituent atoms. Thus, for example, hematite (α Fe_2O_3) is antiferromagnetic, whereas maghemite (δ Fe_2O_3) is ferrimagnetic (Mullins, 1977).

In the literature of soil magnetism, the most common technique to characterize the soils is the measurement of magnetic susceptibility (χ), perhaps because it is a simple and non-destructive method (Oades and Townsend, 1963; Mullins, 1977). Magnetic susceptibility (χ) is the ratio of induced magnetization to applied field, or, more simply, a measure of the "magnetizability" of the sample (Oldfield et al., 1979). Table 1, modified from Mullins (1977), summarizes the normal range

of magnetic susceptibility measurements for the most common ferrimagnetic (magnetite and maghemite) and antiferromagnetic (ilmenite, hematite and goethite) minerals occurring in soils. In Brazilian Oxisols (as indicated by literature), magnetite and ilmenite occur in the sand and silt fraction, hematite is mostly present in the clay fraction, and goethite and maghemite occur only in the clay fraction.

Table 1. Magnetic susceptibility data for the most common ferromagnetic minerals occurring in soils (After Mullins, 1977).

Mineral	χ
	10^{-8} m^3 kg^{-1}
Ilmenite ($FeTiO_3$)	170
Hematite (α Fe_2O_3)	27, 31 up to 63
Goethite (α FeOOH)	35 up to 126
Maghemite (γ Fe_2O_3)	41,000 - 44,000
Magnetite (Fe_3O_4)	50,000 - 100,000

The presence of magnetite in basalt, andesite, and to a lesser extent in other igneous rocks is well known. It occurs mainly as sand-size equidimensional grains in the rocks and in soils developed from them (Mullins, 1977). The weathering of igneous rock is accompanied by a decrease in magnetic susceptibility (Vadyunina et al., 1974). Le Borgne (1965) also has said that, as a general rule, alteration tends to lead to a decrease in susceptibility due to the decomposition of amphiboles and pyroxenes; but with rocks containing resistant magnetic minerals such as ilmenite and magnetite, alteration may lead to an increase in susceptibility because of concentration of these minerals. This effect also was observed by Mullins (1977); however, he noted that a single generalization cannot be made, as weathering of magnetites relative to other minerals will depend on the nature of the other minerals and the type of weathering regime.

Soils lacking magnetite but with a high susceptibility will almost certainly contain maghemite, which forms by poorly understood pedogenic processes. Taylor and Schwertmann (1974) mentioned that maghemite formation is favored by lower oxidation rate, higher total Fe concentration, high temperature and neutral pH. They believe that green rust is an essential precursor of maghemite; on slow oxidation it will form maghemite, probably via magnetite. A common association between maghemite and hematite in soils was postulated by these authors. Le Borgne (1955, 1960) emphasizes the conversion of hematite to maghemite by burning and fermentation.

Longworth and Tite (1977), using Mossbauer and magnetic susceptibility measurements carried out on agricultural surface soil, found that the observed high susceptibility of the top soil after heating in air was the result of formation of ferrimagnetic maghemite from antiferromagnetic goethite. Mullins (1977), reviewing exhaustively the subject, provides a more detailed discussion of the way in which maghemite may be produced in the soil. He concluded that there are four different ways in which maghemite can be formed: 1) by low temperature oxidation of magnetite present in rocks or soil; 2) as a result of burning; 3) by dehydration of lepidocrocite (δ FeOOH); and 4) via a reduction-oxidation cycle occurring under normal pedogenic conditions. Since maghemite commonly occurs in soils whose parent material contains only a trace if any of magnetite or titano-magnetite, Mullins concluded that the reduction-oxidation cycle is likely to be the dominant mode of formation.

The $FeO-Fe_2O_3-TiO_2$ ternary system that comprises almost all the simple oxides of interest in soil magnetism is very prone to isomorphous substitution: there are solution series with varying amounts of Fe and Ti (hematite-ilmenite, magnetite-titano-maghemite) or amounts of oxidation (titanomagnetite-titanomaghemite) (Nagata and Akimoto, 1961). Trace element contents, crystal defects and other kinds of solid solution may also vary the system and influence the magnetic properties of the mineral. In fact, several authors have identified the ferrimagnetic minerals in the soil as impure maghemite (e.g., Longworth and Tite, 1977), non-stoichiometric magnetite (e.g., Longworth et al., 1979), or

they could approximate the solid-solution series between magnetite and maghemite (e.g., Oldfield et al., 1979).

In summary, ferrimagnetic iron oxides present in many soil profiles are inherited from the parent material or are formed as a result of normal pedogenic physical chemical processes. The chemical composition of the magnetic minerals so formed is the subject of some debate, though they appear to lie close to the solid-solution series between magnetite and maghemite, and vary according to the nature of the initial iron compounds present, degree of substitution by other cations, and dominant modes of transformation operating in the soil.

In most soils there are only two strongly magnetic minerals likely to be of significance: magnetite (including oxidised titanomagnetites) and maghemite (including titanomaghemites). However, Hedley (cited by Mullins, 1977) found an unusually high value of magnetic susceptibility for hematite, up to 63×10^{-8} m^3 kg^{-1} compared with normal values which average around 27 to 31×10^{-8} m^3 kg^{-1}; he attributed this to the very-fine grain-size hematite. Resende (1976), in the absence of positive evidence for the presence of maghemite and magnetite in the clay fraction of highly magnetic hematite-rich Oxisols in Brazil, suggested that the very small grain size and relatively high isomorphous substitution of hematite could be responsible for the high magnetic susceptibility of those soils.

Magnetic susceptibility, observed in the field with a hand magnet, is used in Brazilian soil survey work to help identify classes of soil

developed from mafic rocks (Comissão de Solos, 1960). Russian workers also have been using this soil characteristic for mapping soils (Vadyunina and Smirnov, 1978) and as evidence of soil forming processes (Vadyunina and Babanin, 1972). The use of magnetic susceptibility in studying soil developed on uniform parent material suggests that it can play a similar role to that of soil color because it is readily measured and can indicate local variations in soil forming conditions (Mullins, 1977).

Brazilian Latosols

Most of the soils previously called Latosols are included in the Oxisols order. However, the requirement of a high degree of weathering, low cation exchange capacity, and absence of an argillic horizon for a soil horizon or layer to qualify as an oxic horizon eliminated from the Oxisols order many Latosols.

Latosols recognized in Brazil are defined as having a latosolic B horizon, which is similar to the oxic horizon concept of the of U.S.A. Soil Taxonomy. There is, however, one important difference: in the Brazilian concept the latosolic B horizon should have a cation exchange capacity (CEC) of less than 13 meq/100g clay after correction for organic matter (Bennema, 1966), whereas in the American concept the oxic B horizon should have a cation exchange capacity (CEC) of less than 16

meq/100 g clay (Soil Survey Staff, 1975). The CEC as determined by the Brazilian method is somewhat lower than that determined by the U.S. National Soil Survey Laboratory as demonstrated by Ikawa (1978). Without correction for carbon some Latosols are excluded from Oxisols (Bennema and Camargo, 1979).

Latosols in the Central Brazilian landscapes, are, by far, the most widespread soils. In well drained areas color and texture change with changes in parent rock. In these areas, color has been used as an outstanding field criterion for mapping. Using color as one of the main differentiating characteristic, Bennema and Camargo (1979) recognized three main kinds of Latosols for these areas.

1. Red Yellow Latosols in general have hues 5YR or yellower, and values and chromas 4 or higher. Within this "assemblage" are soils low in iron oxides (less than 9% Fe_2O_3 by H_2SO_4 digestion) often derived from felsic crystalline rocks, sandstones poor in iron, or other sediments.

2. Dark Red Latosols commonly with hues 2.5YR or redder, values 4 to 3, chromas 4 to 7. The iron content is intermediate (9 to 18% Fe_2O_3 by H_2SO_4 digestion) and they are often derived from shales, slightly acidic (intermediate content of silica) igneous or metamorphic rocks, limestones, and sandstones high in iron content.

3. Dusky Red Latosols usually hue 10 R (but also 2.5YR) value 3, chromas 3 to 6. The iron content is high (more than 18% Fe_2O_3 by H_2SO_4 digestion) and they are derived from mafic rocks (basic rock in which ferromagnesian minerals predominate). It is not always easy for a soil

surveyor to determine the limit of Dusky Red soils and dark red soils on the basis of color alone. Sometimes H_2O_2 is used to detect the presence of Mn-compounds and a magnet often is used with a dry, crushed sample to estimate the content of magnetic minerals. The magnet will attract a large amount of soil particles unless it is a soil of restricted drainage.

BACKGROUND OF THE AREA

Setting

The region studied is located in the Brazilian Central Plateau, in Minas Gerais State, in the Patos de Minas region, about half-way between Belo Horizonte (the state capital) and Brazilia (the Federal capital) (Figure 1).

Climate

The average monthly temperature of 20.5°C is almost constant throughout the year (Figure 2). The total annual rainfall in the region is around 1400 mm; its distribution is characterized by distinct wet and dry seasons, with approximately 90% of the total precipitation falling between October and March. The length of the dry season is about 3 months and corresponds to the low-sun period of winter, June, July, and August. Short-term droughts occur commonly during the rainy season and may be detrimental to crop growth because of high evapotranspiration rates, low soil water retention capacity and adverse soil chemical

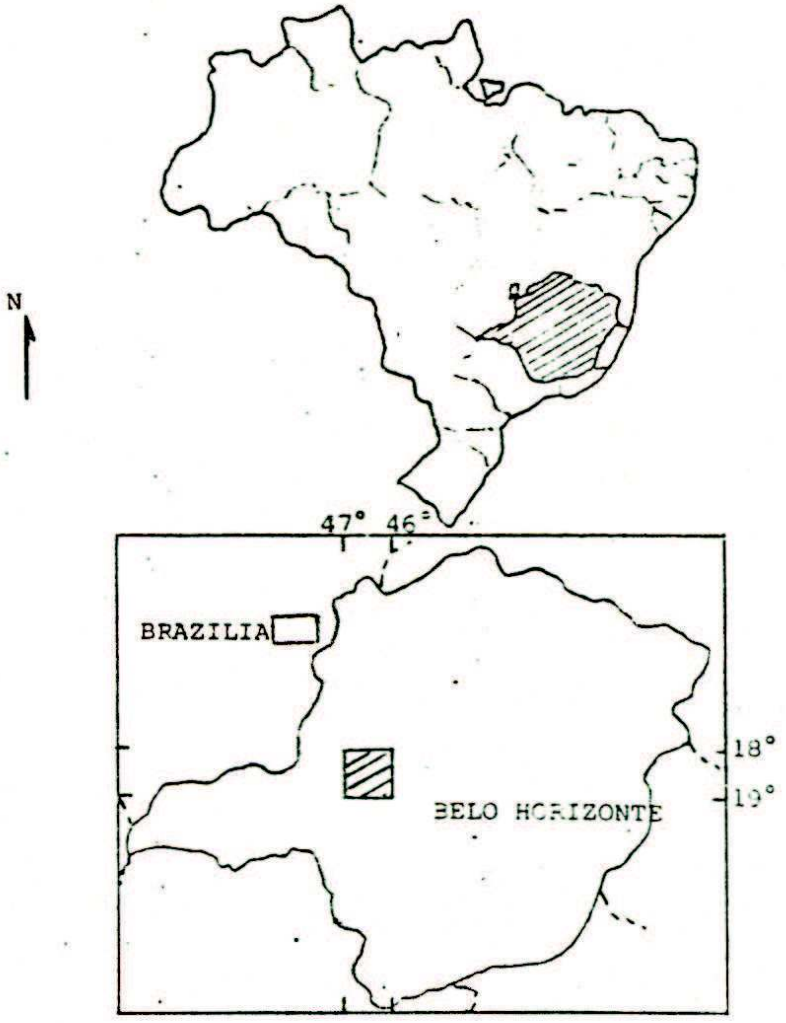

Figure 1. Brazil map showing the location of Minas Gerais State and enlargement showing the area studied (cross-hatched).

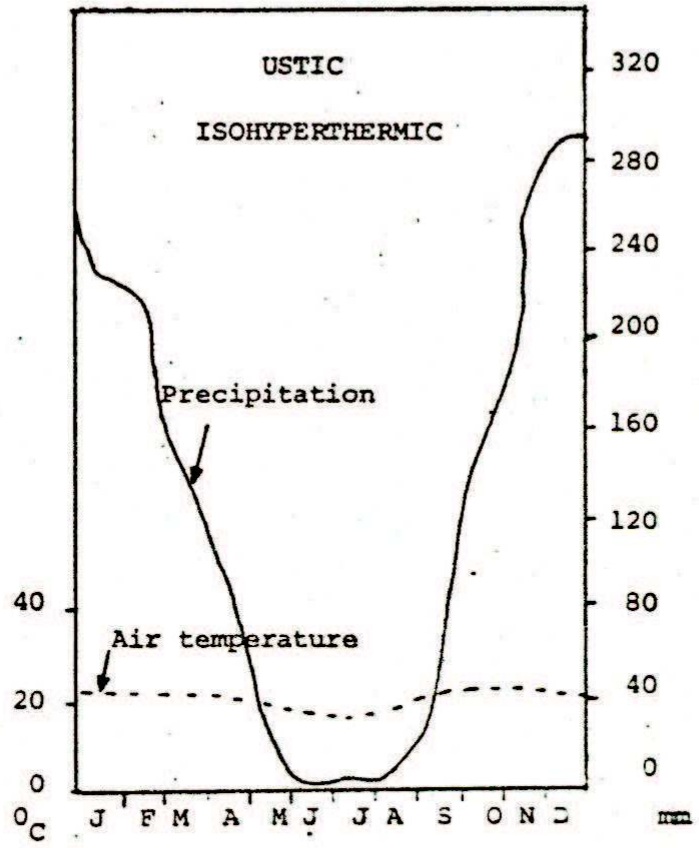

Figure 2. Diagram according to Gaussen and Bagnouls showing annual average distribution of precipitation and temperature for the Patos de Minas Region (After Silva and Antunes, 1980)

conditions for plant growth. Very likely, all soils sampled are under an ustic soil moisture regime and isohyperthermic temperature regime.

Vegetation

Cerrado, in the broad sense, is the main phytogeographic unit. "Cerrado" is the name given to the characteristic vegetation of the Central Plateau of Brazil, and may be defined as subhumid wooded savanna (Eiten, 1972, Ferri, 1977). It grows in a large range of natural physiognomies, from pure grassland to closed tree canopy (Eiten, 1982). The cerrado covers the larger portion of the area, and the remainder is forest, mostly semideciduous, on valley slopes of more rolling landscape.

Geology

Geologically the area has been described (Guimaraes, 1955) as a Precambrian basement, with structurally deformed felsic rocks, that are covered by pyroclastic-rich fluvio-lacustrine sediments (Figure 3).

Thick lava flows spread over a large Mesozoic desert on the Gondwana continent during Cretaceous, time covering eolian sandstones of the lower São Bento series (Botucatu's sandstones). Volcanic activity followed, spreading ash around the activity area. Eventually, a lacustrine environment was established and the volcanic ash accumulated in lakes with subsequent sedimentation and consolidation to form

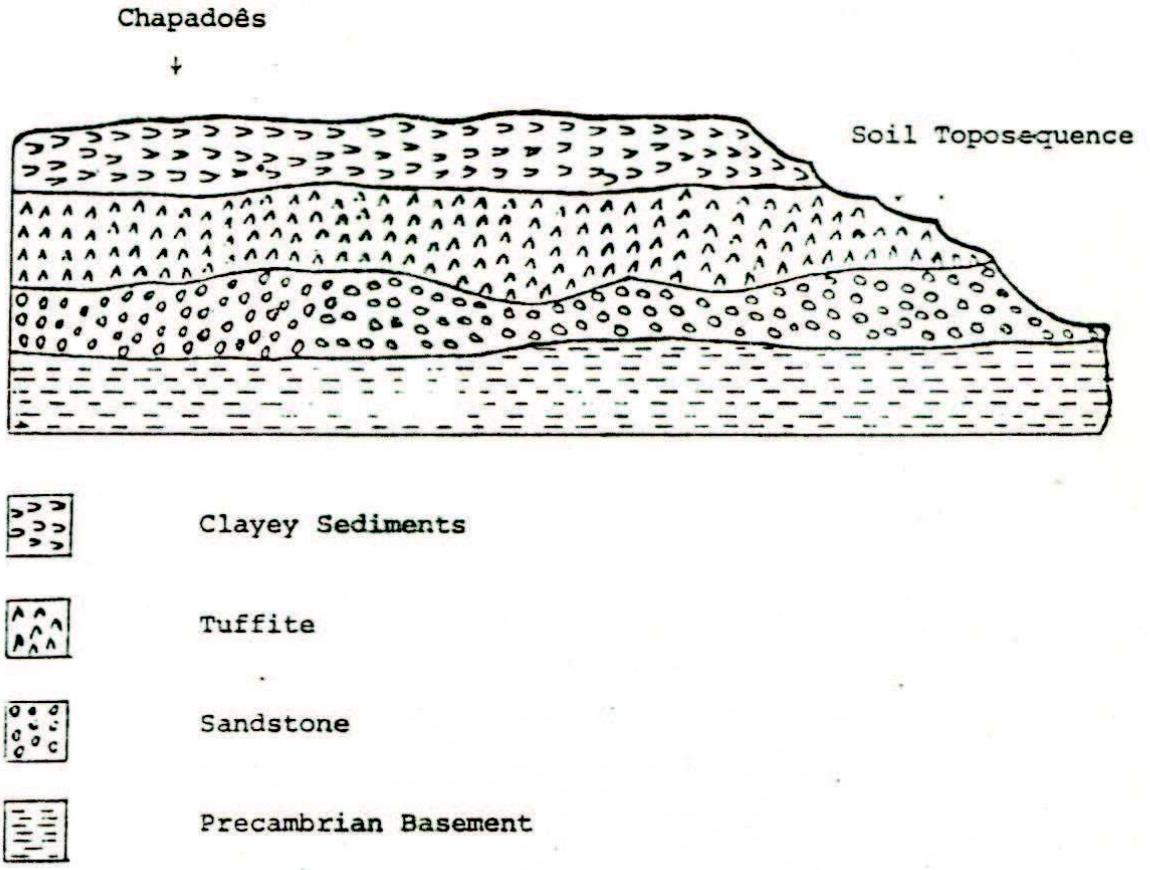

Figure 3. Idealized relationship between geomorphology, and lithology, showing the location of the toposequence studied.

tuffite. The variations in thickness of the deposit and lack of irregular deposition suggest that sedimentation occurred across pre-existing dissected surface (Barbosa et al., 1970).

In Neocretaceous time eolian and fluvial-lacustrine formation covered most of the area (Bauru Group).

Cenozoic sediments are reported as stone lines, lacustrine deposits on the "chapadões", lateritic material (mainly along the slope breaks) and colluvial and alluvial deposits (Resende, 1976).

Geomorphology

The present landscape is best visualized as a broad tableland - the "chapadões", which locally is dissected giving very deep valleys with large sloping pediments (Figure 4).

The "chapadões" are part of the vast plateau that makes up the "Brazilian Central Plateau", believed to date from the Tertiary (Miocene-Pliocene) (Braun, in Barbosa et al., 1970). Altitudes are generally above 1,000 m and the surface is extremely planar being almost flat in many stretches. Arc-shaped drainageways, covered mostly by grasslike vegetation, originate in open circular depressions with poorly drained soils. At the edges of many of these broad "chapadões" there is a surface deposit of lateritic (ironstone) gravel that protects these old surfaces against further erosion. Furthermore, the nearly level

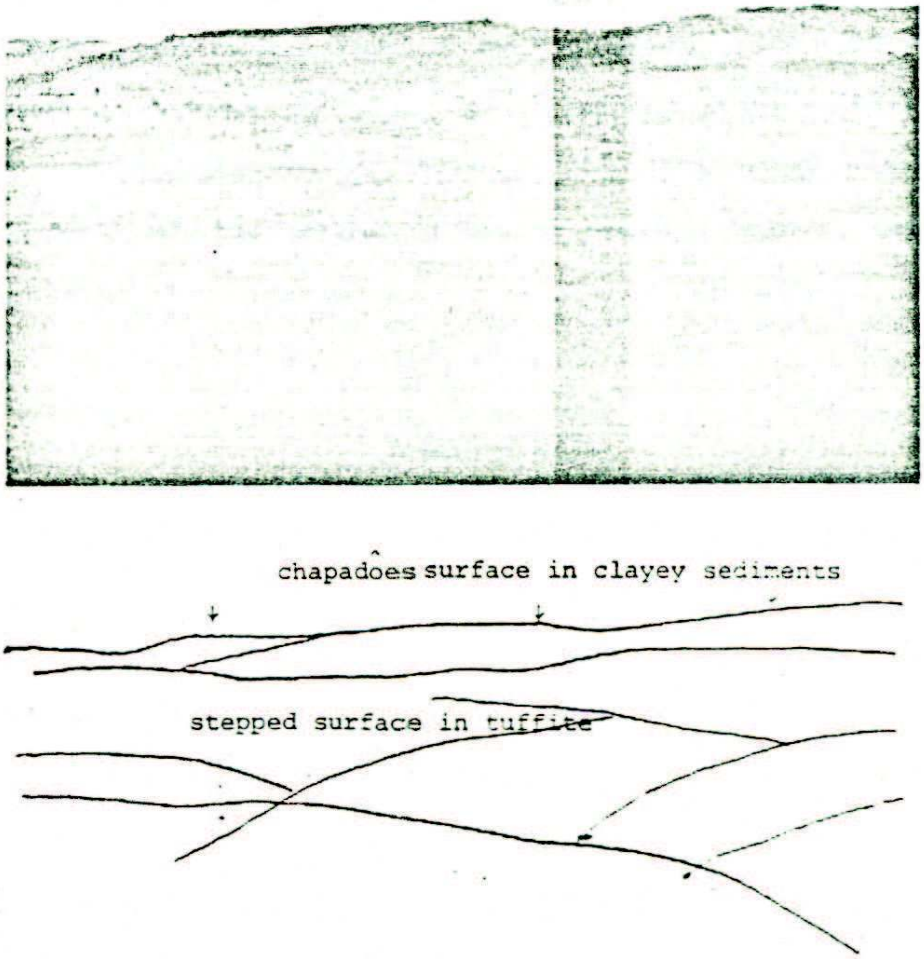

Figure 4. View of the area showing the chapadoes surface in clayey sediments and the stepped surface in tuffite.

surface and high permeability of the soils leads to reduced runoff, helping to stabilize the landscape as suggested for some areas of southern Minas Gerais by Comissaõ de Solos (1962) and of Minas Triangle by Resende (1976).

In the "chapadoês" the various pediments form stepped surfaces and have a tendency to be concave in profile. Now some of these pediments are eroding and forming segments tending towards a convex form. The dissection processes that gave rise to the valleys are probably related to the "Velhas Erosion Cycle" (King, 1956) that in Plio-Pleistocene times dissected the dominant surface of Brazil (Braun, in Barbosa et al., 1970).

Parent Material

The parent material of the "chapadoês" is clayey sediments of still questionable origin. Pelitic Precambrian rocks definitively affected these sediments. Cenozoic clayey deposits have been suggested also as being an important contributor.

Through exposure by erosion, tuffite became the main parent material for soils along major slopes in the valleys. Tuffite is an indurated rock composed of a mixture of pyroclastic and sedimentary detritus, especially ash and fine sediment.

Tuffite has always been an item of interest and curiosity because of its peculiar occurrence, beauty, and potential for agriculture.

Guimarães (1955) found great variability in this material, but consistently found high contents of iron, calcium, potassium, and phosphorus and indications of high levels of cobalt. Ilchenko (1955) reported high values for micronutrients such as Co, Ni, Cu, and Cr. Novais (1969), using tuffite as fertilizer, greatly increased corn production in an acid soil under cerrado vegetation. Barbosa et al. (1970), although stressing the variability among samples, suggested an economic study for the use of tuffite as a fertilizer. Tuffite mainly occurs in the Patos de Minas Region, Minas Gerais State, covering a relatively large area - 2170 km^2 (Barbosa et al., 1970). The fertility status of this region, considered an outstanding crop producing area, is thought to be related to the influence of tuffite in these soils.

In lower landscape positions, tuffite outcropping is common and in the very bottom of many of the valleys sandstone is present.

Soils

The soils on the "chapadoês" typically are Red Yellow Latosols and Dark Red Latosols (Oxisols). About soils of these "chapadoês" there is an interesting fact to point out. Carmo (1977) classified a soil with color 5YR5/6 and 15% Fe_2O_3 (by H_2SO_4 digestion) as a Red Yellow Latosol, using color as the basic criterion, and stressed that the amount of Fe_2O_3 is atypical for this soil class (generally the Fe_2O_3 is less than 9% for a Red Yellow Latosol). On the other hand, Gomes et al. (1980) classified a similar soil as Dark Red Latosol, using

Fe_2O_3 content (by H_2SO_4 digestion) as the basic criterion, and pointed out that the abnormal yellowish color was atypical for this soil class (usually a Dark Red Latosol has hue of 2.5YR or 10R). Thus we have a very important philosophic question -- which is more important, color or Fe_2O_3 content? The New Brazilian Soil Classification System, now in progress, needs data to help decide this basic dilemma: which comes first?

Along the valley slopes, Dusky Red Latosols (Oxisols) are widespread. According to Carmo (1977) the Dusky Red Latosol is usually dystrophic (less than 50% base saturation) in the flatter stretches, and euthrophic (more than 50% base saturation) on the steeper relief. Carmo also stated that these soils become increasingly shallow towards the valley bottom, reflecting more intensive erosion. Cerrado vegetation occurs only on the flatter stretches, being replaced by semideciduous forest on steeper slopes.

In the lower landscape positions there are more weakly developed soils (Inceptisols and Entisols) from tuffite, and also from sandstone in the lowest part of the valleys.

MATERIAL AND METHODS

Field Methods

The area was intensively investigated and particular attention was given to the distribution of soil classes in the landscape, their relationship to the factors of soil formation, color characteristics and magnetic susceptibility.

In selecting the sampling site, the amount of tuffite influence was deduced from field relations and from field tests of attraction of soil material by a hand magnet. By these tests, tuffite-derived soils have great attraction. Ideally, in selecting sites for such studies the nature of the parent material (independent variable) should be determined independently of other soil properties (dependent variable). However, in this deeply weathered tropical area, this was impossible and the magnetic attraction approach, used by soil surveyors in Brazil (Comissão de Solos 1960), is a valid method of retroactively judging the nature of the parent material.

A sequence of soils was sampled approximately 40 km east of Patos de Minas in the direction of São Gotardo (BR-354 Highway) immediately after the São Bartolomeu River.

Using a combination of soil pits and auger sampling, 10 profiles were collected to a depth about 3.20 m from summit to footslope positions. The sampling interval was closer where changes in soil properties were greatest. Horizon depth, color description, and observations about special features constituted the brief profile descriptions. Soil samples selected by color pattern and special pedological features were chosen for more detailed studies.

A smooth surface with 10% slope characterizes the topography of the sequence of soils collected (Figure 5). The erosion surface on which the soils were sampled is probably related to the "Velhas cycle of erosion" (King, 1956) of Plio-Pleistocene age. The soils are apparently all developed from the same tuffite-rich parent material of Cretaceous time. However, profile F1 (Figure 5) seems to be on a different landscape surface and it might have a different source of sediments. The natural vegetation is cerrado, grading to semideciduous forest in lower landscape positions. When sampled, sites F1 through F6 were in field crops (corn and rice), and F7 through F9 were in natural vegetation. Very likely all soils sampled are under an ustic soil moisture regime and isohyperthermic soil temperature regime.

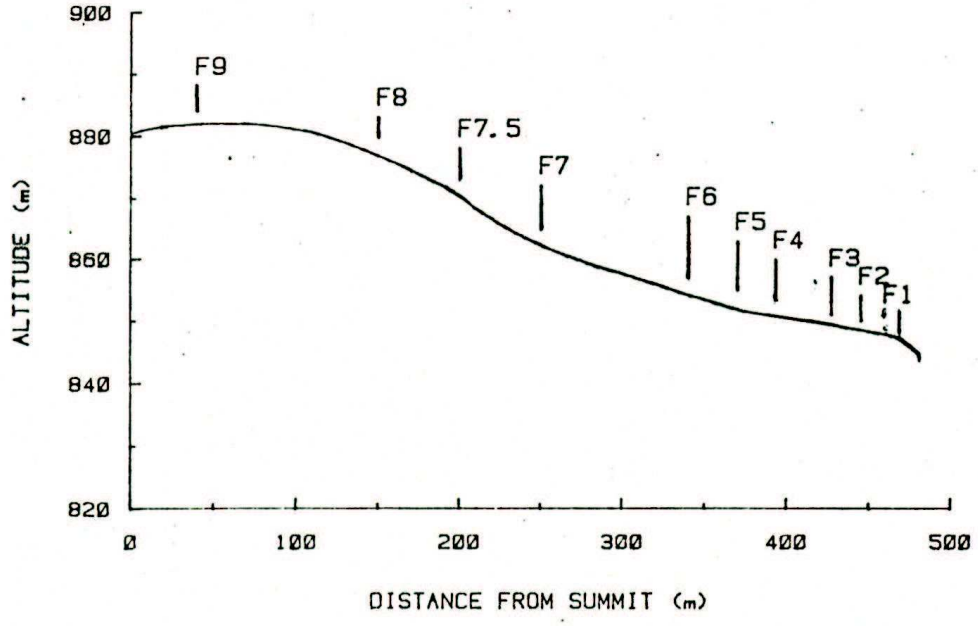

Figure 5. Schematic representation of the toposequence studied indicating the location of the profiles sampled.

Laboratory Methods

Physical and Chemical Characterization

Some of the analyses are those done routinely in the Brazilian soil survey (Vettori, 1969; EMBRAPA, 1979) and were carried out in the Department of Soil Science of the Escola Superior de Agricultura de Lavras, Minas Gerais State, Brasil[1].

Particle size distribution - dispersion with NaOH, clay fraction (< 2μm) measured in suspension by hydrometer, sand (> 20 μm) content obtained by sieving, and silt (2-20 μm) calculated by difference. Particle density - determined on 20g air dried sample using 95% ethyl alcohol to measure the volume in a 50 ml volumetric flask. Moisture equivalent - centrifuge method (Piper, 1944). pH - determined by glass electrode in water and 1 M KCl. Exchangeable cations - extraction with 1 M KCl (1:10) and determination of Ca, Mg, and Al in the extract; extraction with 0.05 M HCl + 0.05 M H_2SO_4 and determination of K and Na in the extract; extraction with pH 7.0 $Ca(OAc)_2$ and determination of acidity by titration with NaOH solution (extractable H equals this acidity minus that from KCl-extractable Al). Base Saturation (BS) - (Extractable bases x 100)/CEC. Organic C - wet oxidation with $K_2Cr_2O_7$. Available P - extraction with 0.05 M HCl and 0.05 M H_2SO_4 and determined colorimetrically. Extractable Si, Al, Fe, Ti, and P with H_2SO_4 - 2 g

---

[1] We are indebted to Prof. Victor G. Bahia who supervised those analyses.

boiled in 50 ml 50% (about 9 M) H_2SO_4 for 1 hr; Al, Fe, Ti, and P in extract determined by colorimetric or volumetric methods; Si in solid portion of extract dissolved in 5% Na_2CO_3 and determined colorimetrically. This extraction approximates the chemical composition of the clay fraction.

Mineralogical Characterization

X-ray diffraction analysis (XRD) - Clay samples were analysed by XRD using randomly oriented powder samples or oriented samples. Clay samples were collected by sedimentation and decantation after dispersion by ultrasonic treatment (5 minutes at 100 watts) followed by adjusting the suspension of deionized water and soil to pH 10.5 with 1N NaOH (this pH was the lowest pH at which good dispersion was reached in a preliminary test). Fine clay (< 0.2 μm) was separated by centrifugation. Diffraction data were obtained using Cu Kα radiation (30 KV, 28 mA) and a Siemens Type F goniometer equipped with a 1° divergence slit, a 0.28 mm receiving slit, and a diffracted beam graphite monochromator, using an Ortec axis controller with digital stepping motor drive. Scanning rate was 1 or 2°2θ/min. The identification of the crystalline species present in the sample was based on Mg-saturated and glycerol solvated samples and air-dried K-saturated samples at room temperature, after heating to 300°C and after heating at 550°C (Jackson, 1975). Table 2 summarizes the main x-ray diffraction characteristics used in the qualitative identification of the clay minerals.

Table 2. Characteristic d-spacings and how they behave with the diagnostic treatments used in the identification of clay minerals.

Mineral	d-spacing	Diagnostic treatment
	nm	
HIV (hydroxyinterlayered vermiculite)	1.4	Collapsed irregularly from 1.40 to 1.00 nm upon K-550[1/]
Mica	1.0, 0.5, 0.33	No changes with any treatment
Kaolinite	0.710, 0.358	Disappears after treating at 550°C
Gibbsite	0.482, 0.434	Disappears after heating at 300°C
Anatase	0.352	Appears after disappearance of kaolinite.

[1/] K-550 = Potassium saturated and heated at 550°C.

Differential thermal analysis (DTA) was carried out on clay fractions with a Dupont 990 Differential Thermal Analyzer with a Pt, Pt-13%Rh thermocouple using a heating rate of 10°C/minute in an intermediate temperature cell base and 50 mg of DCB-treated samples. Fired Al_2O_3 was used as the reference material. Standard curves were prepared for both kaolinite (Huber Company) and gibbsite (Reynolds Metals Company, Richmond, Virginia).

HF dissolution for total elemental analyses was done by the method of Bernas (1968). As a slight modification of the method, sealed 100 ml

Nalgene bottles were used instead of acid digestion vessels. The samples were shaken without heat for 12 hours (or longer until a clear homogeneous solution indicating total dissolution was obtained) in a mechanical shaker. After dissolution was completed, the flask was opened, about 2.8g of H_3BO_3 mixed with about 70 ml deionized water was added quickly and immediately recapped and the solution stirred and then the volume was brought to 100 ml with deionized water. Aliquots of the solution were used to determine K by atomic absorption and the % K_2O was used to estimate mica content (Kieley and Jackson, 1965).

Dithionite-citrate bicarbonate (DCB). The procedure of Mehra and Jackson (1960), using one or two extractions, was used to estimate the amount of iron oxide present in the clay fraction. As a slight modification of the original procedure, 10 (instead of 5) minutes of reaction time was allowed between the 3 subsequent dithionite additions. After the reaction was completed the samples were centrifuged, washed once with the citrate-bicarbonate buffer and the two supernatant solutions were combined. Fe and Al were determined on the extracts by the phenanthroline colorimetric method as described by Franzmeier et al. (1977).

Ammonium oxalate. Oxalate extractable iron was extracted using pH3 ammonium oxalate (Schwertmann, 1964; McKeague and Day, 1966) and determined colorimetrically according to the procedure used for DCB extracts.

Differential x-ray diffraction analysis (DXRD) as described by Schulze (1981) was used to obtain diffraction patterns for iron oxide minerals. Ten percent (w/w) of 1.0 μm α-Al_2O_3 (Buehler Micropolish Linde C 1.0 Micron Alpha Alumina, No. 40-6310.008 Buehler Ltd., 2210 Greenwood Street, Evanston, Illinois, U.S.A. 60221) was added as an internal intensity and peak position standard (Bryant et al., 1983). Samples were thoroughly mixed by gentle stirring and grinding in an agate mortar. The samples were then split in two halves; one half was treated with DCB (described above) and the other half received the same treatment except there was no dithionite in the extracting solution (only citrate and bicarbonate).

After the extraction was completed all the samples were washed twice with 0.1N $MgCl_2$, once with distilled water and with ethyl alcohol until salt free. After air drying at room temperature the samples were gently ground in an agate mortar to pass a 60 mesh sieve. Self-supporting powder mounts were prepared by back-filling 500-600 mg of sample into an Al sample holder (19 x 19 mm sample area) and gently pressing the material against unglazed paper to minimize preferred orientation (Schulze, 1982). Diffraction data were obtained in the same instrument already described. The diffraction patterns were obtained by step-scanning every 0.05 2θ, using a counting time of 70 sec. per increment, from 18 to 44° 2θ . The digitized data were recorded on magnetic tape and computer processed as follows: 1) The raw data were used to plot intensity versus goniometer angle, 2) the position of the (113) α-Al_2O_3

line as originally recorded was determined and a 2θ correction factor was obtained to adjust it to exactly 43.40° 2θ (Joint Committee on Powder Diffraction Standards, 1980). (The corrections were mostly around 0.02° 2θ and ranged from 0.01 to 0.04° 2θ.) 3) the intensities of the 2.085 Å α-Al_2O_3 peak (43.40° 2θ) in the treated and untreated subsamples were determined and the scale factor was calculated by dividing the intensity of the peak from the untreated sample by that from the treated one (Bryant et al., 1983), 4) the curves were smoothed by a 5-point cubic polynomial smoothing routine (Savitzky and Golay, 1964), 5) all intensities in the diffraction pattern for the treated sample were multiplied by the scale factor, 6) the scaled diffraction pattern of the treated sample was subtracted from that of the untreated one, 7) the three patterns, treated, untreated, and difference were displayed on the screen of an IBM Personal Computer XT and slightly different scale factors and shifting factors were tried to give an overall good fit of the curves, 8) the resulting differential pattern (subtracted) as in step 6 was then plotted on a HP flat-bed plotter.

The iron oxides present in the samples were identified based on the Joint Committee on Powder Diffraction Standards (1980) diffraction files (Table 3). Integrated peak areas were determined using a HP digitizer. Peak positions and widths at half height (WHH) were determined from expanded plots. The exact peak position was considered to be the midpoint of the WHH line of the peak and was corrected relative to the position of the internal standard peak (Klug and Alexander, 1974). The widths at half height (WHH) were corrected for instrumental and $\alpha 1$-$\alpha 2$

dispersion broadening by subtracting WHH from the 2θWHH of the well crystalline novaculite (quartz) which exhibits no line broadening due to particle size or disorder. The corrected WHH, WHHc, was used to calculate the mean crystallite dimension perpendicular to hkl, L_{hkl}, using the Scherrer equation (Klug and Alexander, 1974, p. 687-692). Al substitution in goethite was estimated by calculating the c dimension from the (110) and (111) line positions and relating the c dimension to aluminum substitution (Schulze, 1984). Al substitution in hematite was estimated from the a dimension (Schwertmann et al., 1979).

Table 3. XRD and crystal lattice characteristics of goethite, hematite, maghemite and α-alumina (Joint Committee on Powder Diffraction Standards, 1980).

Mineral	Peak position (CuKα)	d-spacing	Relative intensity	hKl
	°2θ	nm		
Goethite	21.25	0.418	100	110
	33.30	0.269	35	130
	36.67	0.245	50	111
Hematite	24.25	0.367	25	110
	33.30	0.269	100	104
	35.77	0.252	50	110
Maghemite	30.26	0.295	30	220
	35.76	0.251	100	313
	43.28	0.209	15	400
α-Alumina (Corundum)	25.60	0.348	75	012
	35.17	0.255	90	104
	37.77	0.238	40	110
	43.40	0.2085	100	113

Quantitative DXRD. The DXRD patterns of the iron oxide minerals can be used for quantitative analysis of the phases present. Quantitative analysis using x-ray patterns is based on the assumption that the diffraction intensity of each component's pattern is proportional to the amount present. Thus, the weight fraction of component p in the mixture (Wp) is given by

$$W_p = K_p \times I_p,$$

where K_p is a constant which depends on the nature of the component, the particular reflection considered, and the experimental arrangement, and I_p is the diffracted intensity of a given x-ray line of component p. However, absorption effects are present which usually prevent us from directly comparing pattern intensity of a component in a mixture with the pattern of the pure component prepared under identical conditions. On the other hand, if an internal standard is added in a constant proportion, s the concentration of component p will be a linear function of the intensity ratio Ip/Is (Klug and Alexander, 1974, p. 537). Thus, we can rewrite our equation as :

$$W_p = K_p \cdot \frac{I_p}{I_s}$$

For a mixture m of components p, q, r ..., the total weight fractions of all Fe oxide components, W_m will be the summation of W_p, W_q, W_r, ... or

$$W_m = K_p \cdot \frac{I_p}{I_s} + K_q \cdot \frac{I_q}{I_s} + K_r \cdot \frac{I_r}{I_s} + \ldots$$

The total of all Fe oxide components W_m can also be estimated from chemical analysis (DCB). The peak intensities of each iron oxide component can be easily obtained in the DXRD patterns of the samples and the intensity of the internal standard peak can be obtained from the diffraction pattern of the untreated sample. So, the only unknown elements of the equation will be the K factors. K can be expressed as:

$$K = A \times f,$$

where f is the weight fraction of Fe in a specific mineral and A is the coefficient that relates the amount of that mineral to its peak intensity ratio (I/Is). It accounts for the nature of the component and the particular reflection used. As an illustration, consider a goethite with $\underline{x}$ mole fraction of Al-substitution in the structure $(Fe_{1-x}, Al_x)OOH$. The f factor will be:

$$f_{Gt} = \frac{55.8(1-x)}{55.8(1-x)+27.0x+33.006}$$

Similar factors can be calculated for hematite and maghemite.

$$f_{Hm} = \frac{55.8(1-x)}{55.8(1-x)+27.0x+24.0}$$

$$f_{Mh} = \frac{55.8(1-x)}{55.8(1-x)+27.0x+24.0}$$

For maghemite, x was assumed to equal zero.

The $\underline{A}$ coefficient can be obtained by a linear regression analysis. For example, in the clay system studied, the iron oxides present were

goethite, hematite and maghemite, so the equation for the multiple regression was:

$$Fe_d = A \cdot f_{Gt} \cdot \frac{I_{Gt_{110}}}{I_{S_{113}}} + B \cdot f_{Hm} \cdot \frac{I_{Hm_{012}}}{I_{S_{113}}} + C \cdot f_{Mh} \cdot \frac{I_{Mh_{220}}}{I_{S_{113}}}$$

where:

Fe_d = DCB-extractable iron

A, B, C, = regression coefficients for goethite, hematite and maghemite, respectively.

f_{Gt} = Fe-goethite factor

f_{Hm} = Fe-hematite factor

f_{Mh} = Fe-maghemite factor

$I_{Gt_{110}}$ = intensity of the (110) line at 0.418 nm for goethite

$I_{Hm_{012}}$ = intensity of the (220) line at 0.367 nm for hematite

$I_{S_{113}}$ = intensity of the (113) line at 0.2085 nm for α-Al_2O_3

The model was solved by a multiple linear regression analysis subprogram REGRESSION in the program package Statistical Package for the Social Sciences - SPSS (Vogelbech Computing Center, Northwestern University, Evanston, Illinois).

Magnetic characterization

Magnetic susceptibility was determined on the whole soil, total sand, silt, and clay fractions, using a double beam analytical balance with pans not attracted by the magnet (Matsusaka and Sherman, 1961; Oades and Townsend, 1963; Jones and Beavers, 1964; Resende, 1976). Ferrous ammonium sulfate, mercury tetrathiocyanatocobaltate and manganese chloride, which have known magnetic susceptibilities (Figgis and Lewis, 1965; Quickenden and Marshall, 1972; Weast, 1982), were used as standards.

Magnetic separation was done in an attempt to concentrate the magnetic minerals in the clay fraction using a device that, although not as sophisticated as the one used by Schulze and Dixon (1979), basically followed their ideas and procedures. The device consisted of a Pyrex glass tube, 7.0 cm i.d. by 8.5 cm o.d. by 10.0 cm long, containing approximately 1g of "fine" magnetic stainless steel wool (International Steel Wool Corp., Springfield, Ohio) occupying 8.0 cm of the length of the tube. The assembly was placed between two horseshoe permanent magnets (General model 370.6) using a wooden support (Figure 6). The steel wool was cleaned by soaking in carbon tetrachloride, then in soap solution, and then rinsing with deionized water. The inlet was connected by plastic tubing to a large funnel which served as a feed reservoir. The outlet was connected to a metering orifice made from a disposable pipet. The flow rate was adjusted to approximately 100

ml/min using a screw clamp and/or changing the hydraulic head by raising or lowering the funnel. During the separation procedure, the flow rate was kept constant by maintaining the level of the liquid at a level marked on the side of the funnel by constantly adding more solution. The solution draining from the orifice, after passing through the steel wool was collected in a beaker. After the clay suspension had been passed through the filter 5 times, the magnets were removed and the magnetic fraction was flushed out. After the filter was cleaned the tailings were passed through the filter one additional time to make sure all the magnetic material had been trapped. After the separation, oriented slides were prepared from both the magnetic fraction and the tailings, and x-ray diffraction patterns were obtained.

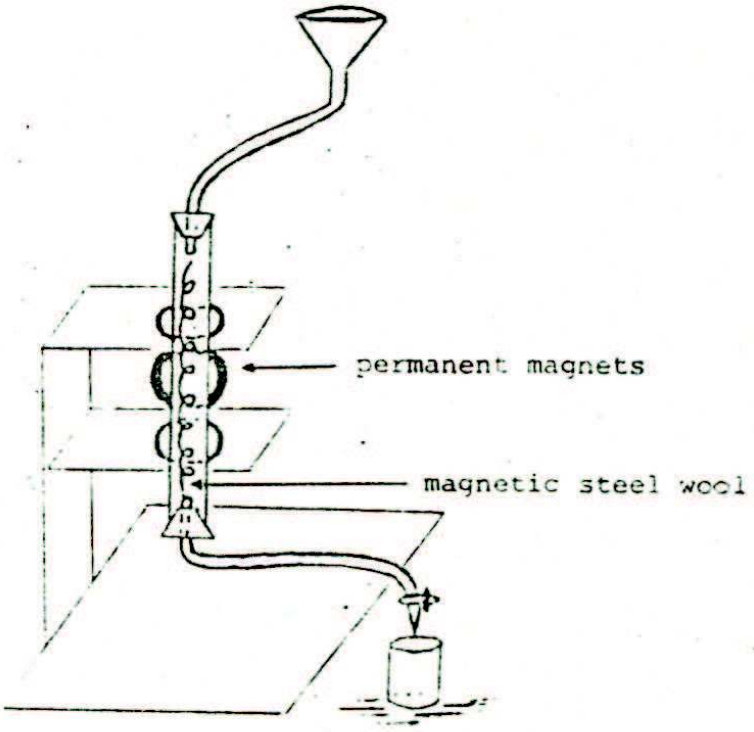

Figure 6. Schematic representation of the magnetic separator device.

RESULTS AND DISCUSSION

Morphology

Dark red colors predominate and are uniform throughout the control section (2.00 m for Oxisols), an exception being profile F1 where somewhat brownish colors predominate and mottling starts at 0.70 m depth (Table 4). The position at profiles in the landscape is shown in Figure 7 which is based on an instrumental survey. In the lower landscape positions brownish and reddish mottles were observed in the wettest portions of the profiles. There are also some black spots and gray mottles (chroma 2 or less) (Figure 7). This type of mottling is associated with short periods of saturation and periods of several months in which the horizon is close to saturation (Veneman et al., 1976). The development of mottled coloration is generally accepted as the result of seasonal fluctuations of water tables. A perched water table, supplied by rainfall with dissolved oxygen, may seasonally develop. The zone through which the water table frequently fluctuates is well enough aerated most of the growing season to provide conditions for vigorous root growth. Roots growing in this zone, through exudates and their own biomass, provide organic matter as an energy source of microorganisms.

Table 4. Soil profile description.

Layer	Depth	Moist Soil Color		Observations
		Matrix	Mottles	
	--m--			
			Profile F9 (Summit position)	
1	0-0.20	10R3/3		Sampling depth limited by concretions up to 1 cm diameter in layer 6
2	0.20-0.70	10R3/3		
4	1.20-1.70	10R3/4		
5	1.70-2.40	10R3/4		
6	2.40-2.60	10R3/4		
			Profile F8 (Shoulder position)	
1	0-0.20	1.5A3/3		Few concretions up to 1 cm diameter at layer 6, but high amount in layer 7 limiting the sampling depth
2	0.20-0.70	1.5R3/4		
3	0.70-1.20	1.5R3/4		
4	1.20-1.70	1.5R3/4		
5	1.70-2.20	1.5R3/4		
6	2.20-2.60	1.5R3/4		
7	2.60-2.70	1.5R3/4		

Table 4 (Cont.)

Layer	Depth	Moist Soil Color		Observations
		Matrix	Mottles	
			Profile F7.5 (Backslope position)	
1	0-0.60	2.5YR3/4		Some concretions up to
2	0.60-1.00	2.5YR3/4		1 cm diameter in layer
3	1.00-1.60	2.5YR3/4		5 increasing to high
4	1.60-2.00	2.5YR3/4		amount in layer 6
5	2.00-2.40	2.5YR3/4		where the concretions
6	2.40-2.60	2.5TY3/4		limited further digging.
			Profile F7 (Backslope position)	
1	0-0.25	2.5YR3/4		Concretions up to 1 cm
2	0.25- .60	2.5YR3/4		diameter limited further
3	0.60-1.20	2.5YR3/4		digging in layer 6.
4	1.20-1.70	2.5YR3/4		
5	1.70-2.20	2.5YR3/4		
6	2.20-2.50	2.5YR3/4		

Table 4 (Cont.)

Layer	Depth	Moist Soil Color		Observations
		Matrix	Mottles	
			Profile F6 (Footslope position)	
1	0-0.25	2.5YR3/4		No concretions
2	0.25-0.60	2.5YR3/6		
3	0.60-1.20	2.5YR3/6		
4	1.20-1.70	2.5YR3/6		
5	1.70-2.20	2.5YR3/6		
6	2.20-2.70	2.5YR3/6		
7	2.70-3.20	2.5YR3/6		
			Profile F5 (Footslope position)	
1	0-0.25	2.5YR3/4		No concretions
2	0.25-0.60	2.5YR3/4		
3	0.60-1.20	2.5YR3/6		
4	1.20-1.70	2.5YR3/6		
5	1.70-2.20	2.5YR3/6		
6	2.20-2.70	2.5YR3/6		
7	2.70-3.10	2.5YR3/6		
8	3.10-3.20	2.5YR3/6		

Table 4 (Cont.)

Layer	Depth	Moist Soil Color		Observations
		Matrix	Mottles	
			Profile F4 (Footslope position)	
1	0-0.25	2.5YR3/4		Few iron and manganese concretions smaller than 1 cm diameter in layer 6.
2	0.25-0.60	2.5YR3/5		
3	0.60-1.20	2.5YR3/6		
4	1.20-1.75	2.5YR3/6		
5	1.75-2.30	2.5YR3/6		
6	2.30-2.70	2.5YR3/6	f black (N), f 10YR7/2	
7	2.70-2.95	7.5YR5/6	c 10YR4/6, f 10YR7/2	
8	2.95-3.20	7.5YR5/6	c 10YR4/6, c 10YR7/2	
			Profile F3 (Footslope position)	
1	0-0.20	2.5YR3/4		Few iron and manganese concretions smaller than 1 cm diameter in layers 5 and 6. Manganese stain in layer 7.
2	0.20-0.60	2.5YR3/4		
3	0.60-1.20	2.5YR3/6		
4	1.20-2.10	2.5YR3/6		
5	2.10-2.30	2.5YR3/6		
6	2.30-2.40	7.5YR5/8	c 2.5YR3/6	
7	2.40-2.90	7.5YR5/8	c 10R5/6	
8	2.90-3.10	7.5YR5/8	c 10R5/6, c 7.5Y7/2	
9	3.10-3.20	7.5YR5/6	c 10R5/6	

Table 4 (Cont.)

Layer	Depth	Moist Soil Color		Observations
		Matrix	Mottles	
			Profile F2 (Footslope position)	
1	0-0.20	2.5YR3/4		Some iron concretions smaller than 1 cm diameter in layer 6 and decreasing throughout layers 7 and 8.
2	0.20-0.60	2.5YR3/4		
3	0.60-1.20	2.5YR3/6		
4	1.20-1.50	2.5YR3/6.5		
5	1.50-2.60	2.5YR3/6	m 7.5YR4/6	
6	2.60-2.70	2.5YR3/6		
7	2.70-2.90	5YR3/6	c 10R6/8, f 2.5YR3/6	
8	2.90-3.20	10YR5/6	m 2.5YR6/4, c 7.5YR5/8, f 10R3/6	
			Profile F1 (Footslope position)	
1	0-0.20	5YR3/4		
2	0.20-0.60	7.5YR4/6		
3	0.60-0.70	variegated	7.5YR4/6+5YR5/8	
4	0.70-1.00	7.5YR4/6	m 7.5YR5/8, c 10YR5/1	
5	1.00-1.50	5YR3/4	c 7.5YR5/8, c 10YR5/1	
6	1.50-2.30	5YR3/4	c 7.5YR5/8, f 2.5YR5/8	
7	2.30-2.90	5YR3/4		
8	2.90-3.20	5YR3/4	m 2.5YR3/6	

Abbreviations used: m = many, c = common, f = few

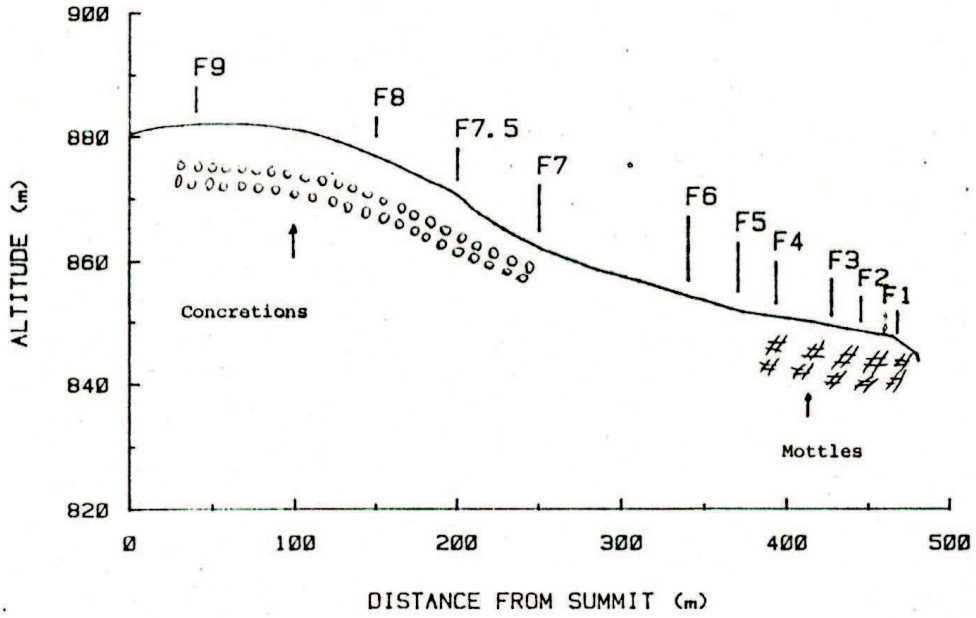

Figure 7. Schematic representation of the profiles in the toposequence sampled indicating the area with concretions and the area with mottles.

When this zone is saturated with water, atmospheric oxygen is excluded and first aerobic microbes consume the remaining dissolved oxygen and then anaerobic organisms dehydrogenate (oxidize) organic matter and donate electrons to reduce NO_3^-, Mn^{3+}, Fe^{3+}, SO_4^{2-}, or other oxidized systems (Jenny, 1980). Manganese compounds are reduced at a higher redox potential than iron compounds. Reduced iron and manganese compounds move with the water in the soil and may be leached from the soil, or may oxidize and immobilize in cutans or nodules when requisite redox potentials occur. These water tables are only temporary and when they disappear the complexing organic ions are biodegraded and the iron and manganese reoxidized. Iron compounds are oxidized at lower redox potentials than are those of manganese (Veneman et al., 1976). Black mottles are assumed to contain iron and manganese, brownish and reddish soil colors are largely from Fe^{3+} oxide minerals, and grayish, greenish, and bluish colors are from soil materials that have lost most of their free Fe oxides or from clay minerals containing Fe^{2+} (Franzmeier et al., 1983). Gray bodies with chromas of two or less develop in the part of the profile subjected to prolonged saturation. Under these conditions, iron and manganese compounds are both leached from the horizon.

Dark brown and black concretions up to 1 cm diameter make up a few percent of the soil were identified at a depth of 1.70 to 2.60 m in most profiles (Figure 6), suggesting a concretion layer uniformly distributed in the upper portion of the landscape and parallel to the ground

surface. Ollier (1959) pointed out that this kind of occurrence is common in Uganda. According to Ollier ironstone concretions are formed by iron enrichment of certain layers in the soil profile and occur in regions with well marked wet and dry seasons. Iron is leached from upper layers of the soil in the wet season, carried both downslope and down the profile, and redeposited at depths when the soil dries. The maximum concentration takes place where the drainage changes, and this normally coincides approximately with the stone line (Ollier, 1959). According to Duchaufour (1982), in an acid environment water containing organic matter circulates laterally and mobilises and transports the iron oxides which move down slope and, by precipitation and crystallization, give rise to a marked accumulation of concretionary ironstone. McFarlane (1976) sees ironstone concretion layer formation associated with an oscillating water table, presumably a water table lowering in response to renewed land surface incision. The precipitation of Fe-rich materials in voids accumulates as an increasingly thick layer in the lower parts of the soil. When down wasting ceases, the water table stabilizes, the residuum is hydrated and a massive variety of ironstone forms. There are still many questions concerning the formation of ironstone concretion layers and, as MacFarlane (1976) concludes, a closer study relating ironstone concretions and land surfaces should make a positive contribution to an understanding of land surface evolution in the tropics.

Mineralogy

Clay mineralogy

Mica, kaolinite, gibbsite, anatase and a 1.4 nm mineral are the dominant clay minerals (Figures 8 and 9). In most cases, the 0.352 nm anatase peak could not be resolved from the 0.357 nm kaolinite peak until the kaolinite peak was destroyed by heating at 550°C (Figure 10). The 1.4 nm mineral did not expand with Mg-saturation and glycerol solvation and did not collapse on K-saturation and air-drying (Figure 10). Subsequent heating at 550°C of K-saturated clays resulted in a gradual shift of the 1.4 nm reflection toward 1.0 nm. This mineral was identified as hydroxy-interlayered vermiculite-HIV (Rich, 1960, Barnhisel, 1977).

Quantitative data for the clay minerals obtained by DTA (kaolinite and gibbsite), total K content (mica) and relative intensity of XRD peaks (HIV and anatase) are shown in Table 5. The distribution of the clay minerals in the landscape is shown in Figure 11. Mica content increases from summit to footslope positions and also increases with profile depth. Kaolinite content also increases with profile depth and decreases in an irregular fashion from upper to lower landscape positions. Gibbsite and anatase contents decrease from summit to footslope positions and also decrease with profile depth. HIV content also decreases with profile depth; however, it shows no clear trend in relation to landscape positions.

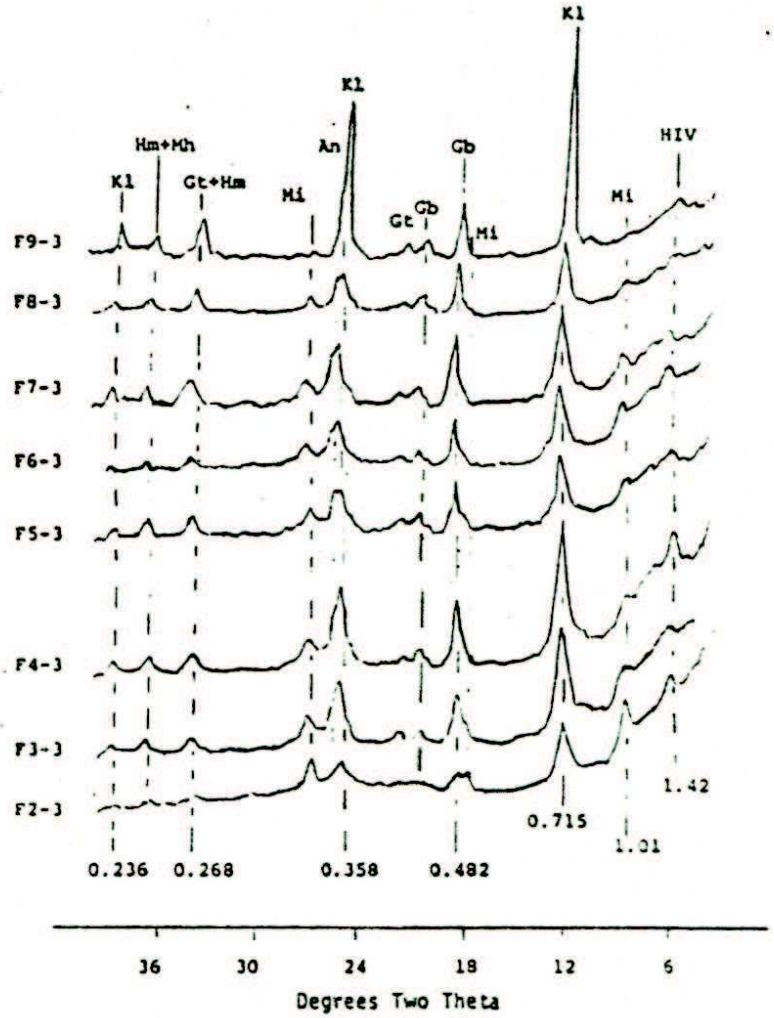

Figure 8. X-ray diffractograms of the NaOH dispersed clay fraction of samples taken at 1 m depth. Units of d-spacing are in nanometers. Kl=kaolinite; Hm=hematite; Mh=maghemite; Gt=goethite; Mi=mica; An=anatase; Gb=gibbsite; HIV=hydroxy interlayered vermiculite.

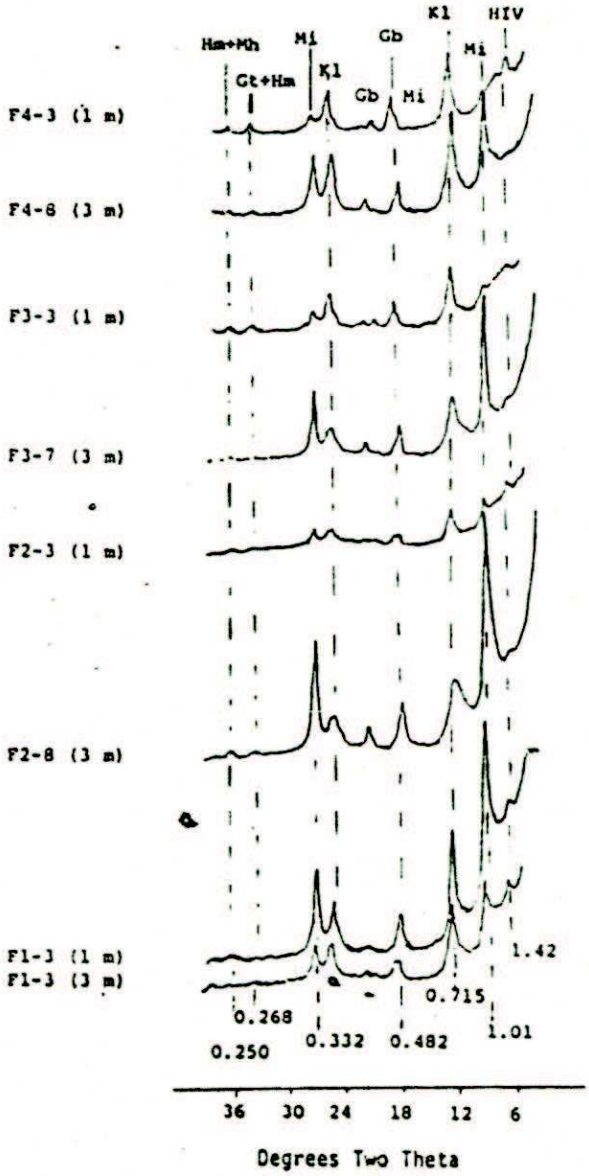

Figure 9. X-ray diffractograms of the NaOH dispersed clay fraction of samples taken at two different depths. Units of d-spacing are in nanometers. Hm=hematite; Gt=goethite; Mi=mica; Kl=kaolinite; Gb=gibbsite; HIV=hydroxy interlayered vermiculite.

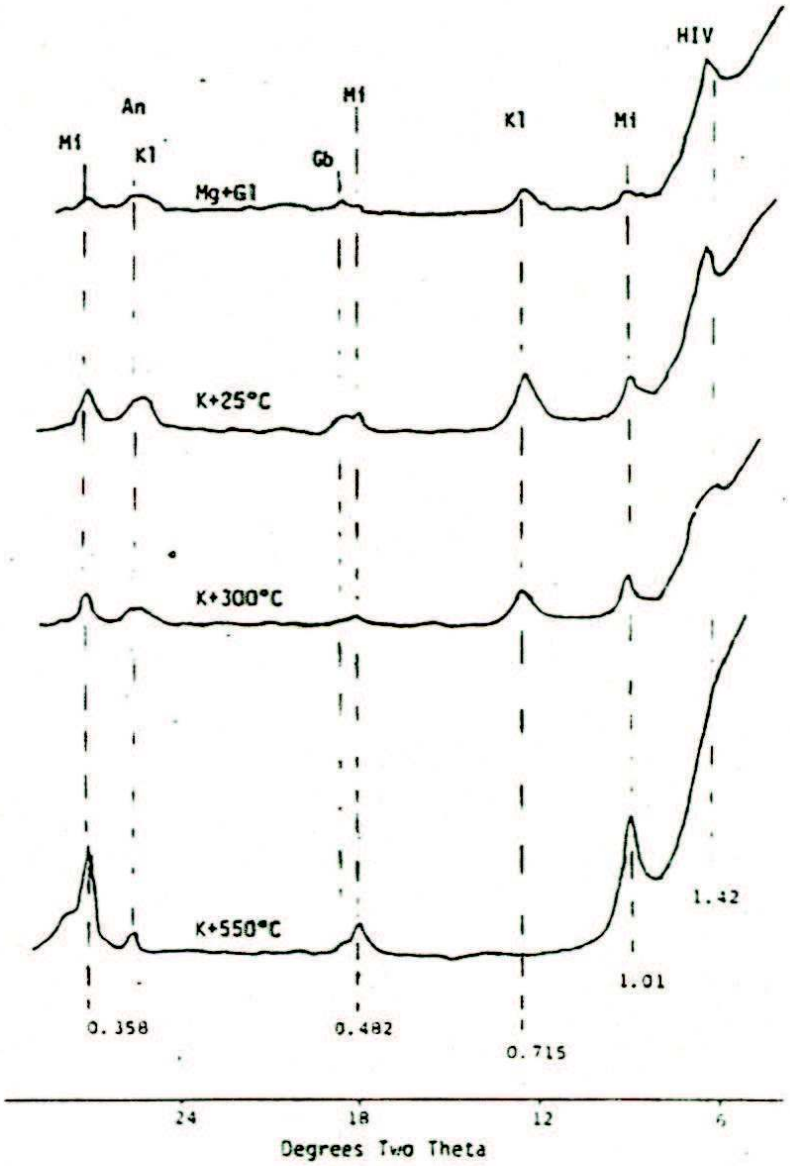

Figure 10. X-ray diffractograms of the clay fraction of sample F2-3 (1 m depth) after Mg saturation and glycerol solvation (Mg+Gl), K saturation at room temperature (K+25°C), heating at 300°C (K+300°C), and heating at 550°C (K+550°C). Units of d=spacing are in nanometers. Mi=mica; An=anatase; Kl=kaolinite; HIV=hydroxy interlayered vermiculite.

Table 5. Content of mica, kaolinite, and gibbsite and relative intensity of hydroxy-interlayered vermiculite (HIV), and anatase XRD peaks.

Soil Sample	Mica	Kaolinite	Gibbsite	HIV	Anatase
	%			I[1/]	
F9-3	1	37	21	4	10
F8-3	10	27	24	3	9
F7.5-3	13	27	21	4	7
F7-3	13	25	19	3	6
F6-3	15	24	17	5	5
F5-3	15	26	17	4	5
F4-3	15	26	16	10	5
F4-8*	34	38	2	1	5
F3-3	19	22	9	4	5
F3-7*	25	32	2	2	4
F2-3	21	21	6	3	5
F2-8*	49	35	1	1	2
F1-3	32	25	1	8	4
F1-8*	26	29	5	4	4

* Samples taken at 3m depth; the others at 1m depth.

1/ Intensities normalized so that the most intense peak has a value of 10.

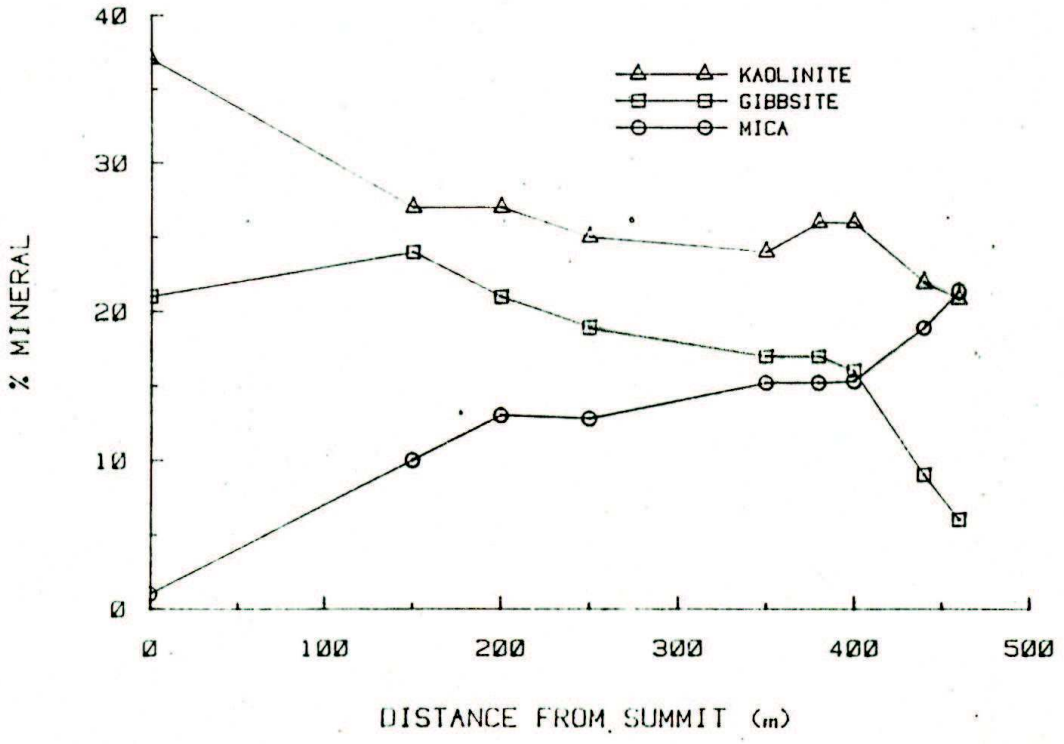

Figure 11. Distribution of the clay minerals at 1 m depth in the landscape.

The landscape trends show essentially that as the weathering intensity increases (from footslope toward summit position) mica content decreases while gibbsite increases. The increase of the mica/gibbsite ratio downslope (Figure 12) suggests that downslope movement of Si or preferential removal of Si from upper slope positions controls the weathering and formation of clay minerals in the landscape. Higher concentration and larger crystal size of mica in lower slope positions have been attributed to a low rate of decomposition of silicate minerals and low loss of Si from the system associated with a wetter environment (Almeida, 1979). The adsorption of Si by Fe oxyhydroxides (McKeague and Cline, 1963) could also contribute to a decrease in the amount of silica in solution in the upper slope positions which have higher Fe content. Similar correlations between iron oxide content and gibbsite content have been reported for some other Brazilian Oxisols (Resende, 1976; Curi, 1983).

Trends with profile depth show that mica and kaolinite contents decrease with increasing weathering intensity (decreasing profile depth) while HIV and gibbsite increase. Kaolinite could weather to gibbsite liberating Si, much of which is lost from the system. Some Al could be incorporated into the vermiculite structure which formed from weathering of mica to form HIV. Under those conditions HIV is resistant to further weathering and would be in a stage of weathering closely related to gibbsite as suggested by Rauen (1980) in a toposequence of soils from basaltic rocks in southern Brazil.

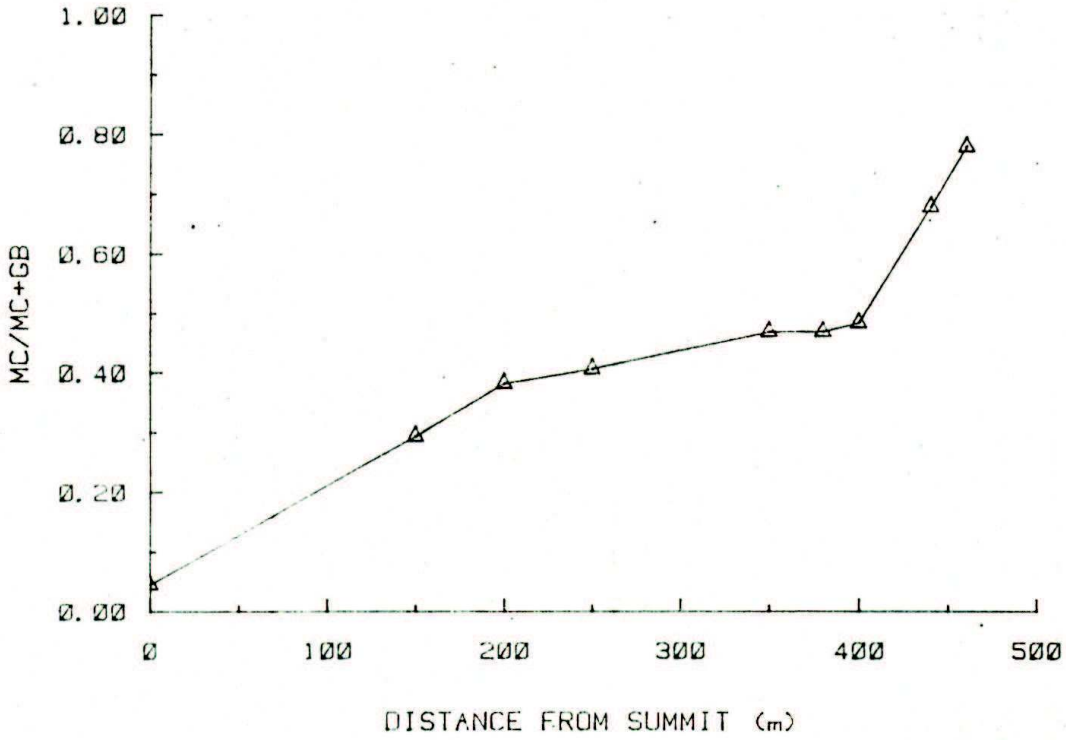

Figure 12. Mica/mica + gibbsite ratio in relation to landscape position.

In general, titanium oxide has been considered to be highly stable so it can be used to judge the degree of weathering of other minerals and the uniformity of parent materials (Hutton, 1977). The steady decrease of anatase content at 1 m depth downslope (Table 5) indicates that soils on upper slope positions are more highly weathered than those on lower slope positions.

For several minerals, the data indicate that profile F1 (samples F1-3 and F1-8 in Table 5) shows different relationships with depth from the other profiles. This profile seems to be on a different landscape surface (see Field Methods section).

Iron Oxides

The iron oxides present in these soils are well crystallized as indicated by the low values for the Fe_o/Fe_d radios (all smaller than 0.01) (Table 6). In most samples the first DCB extraction (Fe_{d1}) was able to extract around 94 to 98.2% of the total DCB-extractable iron (Fe_{d2}). For Al, the first extraction (Al_{d1}) presented a wider range: 75 to 95% of the total DCB-extractable aluminum (Al_{d2}). The ratio of the Fe removed in the first extraction to the total Fe removed is larger for the yellower members than for the redder ones (having larger Fe content and larger hematite/goethite ratios) which agree with Curi (1983) finding.

Goethite, hematite and maghemite are the dominant iron oxides (Figures 13 and 14). Goethite is always present, hematite is absent or virtually so in the deeper samples and maghemite is absent in the deeper samples and also in the upper samples of the footslope position.

Table 6. Oxalate-extractable iron (Fe_0) and DCB-extractable iron (Fe_d) and aluminum (Al_d) contents of the clay samples. (Fe_{d_2} and Al_{d_2} represent the total of the first and second extractions).

Sample no.	Fe_0	Fe_d		Al_d	
		Fe_{d_1}	Fe_{d_2}	Al_{d_1}	Al_{d_2}
	% (wt/wt)				
F9-3	0	13.1	14.3	0.9	1.1
F8-3	0	13.5	14.3	1.0	1.2
F7.5-3	0	12.6	13.3	1.1	1.2
F7-3	0.01	12.0	12.7	1.2	1.3
F6-3	0	10.5	11.0	1.1	1.2
F5-3	0	10.8	11.1	1.2	1.3
F4-3	0	10.8	11.2	1.2	1.3
F4-8*	0.03	7.5	7.9	1.0	1.0
F3-3	0.02	10.5	10.7	1.2	1.3
F3-7*	0.03	4.5	4.5	0.7	0.7
F2-3	0.03	8.3	8.5	1.1	1.2
F2-8*	0.05	5.7	5.8	0.9	1.0
F1-3	0.04	4.8	4.9	0.8	0.9
F1-8*	0.04	4.8	4.9	0.9	1.0

*Samples taken at 3m depth; the others at 1 m depth.

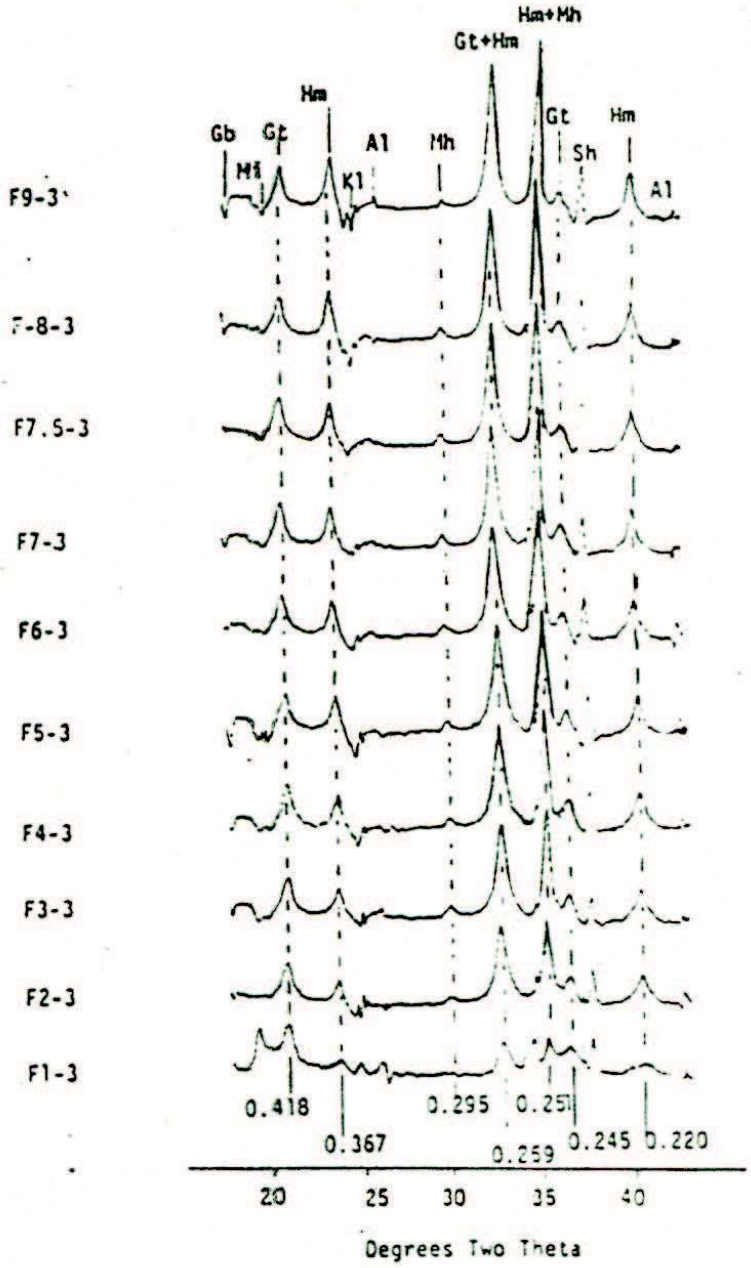

Figure 13. DXRD patterns of the clay fraction of samples taken at 1 m depth. Units for d-spacings are in nanometers; Gb=gibbsite; Mi=mica; Gt=goethite; Hm=hematite; Kl=kaolinite; Al=α-Al_2O_3. Mh=maghemite; Sh=Al metal from sample holder.

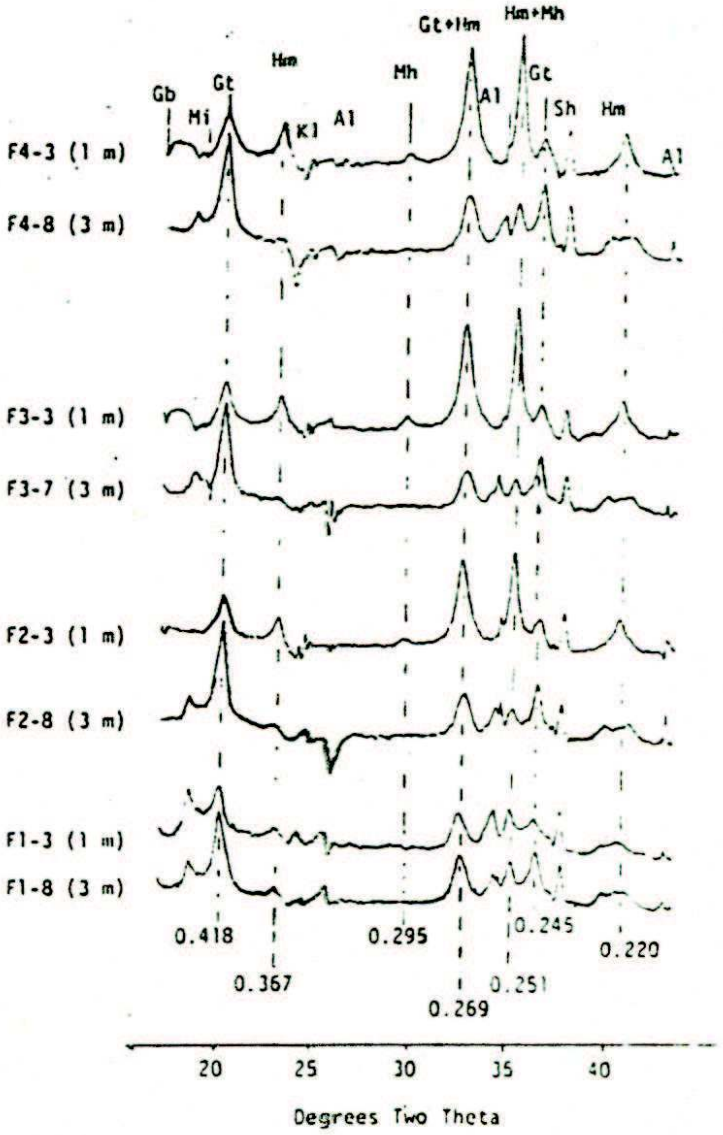

Figure 14. DXRD patterns of the clay fraction of 4 profiles with two different depths. Units of d-spacing are in nanometers. Gb=gibbsite; Mi=mica; Gt=goethite; Hm=hematite; Kl=kaolinite; Al=γ-Al_2O_3; Mh=maghemite; Sh=Al metal from sample holder.

Samples F3-7 and F2-8 at first glance (Figure 14) appear to contain only goethite. On the other hand, the colors of the clay fraction (Table 15) are 7.5YR5/6 and 5YR4/8 for samples F3-7 and F2-8, respectively, which indicate at least small amounts of hematite (Schwertmann et al., 1982). One of the problems in identifying hematite by XRD, however, is that its (104) peak with a relative intensity of 100 and the goethite (130) peak with a relative intensity of 30 both have spacing of 0.269 nm. If, however, for pure goethite the ratio I_{111}/I_{130} is known, it is possible to estimate the contribution of goethite to the 0.269 nm peak from a measurement of the intensity of the 0.245 nm peak. This ratio ranges from 1.8 to 2.2 for pure goethite (Schulze, 1982). Thus, smaller ratios in a mixed system indicate increasing amounts of hematite. This ratio is 0.799 in sample F3-7 and it is 0.978 in sample F2-8, respectively, suggesting the presence of hematite in these samples even though the diagnostic hematite (110) peak cannot be seen. Thus, all samples appear to contain some hematite.

A few samples of fine clay were run to compare with total clay. For one sample, F3-7, there seems to be a small effect of hematite concentration since the characteristic (012) peak at 0.367 nm for hematite does not show up in the total clay but it does show a small hump in the fine clay (Figure 15). Besides that, no other differences due to size of the fraction analyzed were noticed.

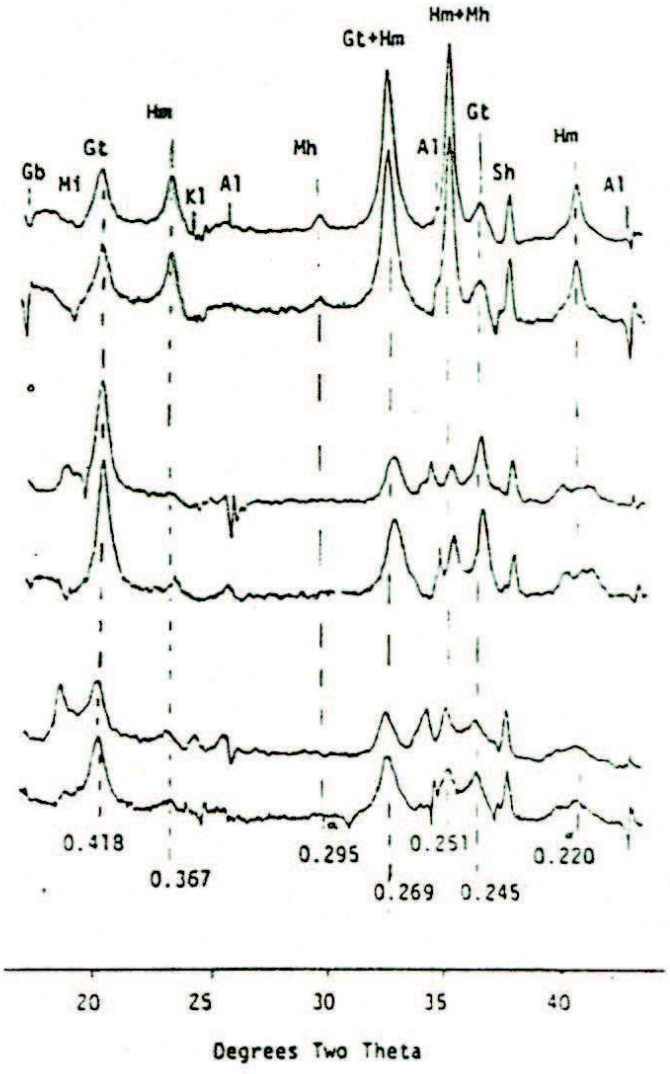

Figure 15. DXRD patterns for total clay and fine clay fractions of three profiles. Units for d-spacings are in nanometers. Gb=gibbsite; Mi=mica; Gt=goethite; Hm=hematite; Kl=kaolinite; Al=α-Al_2O_3; Mh=magnemite; Sh=Al metal from sample holder.

Al substitution is mainly between 11 and 14 mole % for goethite and is zero for hematite (Table 7). This range of Al substitution in goethite is the same as data for soils from Australia (Davey et al. 1975) and smaller than some reported data of Brazilian Oxisols (Resende, 1976; Bigham et al. 1978, Resende, 1980; Curi, 1983). The degree of Al-substitution of goethites may reflect the environment in which they have formed and serve as an indicator of soil-forming processes. Fitzpatrick and Schwertmann (1982) reported that in strongly weathered, non-hydromorphic and more acid conditions, the activity of Al is increased because of the low pH and consequently there is an increasing availability of Al to be incorporated into the goethite structure as it forms. This isomorphous substitution of Al for Fe may also account for the high stability of goethite, possibly by releasing structural strain.

The mean crystallite dimension (Table 7) for goethite is smaller than for hematite and maghemite.

Goethite increases slightly from summit to footslope positions (Figure 16) but increases sharply with profile depth (Table 8). Hematite has the opposite trend; it decreases from upper slope positions to lower slope positions and also decreases with profile depth. Maghemite is absent in the deeper horizons and in all the lower landscape positions, and it is about constant from backslope to summit position.

As soil color becomes redder, DCB extractable Fe increases, similar to previous reports (Schwertmann and Taylor, 1977; Bigham et al., 1978; Torrent et al., 1980; Curi, 1983). Apparently in the wetter conditions

Table 7. Crystallographic parameters, Al-substitution and mean crystallite dimension of goethite and hematite.

Sample	Goethite			Hematite	Al sub.		Mean Crystallite Dimension[3]				
	d_{111}	d_{110}	c	a	Gt[1]	Hm[2]	$Gt_{(110)}$	$Gt_{(111)}$	$Hm_{(012)}$	$Hm_{(113)}$	$Hm_{(110)}$
	nm				mole %		nm				
F9-3	.2442	.4197	.3000	.5051	12	0	26	19	28	23	36
F8-3	.2441	.4197	.3000	.5045	13	0	20	13	30	22	35
F7,5-3	.2440	.4195	.3000	.5060	14	0	18	16	24	24	29
F7-3	.2440	.4195	.3000	.5044	14	0	18	16	24	23	30
F6-3	.2440	.4195	.2999	.5047	14	0	18	18	26	21	29
F5-3	.2440	.4197	.2999	.5043	14	0	18	19	23	20	27
F4-3	.2440	.4195	.3000	.5043	14	0	16	19	24	17	28
F4-8*	.2444	.4201	.3000	-	12	0	18	18	-	-	16
F3-3	.2441	.4197	.3000	.5041	13	0	17	17	20	16	26
F3-7*	.2444	.4203	.3000	-	12	0	18	19	-	-	19
F2-3	.2440	.4195	.3000	.5041	14	0	16	17	24	15	21
F2-8*	.2440	.4195	.3000	.5041	14	0	18	20	-	-	19
F1-3	.2445	.4205	.3000	.5048	11	0	13	13	-	-	20
F1-8*	.2440	.4197	.2999	.5022	14	0	17	15	-	-	16

Al sub. = Al substitution

[1] after Schulze (1982)
[2] after Schwertmann et al., 1979
[3] Scherrer equation (Klug and Alexander, 1974)
*Samples taken at 3m depth; the others at 1m depth.

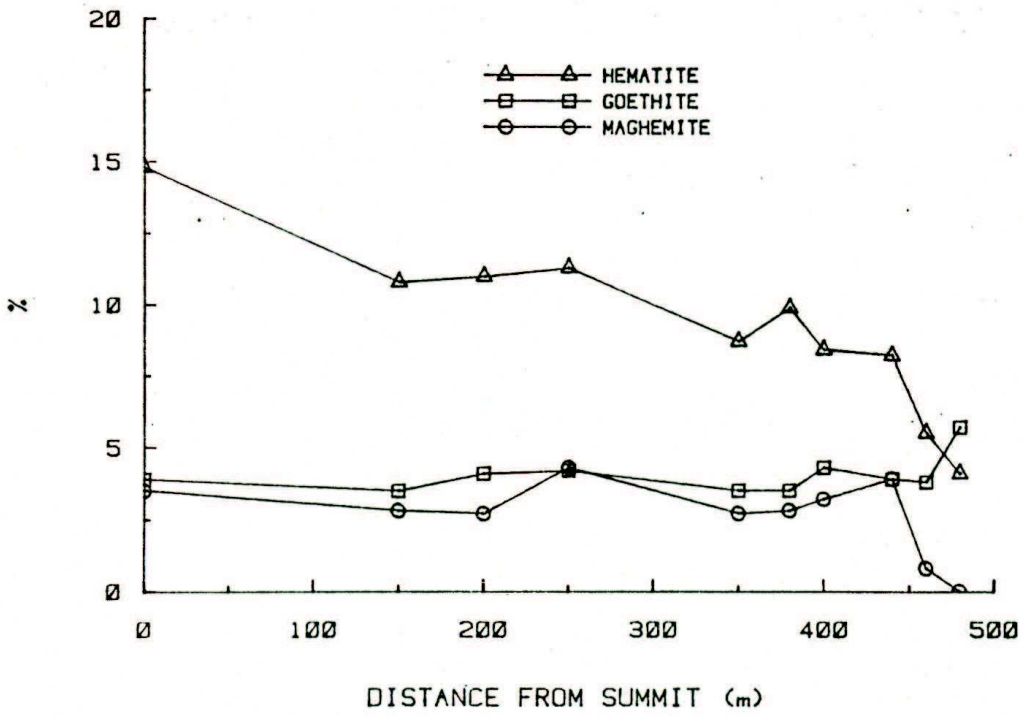

Figure 16. Distribution of iron oxides minerals at 1 m depth in the landscape.

Table 8. Soil color, DCB-extractable iron and quantitative data for goethite, hematite and maghemite.

Sample	Depth	Color	Fed	Gt	Hm	Mh
	- m -		- - - - - % (wt/wt) - - - - -			
F9.3	0.70-1.20	10R3/4	13.1	3.9	14.8	3.5
F8.3	0.70-1.20	1.5R3/4	13.5	3.5	10.8	2.8
F7.5-3	0.60-1.20	2.5YR3/4	12.6	4.1	11.0	2.7
F7.3	0.60-1.20	2.5YR3/4	12.0	4.2	11.3	4.3
F6.3	0.60-1.20	2.5YR3/6	10.5	3.5	8.7	2.7
F5.3	0.60-1.20	2.5YR3/6	10.8	3.5	9.9	2.8
F4.3	0.60-1.20	2.5YR3/6	10.8	4.3	8.4	3.2
F4.8*	2.95-3.20	7.5YR5/6 + mottles	7.5	12.4	0	0
F3.3	0.60-1.20	2.5YR3/6	10.5	3.9	8.2	3.9
F3.7*	2.40-2.90	7.5YR5/8 + mottles	4.5	8.2	0	0
F2.3	0.60-1.20	2.5YR3/6	8.3	3.8	5.5	0.8
F2.8*	2.90-3.20	10YR5/6 + mottles	5.7	9.5	2.6	0
F1.3	0.60-1.00	7.5YR4/6 + mottles	4.8	5.7	4.1	0
F1.8*	2.90-3.20	5YR3/4 + mottles	4.8	7.1	1.1	0

*Samples taken at 3m depth; the others at 1m depth.

(lower slope positions and deeper horizons) goethite formation is favored relative to hematite formation. These environmental conditions probably inhibit hematite formation through Fe complexation by organic compounds and prevent the formation of ferrihydrite and thus hematite, so goethite forms instead of hematite (Schwertmann and Taylor, 1977). Furthermore, dryer conditions in the upper landscape positions may favor hematite over goethite through higher redox potential and higher soil temperature which accelerates the turnover of organic matter yielding a higher Fe^{3+} concentration and favoring the dehydration of ferrihydrite to hematite (Kämpf and Schwertmann, 1983).

As quoted in the literature review there are four different ways in which maghemite can be formed: 1) by low temperature oxidation of magnetite present in rocks or in the soil; 2) as a result of burning; 3) by dehydration of lepidocrocite; and 4) via a reduction-oxidation cycle occurring under normal pedogenic conditions. Of the modes of formation, (1) refers to a situation in which a ferrimagnetic mineral is already present in the parent material, while (2) requires fire, and (3) and (4) require wet and dry cycles. Because of both the depth of occurrence of maghemite and its uniform content over a relative large area, it seems doubtful whether it can be ascribed to the cumulative effect of burning. The repeated reduction-oxidation cycles seems to be an unlikely method of forming maghemite in these soils because where they happen to occur, in the lower landscape positions, neither maghemite nor lepidocrocite is present. So, mode of formation (1) is likely to be the dominant mode of

formation and agrees with magnetite presence in the sand and silt fractions. The occurrence of pedogenic maghemite produced by weathering of magnetite was reported for Hawaiian soils (Matsusaka et al., 1965), a South African soil (Fitzpatrick and Le Roux, 1975), and it is probably more common than has been thought in soils derived from basic igneous parent material (Mullins, 1977). The absence of maghemite in lower landscape positions is probably related to the wetter environment that could be promoting dissolution of maghemite due to the more reducing conditions (Mullins, 1977).

DXRD Problems. In the DXRD method (Schulze, 1981) the diffraction pattern for iron oxide minerals in a sample is obtained by subtracting the pattern for a sample free of iron oxides from that of an untreated sample. The difference in overall intensities before and after dissolution treatment can be compensated for by multiplying all of the line intensities in the pattern from the treated sample by a scale factor that is less than unity before making the subtraction. The scale factor is found by making trial and error subtractions in an attempt to minimize silicate mineral peaks and a DXRD diagram essentially free of peaks due to minerals other than iron oxides is obtained. This approach relies on the assumption that the intensities of the silicate peaks are not affected by the treatment. However, as Schulze (1982) pointed out, it is difficult to correctly cancel out the quartz peaks in the differential diagram when the subtraction is made to cancel out the layer silicate peaks. In most cases the quartz peaks increase

in intensity relative to the peaks of other minerals after the dissolution treatment. The result is that the DXRD diagram contains "negative" diffraction peaks where quartz peaks occur. After considering several possible causes for the negative peaks, Schulze (1982) concluded that only coarse particle size and preferred orientation appear to be important factors in changing the relative intensities of minerals in a sample after selective dissolutions.

Bryant et al. (1983) used an internal standard to calculate the scale factor for the adjustment of intensity. They found negative peaks for quartz, gibbsite, and kaolinite, and they concluded that decreasing absorption of x-rays by iron oxide coatings seems to be the best explanation. Besides negative peaks they also found positive peaks that indicate that the intensity of the original peak is greater than the intensity of the treated subsample peak multiplied by the scale factor. They interpreted the positive peaks as evidence for partial dissolution of some silicate minerals by DCB treatment.

As shown in Figures 13, 14, and 15 there are negative peaks for gibbsite, kaolinite, and mica. It was noticed that it is possible to "create" positive peaks when trying to eliminate negative peaks by using different scale factors. In an attempt to quantify the iron oxides, two methods of calculating scale factors were tried: trial and error attempting to eliminate negative peaks and calculation based on the internal standard. The trial and error method gives an overall better-fitting pattern, and an easily drawn baseline. It can eliminate

or minimize negative peaks of silicate minerals, but it creates some positive peaks especially for the internal standard. The internal standard method gives negative peaks that can be explained, does not give positive peaks for the internal standard, and sometimes gives a pattern for which it is difficult to draw a baseline. The results showed that the two methods of interpretation had no effect for qualitative analysis, as expected, but they did have an effect on peak areas. However, the effect is on the pattern as a whole and because the internal standard approach relies on the relative contribution of each mineral peak area to the total iron oxide peak area (considered as equal to the DCB-extractable iron), the effect is not significant. The occurrence of negative peaks is still not well explained, but the DXRD technique proved once more its validity to identify and quantify iron oxides.

Physical and Chemical Properties

The clay fraction predominates in all profiles (Table 9). Figure 17 shows that the silt fraction is about constant, sand fraction decreases and the clay fraction increases from summit to footslope positions. There is no evidence that clay is moving in the soil profile suggesting a high order of stability or immobility of the clay fraction (Soil Survey Staff, 1975). Stability is further suggested by the very low values of water-dispersible clay in most profiles (Table 9). This

Table 9. Physical properties of the soil samples studied.

Soil Sample	Layer	Depth	Particle size distribution			Water dispersible clay	Flocculation degree[1]	Moisture retained at 15 bar pressure	Particle density
			Sand	Silt	Clay				
		- m -	% (wt/wt)						g/cm^3
F9	3	0.70-1.20	41	14	45	3	93	13.0	2.86
	5	1.10-2.40	42	14	44	9	79	13.5	2.98
F8	3	0.70-12.0	32	14	54	3	94	17.8	2.86
	5	1.70-2.40	31	13	56	9	84	18.6	2.94
F7.5	3	0.60-1.20	31	13	56	3	95	16.8	2.84
	5	1.70-2.20	31	14	55	5	91	18.2	2.92
F7	3	0.60-1.20	31	11	58	3	95	16.6	2.86
	5	1.70-2.20	32	12	56	3	93	18.6	2.90
F6	3	0.60-1.20	28	10	62	2	97	19.9	2.74
	5	1.70-2.20	27	10	63	3	95	21.4	2.94
F5	3	0.60-1.20	24	12	64	2	97	19.9	2.77
	5	1.70-2.20	24	13	63	2	97	21.0	2.86
F4	3	0.60-1.20	27	12	61	2	97	19.8	2.70
	8	2.95-3.20	26	17	57	2	97	22.9	2.82
F3	3	0.60-1.20	25	11	64	2	97	19.8	2.41
	7	2.40-2.90	37	19	44	54	23	24.6	2.78
F2	3	0.60-1.20	19	17	64	2	97	24.1	2.86
	8	2.90-3.20	23	28	49	24	51	25.2	2.86
F1	3	0.60-1.00	3	21	96	12	97	29.1	2.96
	8	2.90-3.20	21	15	64	57	11	21.6	2.70

[1] Flocculation degree = $\frac{\text{total clay-water dispersible clay}}{\text{total clay}}$

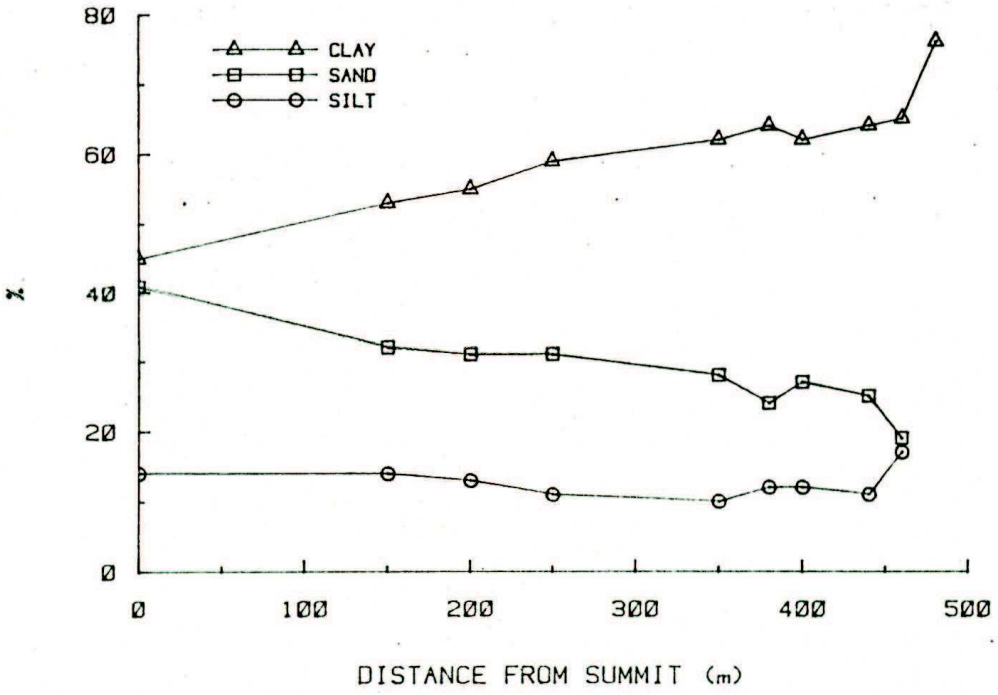

Figure 17. Particle size distribution at 1 m depth in the landscape.

low water dispersible clay value was found to be related to slightly negative or positive surface charge as expressed by ΔpH ($pH_{KCl} - pH_{H_2O}$) for some soils of São Paulo State, Brazil (Dematte et al., 1977). Figure 18 shows that for most profiles the ΔpH values are between -0.5 and +0.5, supporting Dematte's results. According to Uehara and Gillman (1981), ΔpH values in this range are indicative of soils with variable charge minerals.

Oxic horizons usually have silt- and sand-size aggregates of clay that are hard to get dispersed but that contribute to the exchange capacity. Soil Taxonomy (Soil Survey Staff, 1975) recommends the use of the amount of water retained at 15-bar to independently estimate the clay content. Soil Taxonomy states that the ratio, percent 15-bar water to percent clay, does not exceed 0.6 if the clay disperses well. Our data show ratios in the range 0.3 - 0.4, indicating that good dispersion occurred. Soil Taxonomy (p. 38) permits the use of the relationship:

Percent clay = 2.5 x 15-bar gravimetric water

to estimate clay content. Conversely, the relationship 15-bar water = 0.4 x % clay can be used to estimate 15-bar water content. Figure 19 shows that the soils studied hold less water per g of clay than predicted by the Soil Taxonomy relationship. Uehara and Gilman (1981) reported similar results for Brazilian soils studied by Leptsh and Buol (1974).

The values for particle density (Table 9) are similar to those reported for similar soils developed from basalt but are smaller than those derived from itabiritic rocks (Curi, 1983).

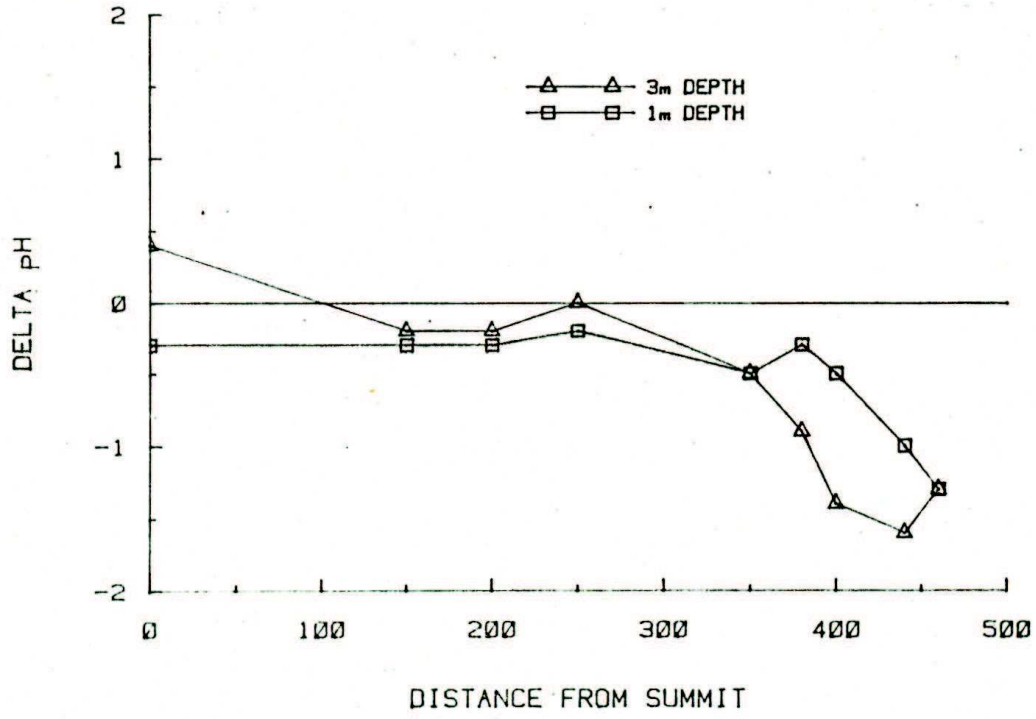

Figure 18. Delta pH ($\Delta pH = pH_{KCl} - pH_{H_2O}$) at two different depths according to landscape positions.

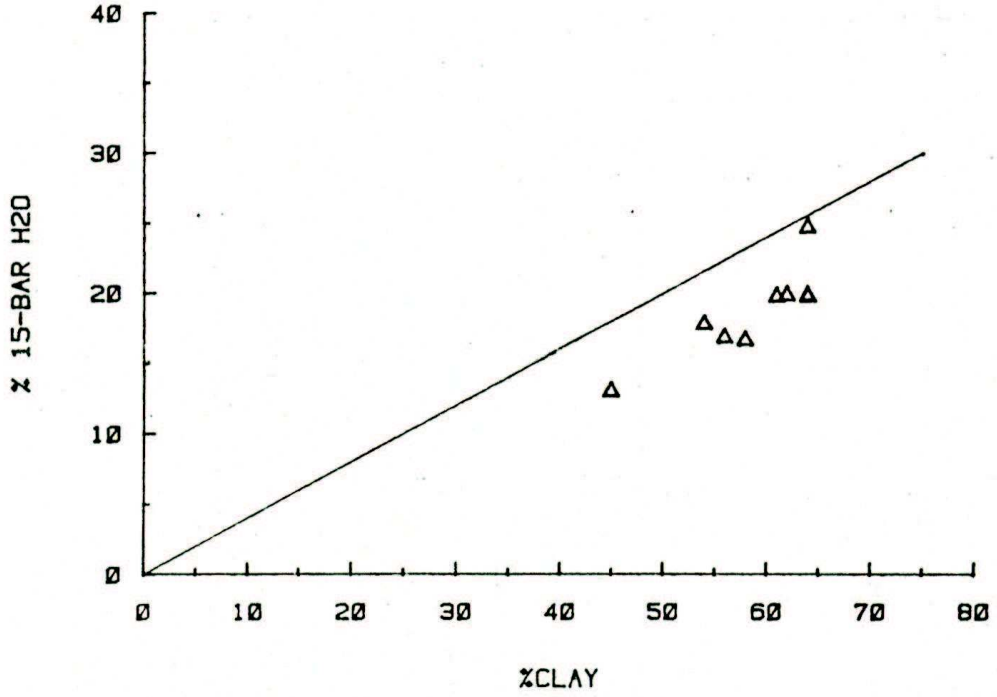

Figure 19. Correlation between clay content and water retained at 15 bar. The solid line indicates the estimate according to U.S.A. Soil Taxonomy.

It is evident by the chemical data (Table 10) that these soils are very much leached and weathered. The CEC and base saturation data increase from upper slope positions to lower slope positions and decrease with profile depth in most profiles. The landscape trend suggests lower weathering rates and a less leaching environment in the lower landscape positions. The profile trend could be associated with the vegetation through mineral recycling and organic matter source.

Sulphuric acid dissolution data is shown in Table 11 and Figure 20. This extractant is assumed to dissolve mainly the clay fraction. Fe and Ti decrease from summit to footslope positions and also decrease with profile depth. Si and Al increase toward downslope positions. Si also increases with profile depth, but Al decreases slightly or it is about constant. The Si/Ti ratio, Si/Fe ratio, and Si/Al ratio distribution in the landscape (Figure 21) emphasizes that loss of silica and relative accumulation of iron and titanium are mainly the result of an increase in weathering intensity. Figure 21 shows also that the CEC seems to correlate with the Si/Ti ratio trends in the landscape. This probably is due to more 2:1 minerals, that have higher CEC, downslope.

The (% Fe/% Clay) x 100 ratio (Figure 22) decreases from summit to footslope positions indicating a smaller association between Fe and clay fraction in the lower landscape positions. This could be related to the concept of the saturation point of clays for free iron (D'Hoore, 1954 in Eswaran and Sys, 1970), i.e., up to a certain iron concentration, the

Table 10. Chemical properties of the soil samples studied.

Soil Sample	Layer	Depth	pH (1:25)		Exchangeable Cations					CEC	BS	Org.C	Avail. P
			H2O	KCl 1M	Ca+Mg	K	Na	Al	H+Al				
		- m -			--------- c mol(p+) Kg^{-1} ----------						- %(wt/wt)-		µg/g
F9	3	0.70-1.20	5.5	5.2	0.2	0.02	0.01	0.1	2.6	2.8	7	0.38	1
	5	1.70-2.40	5.4	5.8	0.2	0.02	0.01	0.1	2.3	2.5	8	0.19	1
F8	3	0.70-1.20	5.5	5.2	0.2	0.06	0.02	0.1	3.0	3.3	9	0.40	1
	5	1.70-2.40	5.7	5.5	0.2	0.07	0.02	0.1	2.6	2.9	10	0.19	1
F7.5	3	0.60-1.20	5.3	5.0	0.3	0.14	0.02	0.1	3.1	3.6	14	0.49	1
	5	1.90-1.20	5.4	5.2	0.2	0.10	0.03	0.1	2.7	3.0	10	0.12	1
F7	3	0.60-1.20	5.0	4.8	0.4	0.23	0.05	0.1	3.3	4.0	18	0.58	1
	5	1.70-2.20	5.0	5.0	0.2	0.11	0.05	0.1	2.6	3.0	13	0.06	1
F6	3	0.60-1.20	4.9	4.4	0.6	0.078	0.02	0.7	4.9	5.6	13	0.45	1
	5	1.70-2.20	5.2	4.7	0.5	0.28	0.06	0.8	3.3	4.1	20	0.12	1
F5	3	0.60-1.20	4.8	4.5	0.4	0.09	0.02	0.5	3.9	4.4	11	0.45	1
	5	1.70-2.20	5.4	4.5	0.2	0.11	0.02	0.3	3.6	3.9	8	0.32	1
F4	3	0.60-1.20	5.0	4.5	0.7	0.09	0.02	0.6	4.3	5.1	16	0.38	1
	8	2.95-3.20	5.6	4.2	0.2	0.13	0.03	1.4	3.3	5.7	7	0.12	3
F3	3	0.60-1.20	5.9	4.9	3.8	0.11	0.02	0.1	3.9	7.8	50	0.38	1
	7	2.40-2.90	5.9	4.3	1.9	0.13	0.04	1.2	3.3	5.4	39	0.06	2
F2	3	0.60-1.20	5.7	4.4	3.1	0.26	0.05	0.7	5.9	9.3	37	0.64	3
	8	2.90-3.20	5.5	4.2	4.1	0.14	0.04	1.6	4.3	8.6	50	0.12	1
F1	3	0.60-1.00	5.8	4.3	7.7	0.31	0.08	0.6	4.9	13.0	62	0.32	2
	8	2.90-3.20	5.6	4.3	3.5	0.12	0.04	0.7	4.3	8.0	46	0.19	2

Table 11. Sulphuric acid dissolution data for the soil samples studied.

Soil Sample	Layer	Depth	Si	Al	Fe	Ti	P
		--m--	----------		% wt/wt		----------
F9	3	.70 - 1.20	3.4	8.2	16.2	2.19	.23
	5	1.70 - 2.40	3.7	8.2	16.2	1.70	.22
F8	3	.70 - 1.20	5.8	10.9	15.9	1.91	.14
	5	1.70 - 2.40	6.2	9.9	15.7	1.69	.20
F7.5	3	.60 - 1.20	5.8	11.0	15.5	1.68	.13
	5	1.70 - 2.20	6.3	9.5	14.7	1.44	.21
F7	3	.60 - 1.20	5.8	11.0	14.9	1.35	.13
	5	1.70 - 2.20	6.4	9.3	14.4	1.28	.23
F6	3	.60 - 1.20	6.5	11.0	12.0	1.16	.09
	5	1.70 - 2.20	8.4	9.3	11.8	1.11	.10
F5	3	.60 - 1.20	6.3	11.0	11.3	1.12	.10
	5	1.70 - 2.20	6.6	11.3	11.1	1.09	.08
F4	3	.60 - 1.20	6.9	10.8	11.1	1.15	.09
	8	2.95 - 3.20	10.0	10.3	9.7	1.13	.18
F3	3	.60 - 1.20	7.6	11.1	10.9	1.05	.12
	7	2.40 - 2.90	13.9	11.3	7.8	.91	.08
F2	2	.60 - 1.20	9.5	10.3	10.0	1.09	.18
	8	2.90 - 3.20	14.6	11.4	7.1	.86	.06
F1	3	.60 - 1.00	10.9	11.0	8.5	.88	.14
	8	2.90 - 3.20	10.0	11.0	7.1	.85	.22

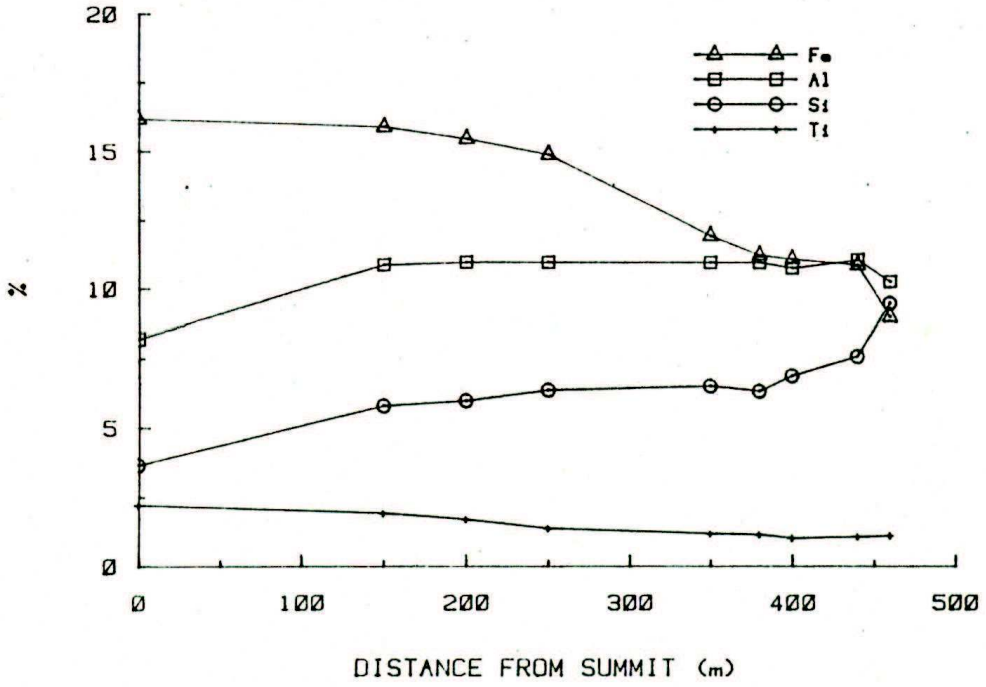

Figure 20. Sulphuric acid dissolution data of samples taken at 1 m depth in relation to landscape position.

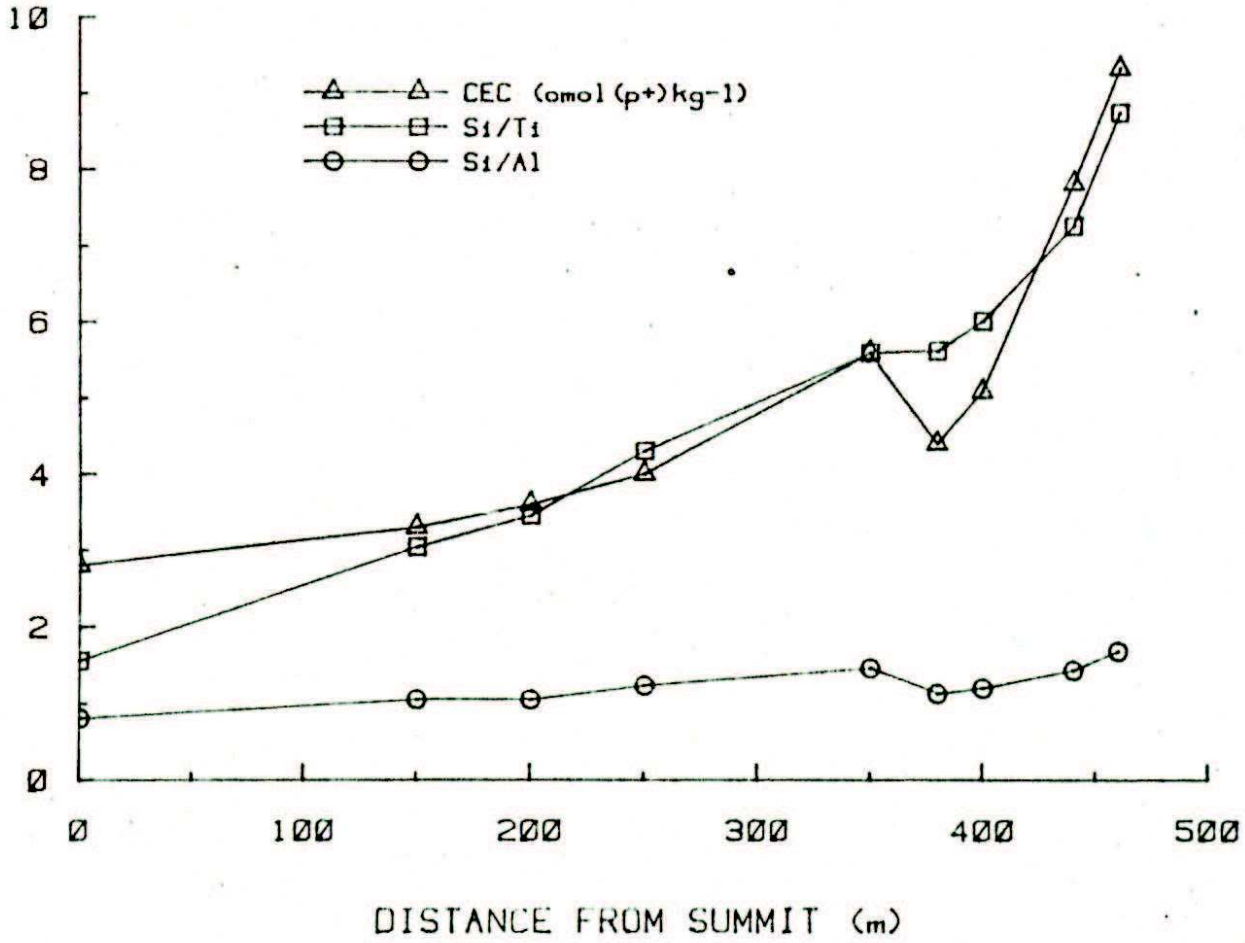

Figure 21. CEC, Si/Ti and Si/Al ratios of samples taken at 1 m depth in relation to landscape position.

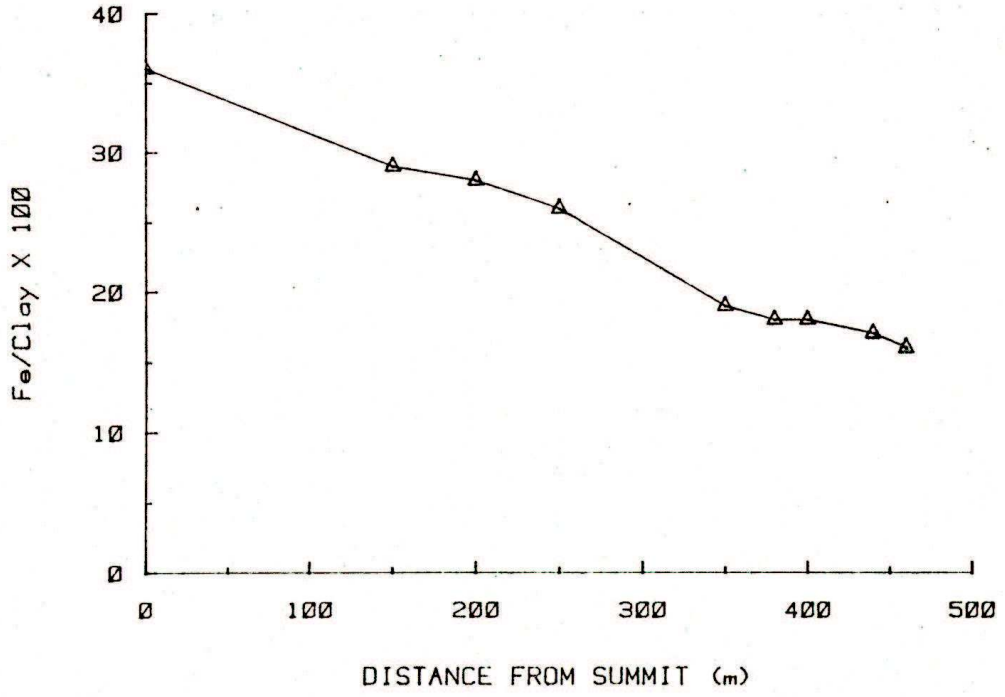

Figure 22. Fe/clay ratio at 1 m depth in relation to landscape position.

iron is mostly present on the clay fraction but over that concentration (saturation point) the iron also settles on other granulometric fractions. The saturation point was reported to be 7 to 10% Fe (Soileau and McCracken, 1967; Eswaran and Sys, 1970). According to these figures most of the soil clays studied are over the Fe-saturation point. From summit to backslope position, the Fe/Clay ratio is greater than 0.2 which, according to Eswaran and Sys (1970), indicates sufficient iron in excess of saturation to bind the soil material. Under these conditions a petroplinthic horizon can result if moisture conditions are favorable. In the toposequence ratios greater than 0.2 correspond with the presence of iron concretions layer (see morphology discussion), which supports the concept of the saturation point.

Overall the physical and chemical characterization data emphasize once more (see mineralogy section) the effect of topography in the genesis of these soils, the weathering stage decreasing from summit to footslope positions with corresponding changes in related soil properties.

Magnetic susceptibility

Figure 23 shows the calibration curve used to convert magnetic attraction (mg/1g) measurements to $m^3kg^{-1} \times 10^{-8}$, the SI units.

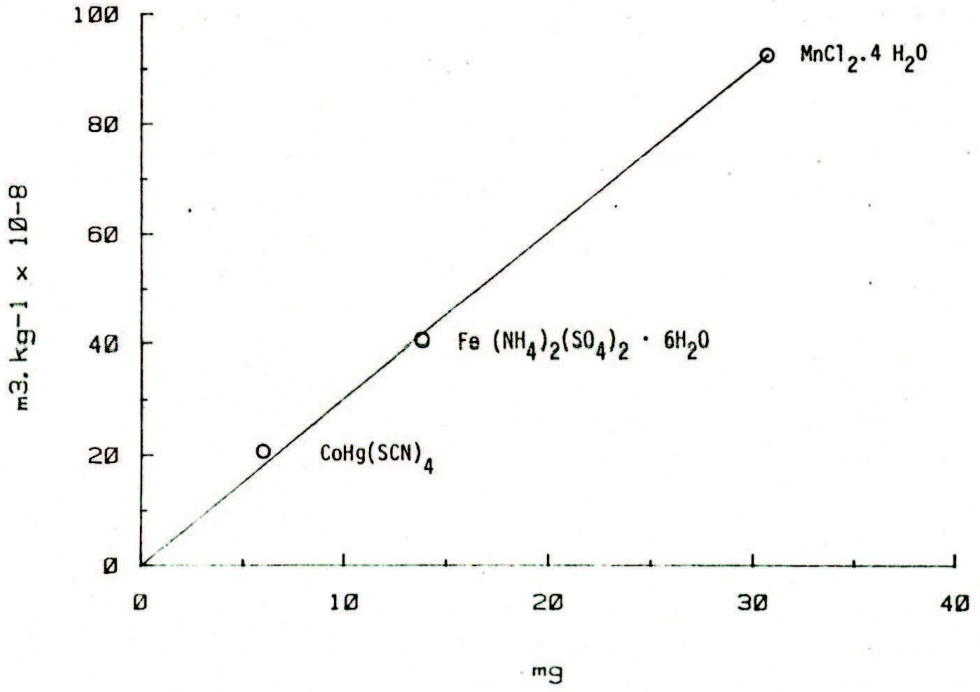

Figure 23. Magnetic susceptibility calibration curve, using three different salts.

Table 12 shows the result of magnetic susceptibility measurements of the separates of some samples. The magnetic susceptibility decreases with particle size, i.e., the sand fraction is the most magnetic fraction, except for profiles F9 and F8 where the silt fraction is more magnetic. Vadyunina et al., (1974) states that the magnetic susceptibility of sand particle size in soils developed on strongly magnetic rocks always exceeds that of the other fractions. These results suggest that the magnetic property was inherited from the parent material. The two profiles in the uppermost positions, F9 and F8, have in the silt fraction their most active magnetic fraction. This probably is due to a more advanced weathering that is breaking down sand size magnetic particles to magnetic silt size particles. Magnetite is probably the mineral related to the magnetic susceptibility of the sand and silt fraction. For the clay fraction maghemite does correlate with magnetic susceptibility (Figure 24).

Magnetic susceptibility measurements (Table 13) were done on the clay fraction before (untreated samples) and after DCB treatment (treated samples). The differential magnetic susceptibility ($\Delta\chi$ = χ untreated - χ treated) is equivalent to the χ of the minerals dissolved. Only those samples having detectable maghemite by DXRD had significant $\Delta\chi$ (>1100 $m^3Kg^{-1}10^{-8}$); those with no maghemite had <350 $\Delta\chi$. Since goethite and hematite have insignificant magnetic susceptibility compared with maghemite, it is reasonable to assume that maghemite is responsible for the differential magnetic susceptibility. A regression

Table 12. Magnetic attraction of 1 g sample and corresponding magnetic susceptibility (χ) of the separates of some soil samples.

Sample	Magnetic Attraction				χ			
	Sand	Silt	Clay	Soil	Sand	Silt	Clay	Soil
	mg				$m^3kg^{-1}10^{-8}$			
F9-3	1,479	5,314	798	1,224	4,365	15,848	2,356	3,612
F8-3	2,784	3,474	845	1,095	8,214	10,250	2,494	3,232
F7.5-3	1,782	1,253	771	867	5,259	3,698	2,276	2,559
F7-3	1,691	1,159	761	625	4,990	3,419	2,247	1,845
F6-3	1,595	799	644	506	4,707	2,359	1,901	1,494
F5-3	1,295	756	623	460	3,822	2,232	1,839	1,359
F4-3	1,000	613	550	451	2,952	1,810	1,624	1,332
F4-8*	482	193	90	100	1,424	571	267	297
F3-3	1,010	553	534	360	2,981	1,633	1,577	1,064
F3-7*	153	323	80	15	453	954	234	46
F2-3	1,060	370	350	276	3,129	1,093	1,034	816
F2-8*	65	55	45	23	193	164	134	70
F1-3	402	192	128	122	1,188	568	379	362
F1-8*	277	82	77	59	819	244	229	176

*/ Samples taken at 3m; the others at 1m.

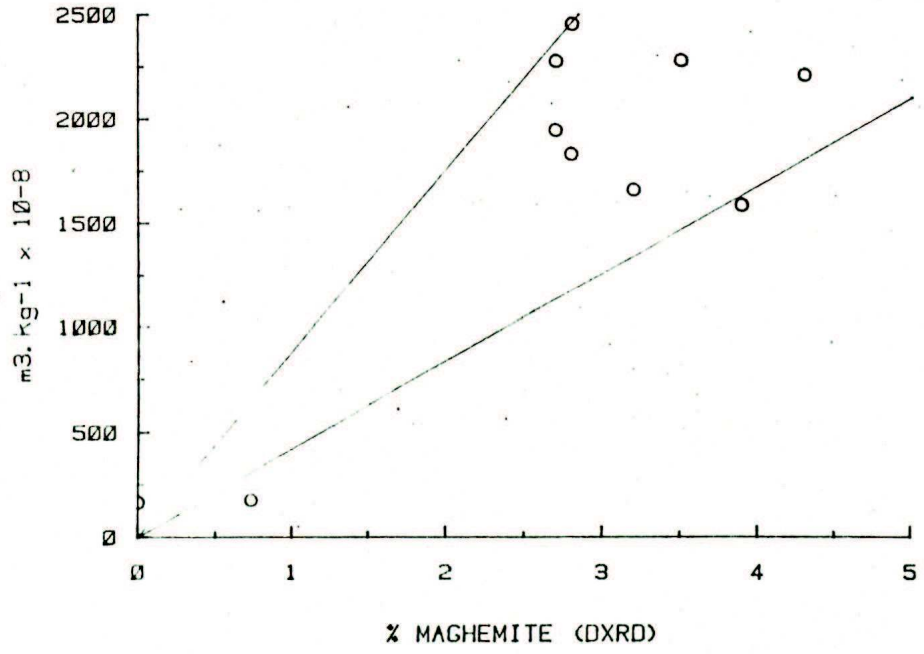

Figure 24. Correlation between maghemite content and magnetic susceptibility of the clay fraction of samples taken at 1 m depth. The two solid lines represent the estimate of magnetic susceptibility of maghemite according to Mullins (1977).

Table 13. Magnetic attraction of 1g of clay sample (χ) before (untreated) and after DCB treatment (treated) and corresponding magnetic susceptibility (χ); maghemite content by DXRD.

Sample	Depth	Magnetic Attraction		χ			Maghemite content
		Untreated	Treated	Untreated	Treated	$\Delta\chi$	
	- m -	------- mg ------		------ $m^3kg^{-1}\ 10^{-8}$		-----	------- % (wt, wt) --------
F9-3	0.70-1.20	794	22	2,344	67	2,279	3.5
F8-3	0.70-1.20	863	32	2,547	96	2,453	2.8
F7.5-3	0.60-1.20	800	29	2,362	87	2,276	2.7
F7-3	0.60-1.20	778	30	2,297	90	2,208	4.3
F6-3	0.60-1.20	679	20	2,005	61	1,946	2.7
F5-3	0.60-1.20	640	20	1,890	61	1,831	2.8
F4-3	0.60-1.20	582	19	1,719	58	1,662	3.2
F4-8	2.95-3.20	86	30	255	142	167	0
F3-3	0.60-1.20	557	19	1,645	58	1,589	3.9
F3-7	2.40-2.90	84	28	249	84	167	0
F2-3	0.60-1.20	404	19	1,193	58	1,137	0.8
F2-8	2.90-3.20	46	10	137	31	108	0
F1-3	0.60-1.00	116	6	344	19	326	0
F1-8	2.90-3.20	71	4	211	13	199	0

regression linear analysis between maghemite content (as estimated by DXRD) and differential magnetic susceptibility give a $r^2 = 0.83$ and $Y = 345.73 + 505.91X$ (Figure 24). The slope of the curve indicates the change in the mean of the probability distribution of Y per unit increase in X, in other words, 1% of maghemite has a magnetic susceptibility of 505.91 x (10^{-8} m^3 kg^{-1}). Mullins (1977) gave a value of 41,000 - 44,000 x (10^{-8} m^3 kg^{-1}) for pure synthetic maghemite and a value of 88,000 x (10^{-8} m^3 kg^{-1}) for what he refers to as "the only available estimate for the susceptibility of non-concretionary pedogenic maghemite". Thus Mullins' data range from 410 - 440 to 880 x (10^{-8} m^3 kg^{-1}) for the magnetic susceptibility of 1% of maghemite, and our data is in the middle of this range (Figure 24).

Magnetic susceptibility decreases steadily from the summit to the footslope positions and also decreases with profile depth. These trends indicate that magnetic susceptibility increases with increase in weathering intensity. As already postulated in the iron oxides discussion this fact is an indication that maghemite is a product of weathering of magnetite inherited from the parent material.

In Brazilian soil survey work magnetic susceptibility, as observed in the field with a hand magnet, is used to help identify those soils formed from mafic rocks. This measurement is only qualitative and it is judged by visual inspection. We devised a simple way to quantify this observation using a spring balance. A permanent hand horseshoe magnet (General model 370-6) was hooked to a spring balance (Homus, model 100g

capacity 100 gm x 1 gm) using a string. The soil samples were placed in a plastic cup container (50 cc), packed well and covered with a thin plastic film. Then the magnet was allowed to touch the plastic cover on the soil sample. The force necessary to pull the magnet away was considered the magnetic attraction. The values obtained with the spring balance (SB) were well correlated with values from the analytical balance (Figure 25). Thus, magnetic profiles like those shown in Figure 26 can be obtained in the field when soils are described. These measurements can be quickly done and can indicate local variations in soil forming conditions, as well as continuity of parent material.

Magnetic Separator

The magnetic separation procedure produces only a small relative concentration of ferromagnetic minerals. The presence of all minerals were detected in both fractions, magnetic and tailing. There is a small concentration of hematite and maghemite (identified by the combined peak of 0.251 nm at 35.7° 2θ) in the magnetic fraction, and HIV, mica, kaolinite, gibbsite, anatase and goethite in the tailings (Table 14).

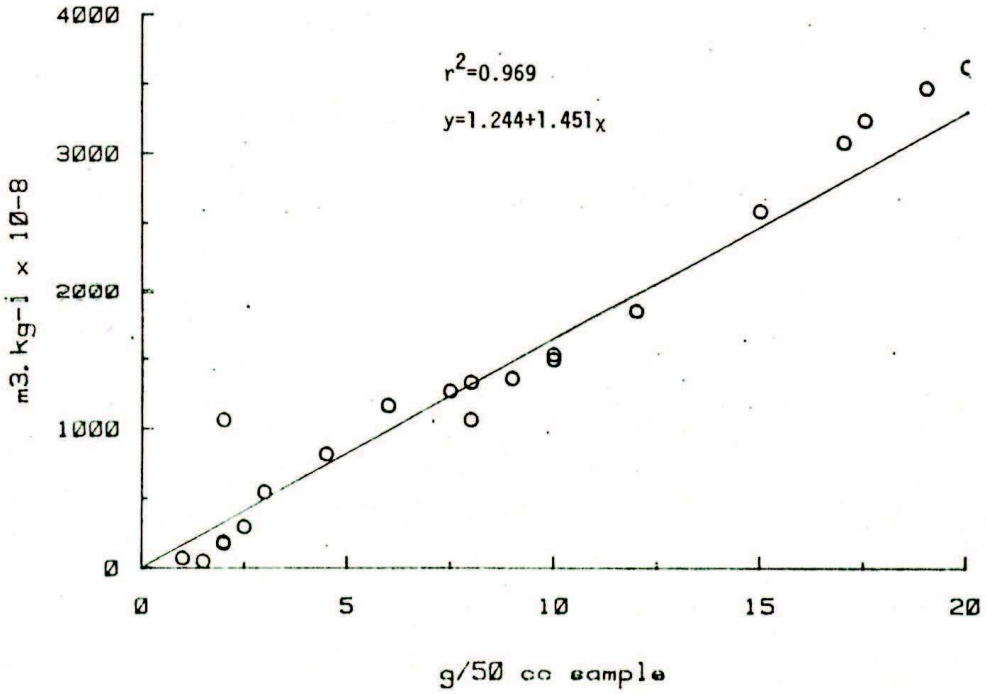

Figure 25. Correlation between spring balance and analytical balance measurements of magnetic susceptibility.

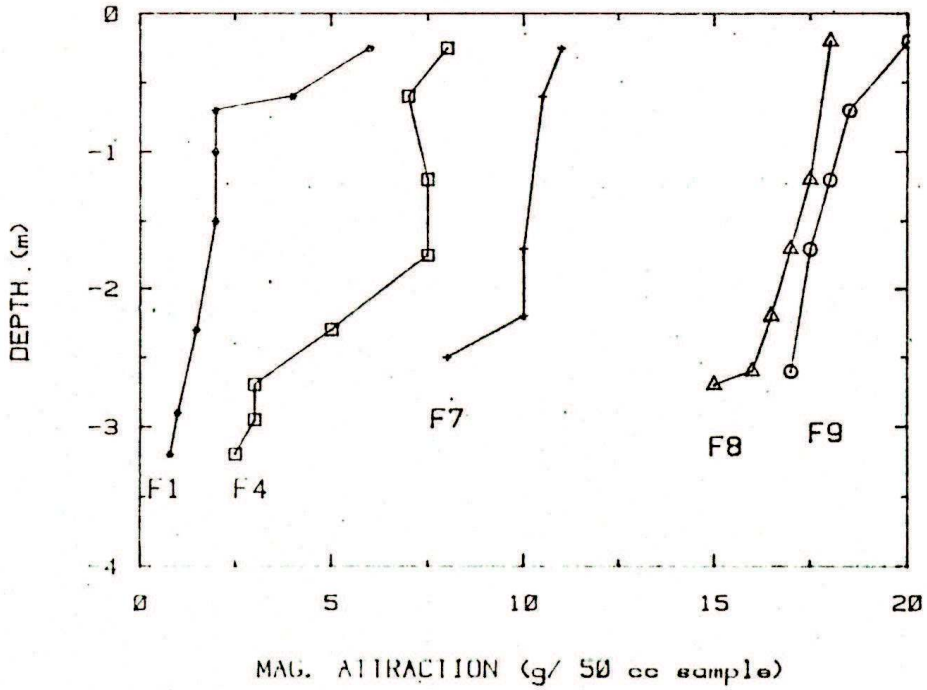

Figure 26. Magnetic susceptibility profiles.

Table 14. Peak areas (WHH x Height) of the minerals identified in the magnetic and tailings fraction of sample F8-3.

Mineral	Peak area (WHHxH)	
	Magnetic Fraction	Tailings
HIV	7	10
Mica	39	60
Kaolinite	117	222
Gibbsite	32	113
Anatase	42	70
Goethite	10	25
Hematite + Maghemite	39	30

According to Schulze and Dixon (1979) there are three possible ways for minerals other than iron oxides to occur in the magnetic fraction: (1) mechanical trapping of particles by the steel wool filter; (2) magnetic trapping of non-iron oxide minerals, and (3) magnetic trapping of compound particles made up of magnetic and non-magnetic minerals.

The extent of mechanical trapping, although not actually measured, was assumed to be small because the low packing densities of steel wool

used would not provide many sites for particles to be mechanically trapped. So, magnetic trapping of compound particles made up of magnetic and nonmagnetic minerals appears to account for the high percentage of non-ferromagnetic minerals in the magnetic fraction.

The presence of ferromagnetics minerals in the tailing probably is because of the small particle size of ferromagnetics like maghemite (Mullins, 1977) and because of some bonding of magnetic minerals to nonmagnetic particles (Schulze and Dixon, 1979). Another possibility would be that the magnet used is not strong enough to trap all ferromagnetic minerals.

Color

Color of the clay fraction, measured in moist samples placed on glass slides in order to get flat surfaces to compare with chips of the Munsell Color Charts under sunlight, correlates well with the soil color as measured in moist samples in the field (Table 15). Clay colors of mottled soil horizons, in general assumed the matrix color of the soil sample. The overall agreement between soil color and clay color indicates the clay fraction is the dominant coloring fraction.

Munsell color of the clay fraction was converted to the Redness Rating (RR) suggested by Torrent et al. (1980) according to the following expression:

$$RR = \frac{H^* \times C}{V}.$$

Table 15. Soil color and color, redness rating (RR), DCB extractable iron (Fe_d), hematite content (Hm) and hematite/hematite + goethite ratio (Hm/Hm + Gt) of the clay fraction.

Sample	Depth	Soil Color		Clay Fraction				
		Matrix	Mottles[1]	Color	RR	Fe_d	Hm	Hm/Hm+Gt
	--- m ---			------- % (wt/wt) ------				
F9-3	0.70-1.20	10R3/4		10R3/4	13.3	13.1	14.8	0.80
F8-3	0.70-1.20	1.5R3/4		2.5YR3/4	10.0	13.5	10.8	0.76
F7.5-3	0.60-1.20	2.5YR3/4		2.5YR3/6	15.0	12.6	11.0	0.74
F7-3	0.60-1.20	2.5YR3/4		2.5YR3/6	15.0	12.0	11.3	0.74
F6-3	0.60-1.20	2.5YR3/6		2.5YR3/6	15.0	10.5	8.7	0.72
F5.3	0.60-1.20	2.5YR3/6		2.5YR3/6	15.0	10.8	9.9	0.74
F4.3	0.60-1.20	2.5YR3/6		2.5YR4/6	11.2	10.8	8.4	0.67
F4.8	2.95-3.20	7.5YR5/6	c 10YR4/6 + c 10YR7/2	7.5YR5/8	4.0	7.5	-	-
F3.3	0.60-1.20	2.5YR3/6		2.5YR4/6	11.2	10.5	8.2	0.69
F3.7	2.40-2.90	7.5YR5/8	c 10R5/6	7.5YR5/6	3.0	4.5	-	-
F2.3	0.60-1.20	2.5YR3/6		2.5YR3/6	15.0	8.3	5.5	0.60
F2.8	2.90-3.20	10YR5/6	m 2.5YR6/4 + c 7.5YR5/8 + f10R3/6	5YR4/8	10.0	5.7	2.6	0.38
F1.3	0.60-1.00	7.5YR4/6	5YR5/8 - variegated	7.5YR4/6	3.8	4.8	4.1	0.43
F1.8	2.90-3.20	5YR3/4	m 2.5YR3/6	7.5YR4/6	3.8	4.8	1.1	0.14

[1] m = many
c = common
f = few

where C and V are the numerical values of the Munsell chroma and value, respectively, and H^* increases with the red color assuming the following values: 12.5 for 2.5R; 10 for 10R; 7.5 for 2.5YR; 5 for 5YR; 2.5 for 7.5YR; and 0 for 10YR or yellower hues. This RR is similar to that of Hurst (1977) but is supposed to provide a better discrimination between yellowish brown and red colors (Torrent et al., 1980). As a whole as the clay fraction becomes redder (higher RR) there is a corresponding increase in Fe_d, hematite content and hematite/hematite + goethite ratio (Table 15) similar to previous reports (Schwertmann and Taylor, 1977; Bigham et al., 1978; Torrent et al., 1980; Curi and Franzmeier, 1984).

Redness Rating was found to be more related to hematite content of soils than to either the hematite/hematite + goethite ratio or the total Fe_d content (Table 16) indicating that hematite is responsible for the reddish color of these soils, in agreement with reported results (Torrent et al., 1980; Schwertmann et al., 1982; Kämpf and Schwertmann, 1983).

However, even the correlation coefficient for hematite was considerably smaller than those reported by Torrent et al. (1980) for soils of Spain derived from acid rocks, and closer to the results of Kämpf and Schwertmann (1983) for Brazilian soils derived from basalt. This means a "redness saturation" as the hematite content increases above about 5% (Torrent et al., 1983). Furthermore, the way the RR is calculated, small variations in chroma (see, for example, samples F7.3 and F6.3) result in large variations in the RR that do not express the

Table 16. Correlation among different redness indices and some clay characteristics.

Redness Index	Hematite	Hm/Hm + Gt	Fe_d
H	$r^2 = 0.84$	$r^2 = 0.31$	$r^2 = 0.78$
	$y = 2.66 + 0.50x$	$y = 5.34 + 0.70x$	$y = 0.69x - 0.30$
H+V	$r^2 = 0.83$	$r^2 = 0.12$	$r^2 = 0.38$
C	$y = 3.20 + 0.50x$	$y = 6.13 + 0.63x$	$y = 3.39 + 0.39x$
H+C	$r^2 = 0.81$	$r^2 = 0.85$	$r^2 = 0.76$
V	$y = 4.26 + 0.51x$	$y = 3.29 + 9.82x$	$y = 1.24 + 0.70x$
Hx V1/	$r^2 = 0.77$	$r^2 = 0.62$	$r^2 = 0.69$
C	$y = 1.42 + 0.32x$	$y = 1.21 + 4.61x$	$y = 0.43x - 0.37$
Hx C2/	$r^2 = 0.61$	$r^2 = 0.20$	$r^2 = 0.59$
V	$y = 4.68 + 0.82x$	$y = 9.04 + 1.58x$	$y = 1.13x - 0.03$

1/ After Hurst (1977).
2/ Schwertmann et al. (1980).

small variation in hematite content. This is also true for the index used by Hurst (1977) and thus these procedures diminish the importance of hue, which seems to be the component most related with the mineralogical changes expressed in the color. A slight change replacing the operator x (times) by + (plus) improved the results (Table 16). Table 16 also stresses the important role played by hue in these high hematite content soils (Figures 27 and 28). Although H^* alone gave the best correlation coefficient with hematite content, the index $H^* + \frac{C}{V}$, hereafter called RF (Redness Factor), was chosen because of its overall best correlation and because its use of all soil color attributes (H, C and V) can be more important in a larger set of samples with a wider variation in color.

The use of a single redness index to represent a horizon with mottles is a problem. An attempt was made to solve this problem by giving "weights" to the indices of matrix and mottles according to the abundance of mottles as described in the field (Soil Survey Staff, 1975). The "weights" were chosen based on the midpoint of each mottle class range, as follows:

Color pattern	% Area covered	"Weight"
Many mottles	20-50	0.35
Common mottles	2-20	0.11
Few mottles	<2	0.01
Matrix	>50	1.00 - mottle fraction

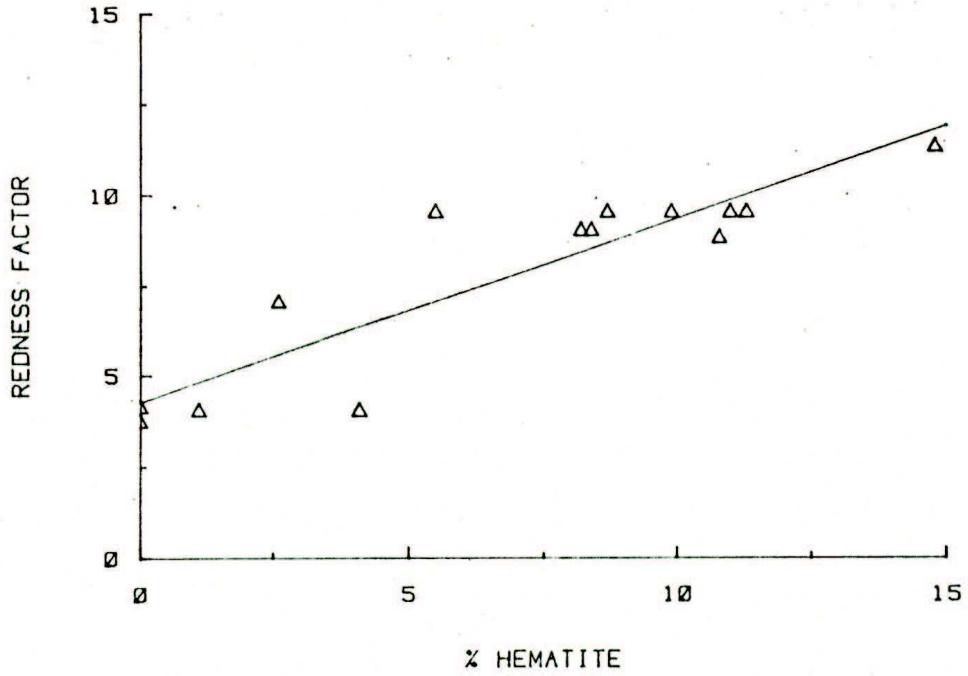

Figure 27. Relationship between redness factor (RF) and hematite content for clay samples taken at 1 m depth.

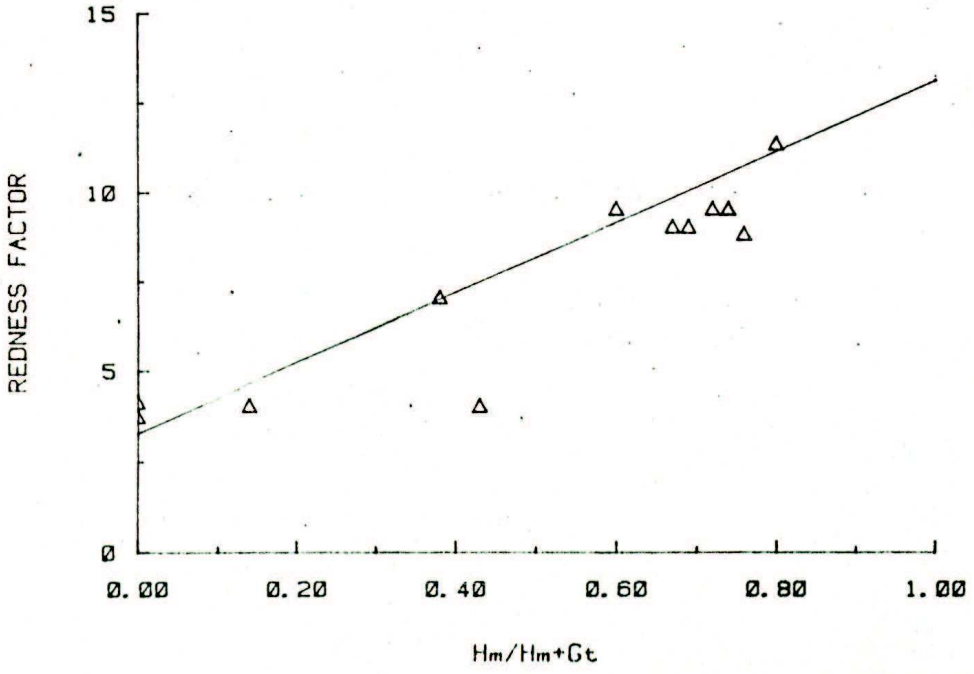

Figure 28. Relationship between redness factor (RF) and hematite/hematite+goethite ratio for clay samples taken at 1 m depth.

As an illustration, consider a sample with matrix 5YR3/4, common mottles 7.5YR5/8 and few mottles 2.5YR3/6. The RF of each color will be 6.33, 4.1 and 9.5 , respectively. Averaging using the corresponding "weights" will give:

$$RF = \frac{6.33\ (0.88) + 4.1\ (0.11) + 9.5\ (0.01)}{0.88 + 0.11 + 0.01} = \frac{6.115}{1} = 6.1$$

Table 17 and Figure 29 show the soil color descriptions and the RF for three profiles. The RF value decreases dramatically in the deeper mottled horizons of profiles F1 and F4, showing that the method of calculating RF (or other factors) for mottled horizons is sensitive to changes in color patterns. The method thus provides a good way of graphically representing mottled horizons. It will also permit the use of a single redness index for mottled soil colors when correlations between color and other soil properties are being studied.

Table 17. Soil color descriptions and Redness Factor (RF) for three profiles.

Sample	Layer	Depth	Soil color		RF
			Matrix	Mottles[1]	
		-- m --			
F1	1	0 -0.20	5YR3/4		6.3
	2	0.20-0.60	7.5YR4/6		4.0
	3	0.60-0.70	7.5YR4/6 + 5YR5/8	variegated	5.3
	4	0.70-1.00	7.5YR4/6	m7.5YR5/8 C10YR5/1	3.6
	5	1.00-1.50	5YR3/4	C7.5YR5/8 C10YR5/1	5.4
	6	1.50-2.30	5YR3/4	C7.5YR5/8 f2.5YR5/8	6.1
	7	2.30-2.90	5YR3/4		6.3
	8	2.90-3.20	5YR3/4	m2.5YR3/6	7.4
F4	1	0 -0.25	2.5YR3/4		8.8
	2	0.25-0.60	2.5YR3/6		9.5
	3	0.60-1.20	2.5YR3/6		9.5
	4	1.20-1.75	2.5YR3/6		9.5
	5	1.75-2.30	2.5YR3/6		9.5
	6	2.30-2.70	2.5YR3/6	C 5YR5/6	9.1
	7	2.70-2.95	10YR5/6	C 10YR4/6 f 10YR7/2	1.22
F9	1	0 -0.20	10R3/3		11.0
	2	0.20-0.70	10R3/3		11.0
	3	0.70-1.20	10R3/4		10.7
	4	1.20-1.70	10R3/4		10.7
	5	1.70-2.40	10R3/4		10.7
	6	2.40-2.60	10R3/4		10.7

[1] m = many
c = common
f = few

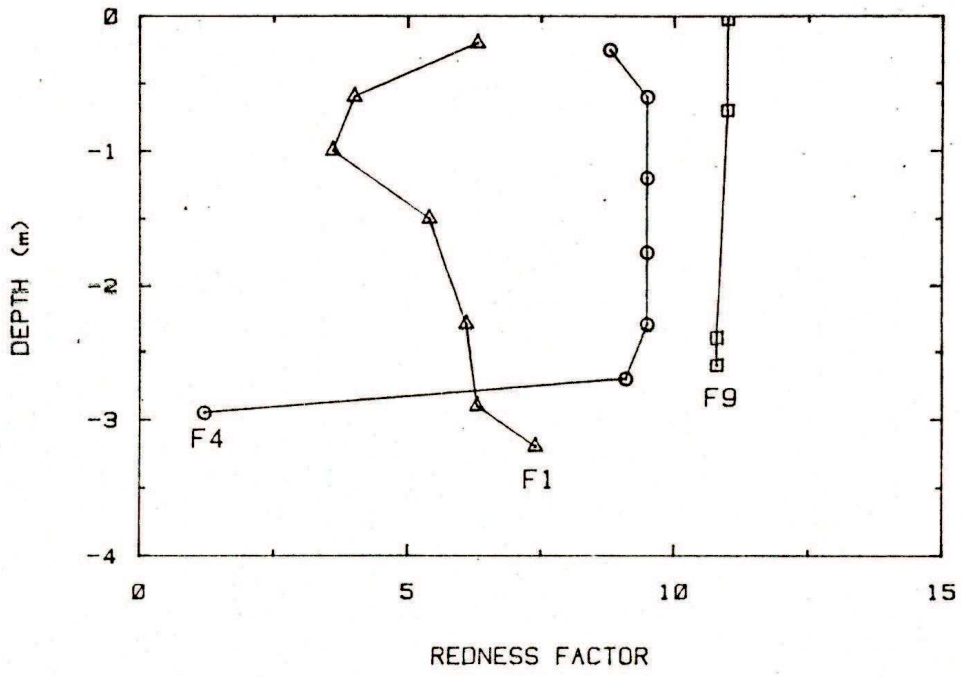

Figure 29. Variation of redness factor (RF) with depth for 3 profiles.

SUMMARY AND CONCLUSIONS

The region concerned in this study is located in the east portion of the Brazilian Central Plateau, in the Patos de Minas Region, Minas Gerais State, Brazil. The average monthly temperature of 20.5°C and a total annual rainfall of about 1400 mm, distributed in distinct wet and dry seasons, results in an ustic soil moisture regime and an isohyperthermic temperature regime for most soils of the region. Cerrado, a subhumid wooded savanna, occurs on flatter stretches but is replaced by semideciduous forest on the steeper slopes. The soils are mainly Ustox. Geologically, the area has been described as a Precambrian basement, with structurally deformed felsic rocks, that are covered by pyroclastic rich fluvio-lacustrine sediments (tuffite). Tuffite is an indurated rock composed of a mixture of pyroclastic and sedimentary detritus, especially volcanic ash and fine sediments.

The present landscape is best visualized as a broad tableland - the "chapadoês" - which is locally dissected by deep valleys merging into broad sloping pediments. The pediments form stepped surfaces and have a tendency to be concave in profile. The dissection process that gave rise to the valleys are probably related to the "Velhas Erosion

Cycle" that in Plio-Pleistocene times dissected the existent dominant surface of Brazil.

The broad tableland is at an altitude of about 1000 m and the broad pediments forming stepped surfaces slope down to about 700 m. This study is concerned with a hillslope located at altitudes around 800 m. Seeking to understand how properties of the Ustox soils relate to landscape positions, ten profiles were sampled in a toposequence with 40 m relief in 500 m. Through exposure by erosion tuffite became the main parent material for the soils along the hillslopes. Weathering of tuffite releases Si, Al, Mg, Fe, Ca, Na and trace elements. The high leaching environment allows most of the released silica to be lost from the weathering zone. Due to the long time factor, although the soil system is very dynamic, there is a tendency for equilibrium conditions to prevail and part of the Si and Al precipitates to form clay minerals (mostly kaolinite) and some gibbsite, which are some of the stable components of the clay fraction of these soils. Significant amounts of iron were oxidized due to the well-drained, well-aerated environment. Ferric forms, mostly hematite, goethite and maghemite, remain in the system because they are insoluble at pH values greater than 3. Anatase, mica and magnetite are present as residual minerals. Mica altered, probably through a vermiculite intermediate, into hydroxy-interlayered vermiculite (HIV).

Along a toposequence located in the flatter stretches of the large valley slopes, the soils grade progressively from dusky red at the

summit to strong brown with mottles on the footslope position. In this toposequence water can move downslope as runoff and subsurface flow carrying silica and other weathering products resulting in a relative accumulation of iron in upper landscape positions. In these ustic moisture regime conditions, the wetter environment in lower slope positions probably results in greater plant growth and organic matter production, and such conditions could affect mineral equilibria. In the toposequence studied, mica content increases from summit to footslope positions, kaolinite decreases in an irregular fashion from summit to footslope positions, HIV shows no clear trends, and gibbsite and anatase decrease from summit to footslope positions. The downslope increase of the mica/gibbsite ratio suggests that downslope movement of Si or slower removal of Si from soils in lower slope positions results in a lower rate of decomposition of silicate minerals, especially mica, in these soils. Among the iron oxides minerals, goethite content increases slightly downslope, hematite content decreases downslope, and maghemite is present in small amounts in summit and backslope positions but is absent in the lower landscape positions. The higher Fe concentration in soils of upper positions, combined with drier conditions that lead to higher average temperature, favor dehydration of ferrihydrite to hematite. On the other hand, in the wetter environment of the lower positions, organic compounds might complex Fe and prevent formation of ferrihydrite and thus hematite, so that goethite forms instead of hematite. Furthermore, the wetter environment also could promote maghemite dissolution under more intense reducing conditions.

In this work, some analytical method advancements were made:

1). The use of differential x-ray diffraction analysis (DXRD) combined with multipleregression analysis made possible a quantitative estimate of the different iron oxide minerals present in the sample.

2) A hand magnet attached to a common spring balance provided a quick and reliable quantitative estimate of soil magnetic susceptibility in the field.

3) A single redness index was calculated for mottled horizons. Also, a new redness index that emphasizes the role of hue in soil color relationships was used.

BIBLIOGRAPHY

Almeida, J. R. 1979. Cromossequencia de solos originarios de rochas peliticas do grupo Bambui. M.S. Thesis. Univ. Fed. Vicosa, MG, Brazil.

Barbosa, O., O. P. G. Braun, R. C. Dyer, and C. A. B. R. Cunha. 1970. Geologia da Região do Triangulo Mineiro. Departamento Nacional da Producão Mineral. Boletim no. 136, Rio de Janeiro, 140 p.

Barnhisel, R. I. 1977. Chlorites and hydroxy interlayered vermiculite and smectite. In J. B. Dixon and S. B. Weed (ed) Minerals in Soil Environments. Soil Sci. Soc. Am., Madison, WI.

Beiser, G. 1969. The Story of the Earth's Magnetic Field. E. P. Dutton and Co., Inc., New York. 128 p.

Bennema, J. 1966. Report to the government of Brazil on the classification of Brazilian soils. FAO Dept. 2197. Rome, Italy. 83 p.

Bennema, J., and M. Camargo. 1979. Some remarks on Brazilian Latosols in relation to the Oxisols of Soil Taxonomy. In F. H. Beinroth and s. Paramananthan (ed.) Proc. Second Int. Soil Classif. Workshop. Part I: Malaysia. p. 233-255.

Bennema, J., M. Camargo, and A. C. S. Wright. 1962. Regional contrast in South American soil formation, in relation to soil classification and soil fertility. Trans. Joint Meet. Comm. IV and V, Int. Soc. Soil Science, New Zealand. pp. 493-506.

Bernas, B. 1968. A new method for decomposition and comprehension analysis of silicates by atomic absorption spectroscopy. Anal. Chem. 40:1682-1686.

Bigham, J. M. 1977. Iron mineralogy of red-yellow hued Ultisols and Oxisols as determined by Mossbauer spectroscopy, X-ray diffractometry and supplemental laboratory techniques. Ph.D. Thesis. North Carolina State Univ., Raleigh. Dissertation Abstracts 77:29662.

Bigham, J. M., D. C. Golden, L. H. Bowen, S. W. Buol, and S. B. Weed. 1978a. Iron oxide mineralogy of well-drained Ultisols and Oxisols: I. Characterization of iron oxides in soil clays by Mossbauer spectroscopy, X-ray diffractometry and selected chemical techniques. Soil Sci. Soc. Am. J. 42:816-825.

Bigham, J. M., D. C. Golden, L. H. Bowen, S. W. Buol, and S. B. Weed. 1978b. Mossbauer and X-ray evidence for the pedogenic transformation of hematite to goethite. Soil Sci. Soc. Am. J. 42:979-981.

Bigham, J. M., D. C. Golden, S. W. Bowen, S. W. Buol, S. B. Weed, and L. H. Bowen. 1978c. Iron oxide mineralogy of well-drained Ultisols and Oxisols: II. Influence on color, surface area, and phosphate retention. Soil Sci. Soc. Am. J. 42:825-830.

Borggard, O. K. 1982. The influence of iron oxides on the surface area of soil. J. Soil Sci 33:443-449.

Borggard, O, K. 1983. Effect of surface area and mineralogy of iron oxides on their surface charge and anion-adsorption properties. Clays and Clay Minerals 31:230-232.

Brailsford, F. 1966. Physical Principles of Magnetism. D. Van Nostrand Company Ltd., London. 274 p.

Brower, G. 1980. Associated minerals. In C. W. Brindley and G. Brown (ed.) Crystal Structures of Clay Minerals and Their X-ray Identification. Mineralogical Society, London. p. 361-410.

Bryant, R. B., N. Curi, C. B. Roth, and D. P. Franzmeier. 1983. Use of an internal standard with differential x-ray diffraction analysis for iron oxides. Soil Sci. Soc. Am. J. 47:168-173

Buol, S. W. 1979. Geomorphology of some Oxisols. In F. H. Beinroth and S. Paramananthan (ed.) Proc. Second Int. Soil Classif. Workshop. Part I: Malaysia. p. 37-43.

Buol, S. W., F. D. Hole, and R. J. McCracken. 1980. Soil Genesis and Classification. 2nd edition. Iowa State University Press, Ames. 404 p.

Camargo, M. N., and Falesi, I. C. 1974. Soils of the Central Plateau and Transamazonic Highway of Brasil. In E. Bornemisza and A. Alvarado (ed.) Soil Management in Tropical America, North Carolina State University, Raleigh. p. 25-45.

Camargo, M. N., and M. N. Beinroth. 1978. Dominant mineralogy of the clay and silt fractions of some soils of Brazil - summary data. In M. N. Camargo and N. N. Beinroth (ed.) Proc. First Int. Soil Classif. Workshop. SNLCS, EMBRAPA, Rio de Janeiro, Brazil. p. 305-308.

Carlisle, V. W., and L. W. Zelazuy. 1973. Mineralogy of selected Florida Paleudults. Soil Sci. Soc. Fla. Proc. 33:136-169.

Carmo, D. N. 1977. Caracterizacão, genese e uso de Latossolos sob cerrado no municipio de Rio Paranaiba, MG. M.S. Thesis. Esc. Sup. Agric. Lavras, MG, Brazil.

Childs, C. W., B. A. Goodman, and G. J. Churchman. 1979. Application of Mossbauer spectroscopy to the study of iron oxides in some red and yellow/brown soil samples from New Zealand. In M. M. Mortland and V. C. Farmer (ed.) Int. Clay Conf., 6th, 1978. Elsevier, Amsterdam. p. 555-565.

Childs, C. W. and D. M. Leslie. 1977. Interelevant relationships in iron-manganese concretions from a catenary sequence of yellow-grey earth soils in loess. Soil Sci. 123:369-375.

Cline, M. G., and S. W. Buol. 1973. Soils of the Central Plateau of Brazil and extension of results of field research conducted near Planaltina, Federal District. Ithaca, Cornell University Agronomy Mimeo 73-13.

Comissao de Solos. 1960. Levantamento de reconhecimento dos solos do Estado de São Paulo. Servico Nacional de Pesquisa Agropecuária. Boletim no. 12. Rio de Janeiro, Brazil.

Comissao de Solos. 1962. Levantamento de reconhecimento dos solos da regias sob influencia do Reservatorio de Furnas. Servico Nacional de Pesquisa Agropecuária. Boletim no. 13. Rio de Janeiro, Brazil.

Curi, N. 1983. Lithosequence and toposequence of Oxisols from Goias and Minas Gerais States, Brazil. Ph.D. Thesis. Purdue Univ. Dissertation Abstracts 44:1674-B.

Curi, N., and D. P. Franzmeier. 1984. Toposequence of Oxisols from the Central Plateau of Brazil. Soil Sci. Soc. Am. J. (in press).

Davey G. G., J. D. Russell, and M. J. Wilson. 1975. Iron oxide and clay minerals and their relation to colours of red and yellow Podzolic soils near Sydney, Australia. Geoderma 14:125-138.

Dematte, J. L. I., and N. Holowaychuck. 1977. Solos do Regia de São Pedro, Estado de São Paulo. II. Mineralogia. Rev. Bras. Cienc. Solo, Campinas, Brazil 1:99-103.

Douglas, L. A. 1965. Clay mineralogy of a sassafras soil in New Jersey. Soil Sci. Soc. Am. Proc. 29:163-167.

Eiten, G. 1972. The cerrado vegetation of Brazil. The Botanical Review 38 (2):201-341.

Eiten, G. 1982. Brazilian "Savannas". In B. J. Huntley and B. H. Walker (ed.) Ecology of Tropical Savannas. Ecological Studies 42, Spring-Verlag, New York. p. 25-47.

EMBRAPA-SNLCS. 1979. Manual de métodos de analise de solos. Rio de Janeiro, Brazil.

Eswaran, H. and C. Sys. 1970. An evaluation of the free iron in tropical basaltic soils. Pedologie 20:62-85.

Fasolo, P. J. 1978. Mineralogical identification of four igneous extrusive rock derived oxisols from the State of Parana, Brazil. M.S. Thesis. Purdue University.

Ferri, M. G. 1977. Ecologia dos cerrados, In M. G. Ferri (ed.) IV° Simposio sobre o Cerrado: Bases para Utilizacão Agropecuaria Edit. Univ. São Paulo, Brazil. p. 15-33.

Fewer, R. 1956. An exploratory investigation of the soils and agricultural potential of the soils of the future Federal District in the Central Plateau of Brazil. Ph.D. Thesis, Cornell University, Ithaca, NY. 432 p. Univ. Microfilms Publ. 16,254.

Figgis, B. N. and J. Lewis. 1965. Magnetochemistry. In H. B. Jonassen and a. Weisaberger (ed.) Techniques of Inorganic Chemistry. Vol. IV, p. 137-248. Interscience Publishers.

Fitzpatrick, R. W. and J. LeRoux. 1975. Pedogenic and solid solution studies on iron-titanium minerals. Proc. Inter. Clay Conf. p. 585-599.

Fitzpatrick, R. W. and V. Schwertmann. 1982. Al-substituted goethite -- An indicator of pedogenic and other weathering environments in South Africa. Geoderma 27:335-347.

Franzmeier, D. P., G. C. Steinhardt, J. R. Crum, and L. D. Norton. 1977. Soil characterization in Indiana: I. Field and laboratory procedures. Purdue Univ. Res. Bull. 943. 30 p.

Franzmeier, D. P., J. E. Yahner, G. C. Steinhardt, and H. R. Sinclair. 1983. Color patterns and water table levels in some Indiana soils. Soil Sci. Soc. Am. J. 47:1196-1202.

Gerrard, A. J. 1981. Soils and Landforms - An Integration of Geomorphology and Pedology. George Allen and Unwin, London. 219 p.

Gomes, I. A. 1976. Oxisols and inceptisols from gneiss in a subtropical area of Espirito Santo State, Brazil. M.S. Thesis Purdue Univ.

Gomes, I. A., M.N. Camargo, F. Palmieri, A. M. Pires Filho, M. Resende, and D. P. Santana. 1980. Estudo expedito de solos da região do Alto Paramaiba, para fins de classificacão, correlacão e legenda preliminar. EMBRAPA-SNLCS, Rio de Janeiro. Bol. Tec. no. 64.

Guimarães, D. 1955. Contribuicao ao estudo dos tufos vulcanicos da Mata da Corda. I.T.I., Boletim No. 18, Belo Horizonte, MG, Brazil. 31 p.

Hall, G. F. 1983. Pedology and geomorphology. In L. P. Wilding, N. E. Smeck, and G. F. Hall (ed.) Pedogenesis and Soil Taxonomy. I. Concepts and Interactions. Elsevier, Amsterdam. p. 117-140.

Heilman, M. D., D. L. Carter, and C. L. Gonzales. 1965. The ethylene glycol monoethil ether (EGME) technique for determining soil-surface area. Soil Sci. 100:409-413.

Herbillon, A. J., M. M. Mestdagh, L. Vielvoye, and E. G. Derouane. 1976. Iron in kaolinite with special reference to kaolinite from tropical soils. Clay Mineral, 11:201-220.

Hutton, J. T. 1977. Titanium and zirconium minerals. In J. B. Dixon and S. B. Weed (ed.) Minerals in Soil Environments. Soil Sci. Soc. Am. Madison, WI. p. 673-688.

Hurst, V. J. 1977. Visual estimation of iron in saprolite. Geol. Soc. Am. Bull. 88:174-176.

Ikawa, H. 1978. Correlation of selected data of Brazil and SCS-USDA laboratories. In M. N. Camargo and F. H. Beinroth (ed.) Proc. First Int. Soil Classif. Workshop. SNLCS, Rio de Janeiro. p. 338-353.

Ilchenko, V. 1955. Os tufos vulcanicos da Mata da Corda e seu emorego na agricultura. Secretaria de Agricultura. Industria, Comercio e Trabalho de Minas Gerais.

Jackson, M. L. 1975. Soil Chemical Analysis. Advanced Course. 2nd ed. Published by the author. Madison, WI.

Jenny, H. 1980. The Soil Resource. Springer-Verlag, New York.

Joint Committee on Powder Diffraction Standards. 1980. Mineral Powder Diffraction File Data Book. Intern. Centre for Diffraction Data, Swarthmore, Pennsylvania.

Jones, R. L., and A. H. Beavers. 1964. A technique for magnetic susceptibility determination of soil materials. Soil Sci. Soc. Am. Proc. 28:47-49.

Juo, A. S. R., F. R. Moorman, and H. O. Maduakor. 1974. Forms and pedogenetic distribution of extractable iron and aluminum in selected soils of Nigeria. Geoderma 11:167-179.

Kämpf, N. and E. Klamt. 1978. Mineralogia e genese de latossolos e solos podzolicos da regias Nordeste do Planalto Sul Riograndense. Rev. Bras. Ci. Solo, Campinas, Brazil 2:68-73.

Kämpf, N. and V. Schwertmann. 1982. Quantitative determination of goethite and hematite in kaolinitic soils by x-ray diffraction. Clay Minerals 17:359-363.

Kämpf, N. and V. Schwertmann. 1983. Relacoes entre oxidos de ferro e a cor em solos cauliniticos do Rio Grande do Sul. Rev. Bras. Ci. Solo, Campinas, Brazil 7:27-31.

Kieley, P. V., and M. L. Jackson. 1965. Quartz, feldspar, and mica determination for soils by sodium pyrosulfate fusion. Soil Sci. Soc. Am. Proc. 29:159-163.

King, L. C. 1962. A geomorfologia do Brasil Oriental. Rev. Bras. Geogr. 18(2):147-256.

King, L. C. 1967. The Morphology of the Earth. 2nd edition. Oliver and Boyd, London.

Klug, H. P., and L. E. Alexander. 1974. X-ray Diffraction Procedures for Polycrystalline and Amorphous Materials. 2nd ed. Wiley, N. Y. 966 p.

Krishna Murti, G. S. R., and Satyanarayana, K. V. S. 1971. Influence of chemical characteristics in the development of soil colour. Geoderma 5:243-248.

Longworth, G., and M. S. Tite. 1977. Mössbauer and magnetic susceptibility studies of iron oxides in soils from archaeological sites. Archaeometry 19:3-14.

Longworth, G., L. W. Becker, R. Thompson, F. Oldfield, J. A. Dearing, and T. A. Rummery. 1979. Mössbauer effect and magnetic studies of secondary iron oxides in soils. J. Soil Sci. 30:93-110.

Leal, J. R., and A. C. X. Veloso. 1973. Adsorcão de fosfato em latossolos sob vegetacao de cerrado. Pesg. Agrop. Bras. Ser. Agron. 8:81-88.

Le Borgne, E. 1955. Abnormal magnetic susceptibility of the topsoil. Am. Geophys. 11:399-419.

Le Borgne, E. 1960. The influence of fire on the magnetic properties of soil, schist and granite. Ann. Geophys. 16:159-196.

Lepsch, I. F., S. W. Buol, and R. B. Daniels. 1977a. Soil-landscape relationships in the Occidental Plateau of Sao Paulo State, Brazil: I. Geomorphic surfaces and soil mapping units. Soil Sci. Soc. Am. J. 41:104-109.

_____. 1977b. Soil-landscape relationships in the Occidental Plateau of Sao Paulo State, Brazil: II. Soil morphology, genesis, and classification. Soil Sci. Soc. Am. J. 41:742-747.

Matsusaka, Y., and G. D. Sherman. 1961. Magnetism of iron oxide in Hawaiian soils. Soil Sci 91:239-245.

Matsusaka, Y., G. D. Sherman, and L. D. Swindle. 1965. Nature of magnetic minerals in Hawaiian soils. Soil Sci 100(3):192-199.

McFarlane, M.J. 1976. Laterite and Landscape. Academic Press, London. 151 p.

McKeague, J. A., and M. G. Cline. 1963. Silica in soils. Adv. Agron. 15:339-396.

McKeague, J. A., and J. H. Day. 1966. Dithionite and oxalate extractable Fe and Al as aids in differentiating various classes of soils. Can. J. Soil Sci. 46:13-22.

McKeague, J. A., J. E. Brydon, and N. M. Miles. 1971. Differentiation of forms of extractable iron and aluminum in soils. Soil Sci. Soc. Am. Proc. 35:33-38.

Mehra, O. P., and M. L. Jackson. 1960. Iron oxide removal from soils and clays by a dithionite-citrate-bicarbonate system buffered with sodium bicarbonate. Clays and Clay Minerals 7:317-327.

Moniz, A. C. 1967. Quantitative mineralogical analysis of Brazilian soils derived from basic rocks and slate. M.S. Thesis. Univ. of Wisconsin, Madison.

Moniz, A. C., and S. W. Buol. 1982. Formation of an Oxisol-Ultisol transition in São Paulo, Brazil: I. Double-water flow model of soil development. Soil Sci. Soc. Am. J. 46:1228-1233.

Moniz, A. C., S. W. Buol, and S. B.Weed. 1982. Formation of an Oxidol-Ultisol transition in São Paulo, Brazil: II. Lateral dynamics of chemical weathering. Soil Sci. Soc. Am. J. 46:1234-1239.

Moura, Filho, W., and S. W. Buol. 1976. Studies of a Latossol roxo (Eutrustox) in Brazil: Clay mineralogy. Experiantiae, Vicosa, Brazil 13:218-234.

Mulay, L. N. 1963. Magnetic susceptibility. In I. M.Kolthoff and P. J. Elving, Treatease on Analytical Chemistry. Part I, Vol. 4, 1751-1883. John Wiley and Sons.

Mulay, L. N. 1976. Definitions and units for magnetic terms. In E. A. Boudreaux and L. N. Mulay, Theory and Applications of Molecular Paramagnetism. p. 477-496. John Wiley and Sons.

Mullins, C. E. 1977. Magnetic susceptibility of the soil and its significance in soil science - a review. J. Soil Sci. 28:223-246.

Murphy, J., and J. P. Riley. 1962. A modified single solution method for the determination of phosphate in natural waters. Analytica Chimica Acta 27:31-36.

Nagata, T., and S. Akimoto. 1961. Magnetic properties of rock-forming ferromagnetic minerals. In T. Nagata (ed) Rock Magnetism 127-146. Maruzen Company Ltd. Tokyo.

Norrish, K., and R. M. Taylor. 1961. The isomorphous replacement of iron by aluminum in soil goethites. J. Soil Sci. 12:294-306.

Novais, R. B. 1969. Estudo preliminar sobre a utilizacao do "tufito" na recuperacão de cerrados de Patos de Minas. Revista Seiva, Vicosa 67:5-13.

Oades, J. M., and W. N. Townsend. 1963. The detection of ferromagnetic minerals in soils and clays. J. Soil Sci. 14(2):179-187.

Oldfield, F.,T. A. Rummery, R. Thompson, and D. E. Walling. 1979. Identification of suspended sediment sources by means of magnetic measurements: Some preliminary results. Water Resources Research 15(2):211-218.

Ollier, C. D. 1959. A two-cycle theory of tropical pedology. J. Soil Sci. 10:137-148.

Pinto, D. C. B. 1971. Formation of a kaolinite from a biotite-feldspar gneiss in four strongly weathered soils profiles from Minas Gerais, Brazil. M.S. Thesis. Purdue University.

Piper, C. S. 1944. Soil and Plant Analysis. New York, Interscience.

Quickenden, T. I., and R. C. Marshall. 1972. Magnetochemistry in SI units. J. of Chemical Education 49(2):114-116.

Prasad, B., and B. P. Ghildyal. 1975. Magnetic susceptibility of lateritic soils and clays. Soil Sci. 120(3):219-229.

Rauen, M. J. 1980. Mineralogical identification of a toposequence of soils from basaltic rocks in the State of Parana, Brazil. M.S. Thesis. Purdue Univ.

Rauen, M. J., and G. C. Steinhardt. 1980. Mineralogy of a toposequence of soils formed from basaltic rocks in Parana, Brazil. Agron. Abstr. 1980 Annual Meetings, ASA, CSSA, and SSSA.

Resende, M. 1976. Mineralogy, chemistry, morphology and geomorphology of some soils of the Central Plateau of Brazil. Ph.D. Thesis. Purdue University. Dissertation Abstracts 37:4803.

Resende, M. 1982. Pedologia., Imprensa Universitaria, Universidade Federal Vicosa, MG, Brazil. 100 p.

Resende, M., and D. P. Franzmeier. 1982. Mineralogy of Brazilian Oxisols - A proposed general model. Univ. Federal Vicosa, MG, Brazil.

Rezende, S. 1971. Estudo de toposequencias de solos em Vicosa, Minas Gerais. M.S. Thesis, Universidade Federal de Vicosa, Vicosa, Minas Gerais, Brasil.

Rezende, S. B. 1980. Geomorphology, mineralogy and genesis of four soils on gneiss in southeastern Brazil. Ph.D. Thesis. Purdue Univ. Dissertation Abstracts 42:118.

Rich, C. I. 1960. Aluminum in interlayer of vermiculite. Soil Sci. Soc. Am. Proc. 24:26-32.

Rodrigues, T. E., and E. Klamt. 1978. Mineralogia e genese de uma sequencia de solos do Distrito Federal (Brazil). Rev. Bras. Ci. Solo 2:132-139.

Sanchez, P. A. 1976. Properties and Management of Soils in the Tropics. John Wiley and Sons, New York.

Santana, D. P. 1973. Estudo de solos do Triangulo Mineiro e de Vicosa: I. Mineralogia; II Adsorcao de fosfatos. M.S. Thesis, Universidade Federal de Vicosa, Vicosa, MG, Brazil.

Santana, D. P., and W. Moura Filho. 1978. Estudo de solos do Triangulo Mineiro e de Vicosa: I. Mineralogia. Experientiae, Vicosa, Brazil 24(6):131-160.

Savitzky, A., and M. J. E. Golay. 1964. Smothing and differentiation of data by simplified least squares procedures. Anal. Chem. 36:1627-1639.

Sawhney, B. L. 1977. Interstratification in layer silicates. In J. B. Dixon and S. B. Weed (ed) Minerals in Soil Environments. Soil Sci. Soc. Am., Madison,WI. p. 405-434.

Schulze, D. G. 1981. Identification of soil iron oxide minerals by differential x-ray diffraction. Soil Sci. Soc. Am. J. 45:437-440.

Schulze, D. G. 1982. The identification of iron oxides by differential x-ray diffraction and the influence of aluminum substitution on the structure of goethite. Dissertation for Dr. Agr., Tech. Univ. Munchen, Fed. Rep. of Germany.

Schulze, D. G. 1984. The influence of aluminum on iron oxides VIII. Unit-cell dimensions of Al substituted goethites and estimation of Al from them. Clays and Clay Minerals, 32(1):36-44.

Schulze, D. G., and J. B. Dixon. 1979. High gradient magnetic separation of iron oxides and other magnetic minerals from soil clays. Soil Sci. Am. J. 43:793-799.

Schwertmann, U. 1964. Differenzierung der eisenoxide des bodens durch extraktion mit ammonium oxalate-losung. Z. Pflanzenernähr., Dung. Bodenkunde 105-194-202.,

Schwertmann, U., and R. M. Taylor. 1977. Iron oxides. In J. B. Dixon and S. B. Weed (ed.) Minerals in soil environments. Soil Sci. Soc. Am., Madison, WI. p. 145-176.

Schwertmann, U., R. W. Fitzpatrick, R. M. Taylor, and D. G. Lewis. 1979. The influence of aluminum on iron oxides. Part II. Preparation and properties of Al-substituted hematites. Clays and Clay Minerals 27:105-112.

Silva, W. J., and F. Z. Antunes. 1980. Aptidão climatica para a cultura do milho. Informe Agropecuário, Belo Horizonte, Brazil 6(72):10-14.

Simonson, R. . 1959. Outline of a generalized theory of soil genesis. Soil Sci. Soc. Am. Proc. 23:152-156.

Soares, M. F. 1980. Caracterizacão quinica e mineralogica de concrecoes ferruginosas de alguns solos brasileiros. M.S. Thesis. Univ. Fed. Vicosa, MG, Brazil.

Soileau, J. M., and R.J. McCraken. 1967. Free iron and coloration in certain well-drained coastal plain soils in relation to their properties and classification. Soil Sci. Soc. Am. Proc. 31:248-255.

Soil Survey Staff. 1975. Soil Taxonomy - A basic system of soil classification for making and interpreting soil surveys. Agriculture Handbook no. 436. SCS, U.S. Department of Agriculture. 754 p.

Taylor, R. M. 1982. Colours in soils and sediments - Review. Proc. VII Intern. Clay Conference, 1981, Bologna, Italy. p. 750-761.

Taylor, R. M., and A. M. Graley. 1967. The influence of ionic environment on the nature of iron oxides in soils. J. Soil Sci 18:341-348.

Taylor, R. M., and U. Schwertmann. 1974. Maghemite in soils and its origin. II. Maghemite synthesis and ambient temperature and pH7. Clay Minerals 10:299-310.

Torrent, J., U. Schwertmann, and D. G. Schulze. 1980. Iron oxide mineralogy of some soils of two river terrace sequences in Spain. Geoderma 23:191-208.

Torrent, J., U. Schwertmann, H. Fechter, and F. Alferez. 1983. Quantitative relationship between soil color and hematite content. Soil Sci. 131(6):354-358.

Uehara, G., and G. Gillman. 1981. The Mineralogy, Chemistry, and Physics of Tropical Soils with Variable Charge Clays. Westview Press, Boulder, Colorado, U.S.A. 170 p.

Vodyanitskiy, Y. N. 1981. Formation of ferromagnetics in Sod-Podzolic soil. Soviet Soil Sci. 1981(3):89-100.

Vadyunina, A. F., and V. F. Babanin. 1972. Magnetic susceptibility of some soils in the USSR. Soviet Soil Sci. (4):588-599.

Vadyunina, A. F., V. F. Babanin, and V. Y. Kovtun. 1974. Magnetic susceptibility of the separates of some soils. Soviet Soil Sci. 1974(6):106-110.

Vadyunina, A. F., and Y. A. Smirnov. Use of magnetic susceptibility in the study and mapping of soils. Soviet Soil Sci. 1978(4):479 (Abstracts).

Valverde, O. 1958. Estudo regional da Zona da Mata de Minas Gerais. Rev. Bras. Geog. 20(1):3-79. Rio de Janeiro, Brazil.

Van Houten, F. B. 1968. Iron oxides in red beds. Bull. Geol. Soc. Am. 79:399-416.

Van Wambeke, A. H. Eswaran, A. J. Herbillon, and J. Comerma. 1983. Oxisols. In L. P. Wilding, N. E. Smeck, and G. F. Hall (ed.) Pedogenesis and Soil Taxonomy II. The Soil Orders, Elsevier, Amsterdam. p. 325-354.

Veneman, P.L. M., M. J. Vepraskas, and J. Bouma. 1976. The physical significance of soil mottling in a Wisconsin toposequence. Geoderma 15:103-118.

Vettori, L. 1969. Metodos de analise de solo. Bol. Tech. no. 7. EPFS, Ministerio de Agricultura, Rio de Janeiro, Brazil. 24 p.

Walker, A. L. 1983. The effects of magnetite on oxalate- and dithionite-extractable iron. Soil Sci. Am. J. 47:1022-1026.

Weast, R. C., and M. J. Astle. 1982. Handbook of Chemistry and Physics. 62nd edition. CRC Press.

VITA

Derli Prudente Santana was born in Tupaciguara, Minas Gerais State, Brazil on October 21, 1948 to Bianor Prudente de Oliveira and Maria José Santana Prudente. He received his B.S. and M.S. in Agronomy from Universidade Federal de Vicosa in 1970 and 1973, respectively. He has been working at Empresa de Pesquisa Agropecuária de Minas Gerais, EPAMIG, a state agency for agricultural research since his graduation. He is married to Maria Célia Nasciutti Prudente and they have three children, Arthur, Cecília and Lucas.